University of Kent

Faculty of Sciences

School of Biosciences

Assay development and efficacy testing of novel and established antimicrobials.

By

Ben Wilson

Thesis for MSc by Research

July 2017

Acknowledgements and Thanks

The author would like to thank Dr Dan Mulvihill and Dr Jennifer Hiscock for their guidance, support and supervision. He would also like to thank the research groups of both supervisors, with special thanks going to L. Blackholly for providing the raw MIC assay verification data, and to L. White for providing the raw characterisation data for the compounds synthesised.

University of Kent

School of Biosciences

Assay development and efficacy testing of novel and established antimicrobials.

By Ben Wilson

Abstract

Over the past 25 years, new antimicrobial discovery has ground to a halt, this combined with a rise in antimicrobial resistance in pathogenic bacteria, is causing the number of effective treatments available to humankind decrease.

For my thesis, I explored the testing methods for screening antimicrobial compounds and found them to be inefficient. One of the limiting factors for the discovery of new antimicrobial compounds are the efficacy testing assays and high-throughput screening methods used by researchers. These methods mainly measure the ability of a compound to diffuse through or across a medium, be it agar, filter papers or testing strips.

Within this thesis I developed new testing assays for a family of novel antimicrobials, as their efficacy wasn't measurable by the standard procedures. I also measured the MIC50 and MIC100 values of all the compounds in the group. They had measurable antimicrobial effect against Gram-Positive bacteria - comparable with established compounds like Vancomycin, and measurable interaction with Gram-Negative bacteria, coating the cells and inhibiting growth.

I then further explored the coating interaction, adding the compounds to bacteria, but also adding solutions of established antimicrobials, I found that the compound boosted the efficacy of the established compounds and was also able to overcome resistance mechanisms developed by the bacteria.

Finally, I developed a modular, 3D printed robot to standardise and increase the accuracy of the new testing methods.

1 Table of Contents

1 Introduction

1.1 Medical Significance of Antibacterial Resistance

The worldwide library of clinically effective antimicrobials is becoming increasingly limited, this is due to a rise in antimicrobial resistance (AMR) exhibited by bacteria [1]. The deaths due to resistant disease causing bacteria are projected by the World Health to rapidly increase within the next 30 years (Figure 1). This is due to three things: the misuse of antimicrobials causing a development of resistance by bacterial organisms, the development of antibacterial resistance within agriculture, and the slowing of novel antibacterial discovery [2]. The human race can take action against two of these factors; stopping the misuse of antibacterials through education and stricter rules on prescription, and developing novel methods of antibacterial discovery and screening. Meanwhile, bacteria will still continue to develop resistance to known antibacterial compounds, so compounds with novel mechanisms of action must be investigated and developed [3].

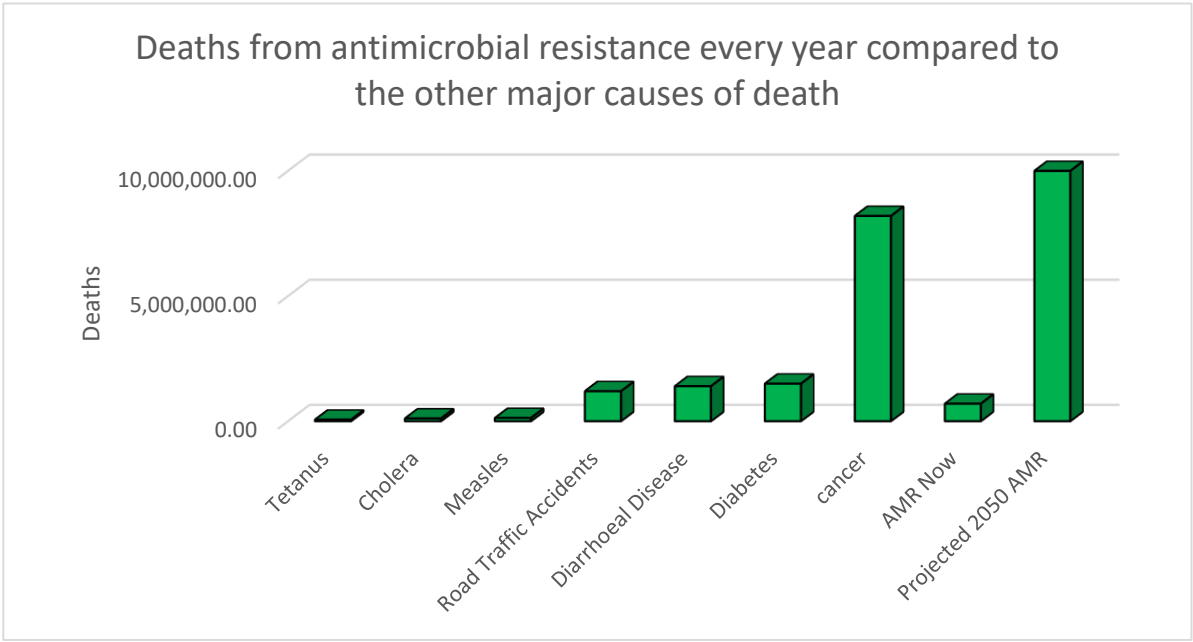

FIGURE 1 - CHART SHOWING DEATHS RELATED TO ANTIBACTERIAL RESISTANCE IN COMPARISON TO OTHER MAIN CAUSES, PROJECTED DEATHS FROM RESISTANT BACTERIAL INFECTIONS WILL OUTNUMBER THE DEATHS FROM CANCER. (DATA FROM WORLD HEALTH ORGANISATION DECEMBER 2014 REVIEW [4])

1.2 Misuse of antibacterials

The misuse of antibacterials is comprised by two problematic behaviours; misprescription of the antibacterial drugs, and improper use of the prescribed drugs. The main misprescription issues are caused by medical professionals unnecessarily prescribing broad spectrum antibacterial therapies such as ampicillin and amoxicillin. The improper use of the prescribed drugs is facilitated by patients not completely finishing full courses of antibacterials, rather stopping when their symptoms are alleviated, this greatly reduces the chance of the target microorganism being eradicated, and increases the likelihood that the remaining population is equipped with modified characteristics that grant them resistance to the therapy [5–7].

Another area where antibacterials are abused is in agriculture. In both first and third world settings, antibacterials are added to the foodstuffs of livestock to promote growth and prevent contraction of infectious disease, an estimated 70% of all antibacterial compounds sold in the USA are used for this purpose [8]. Detection methods have recently shown that resistant bacteria are passed to humans through the ingestion of farmed meat. This is because the livestock act like breeding incubators for resistance, with the ingested antibacterials acting as the selection pressure, killing off most of the bacterial population, and leaving the cells that are resistant. This small population of bacteria will thrive in the body of the host, and be contained within the meat after it is killed and processed [9,10]. Many pathogens such as *Listeria* and *Campylobacter* are incubated within livestock, but the most prevalent are drug resistant strains of *Staphylococcus aureus* [11]. The use of antibiotics in agriculture also effects the environmental microbiome. Around 90% of antibacterials ingested by livestock are excreted in urine and faeces[12]. These excretions are then distributed around the environment by human and natural means. Humans gather up the faeces produced by livestock and spread them on fields as fertilisers. The compounds will leach into the surroundings, accelerated by natural processes like precipitation and surface runoff. This exposes microorganisms in the environment to the compounds, and allows populations to develop resistance.

Lastly, antibiotic cleaning and hygiene products are adding to the misuse of antibacterials as they are increasing the selection pressure placed on bacterial organisms, which will lead to possible increased development of resistance mechanisms [13].

1.3 ESKAPE Pathogens

The ESKAPE pathogens are a group of six bacterial species (***E****nterococcus faecium*, ***S****taphylococcus aureus*, ***K****lebsiella pneumoniae*, ***A****cinetobacter baumannii*, ***P****suedomonas aeruginosa*, and ***E****nterobacter*) [14]. These six organisms have become resistant to a large number of antibacterial compounds, causing a wealth of complications for the medical community. Prevalent in hospital wards and even operating theatres, these opportunistic pathogens can cause a wide variety of infections, which are particularly dangerous to patients in medical care due to the weak and potentially immunocompromised state they are in. One highlighted problem caused by ESKAPE pathogens is the formation of biofilms. S. aureus was first recorded forming a biofilm in 1982, the bacteria had formed a film around the lead of an endocardial pacemaker implanted into patient and had been causing persistent acute bacteraemia infections regardless of the several courses of antibiotic that the patient had taken [15]. The persistence of *S. aureus* biofilms, along with any antibacterial resistant characteristics exhibited make them a potential infection source to anyone that has foreign bodies surgically implanted, like arterial stents, artificial joints and even artificial circulatory valves.

1.4 Mechanisms of Antibacterial Action

Antibacterials are functionalised compounds that are prescribed to patients to combat infections caused by bacteria. After ingestion and reaching the target bacterial cells, the antibacterial compounds have several different routes of attack across the membranes of both Gram-positive and Gram-negative organisms (Figure 2) to cause their therapeutic effect.

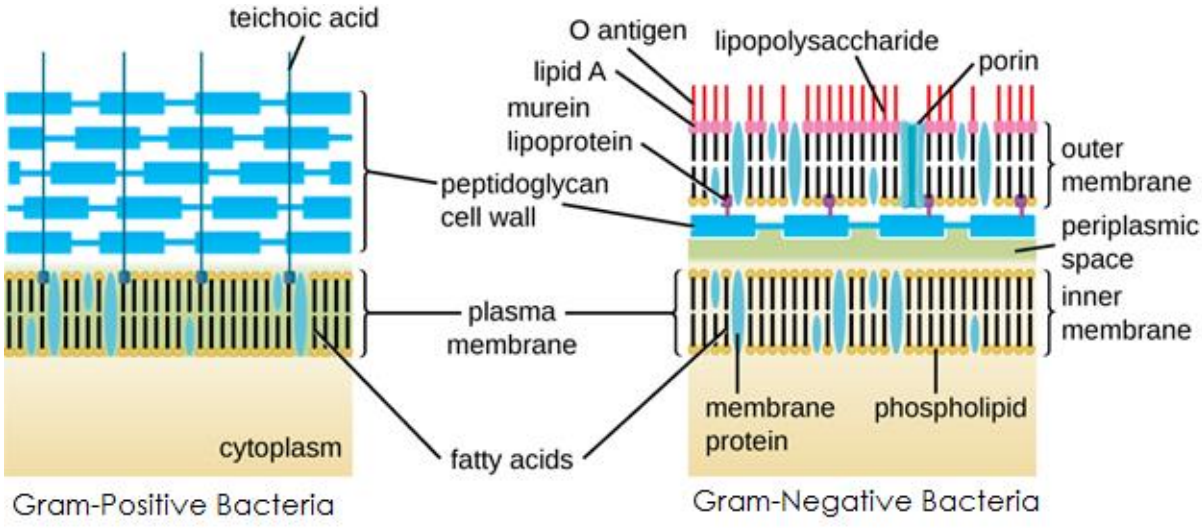

FIGURE 2 - DIAGRAM SHOWING THE DIFFERENCES IN THE BACTERIAL CELL ENVELOPE FOR GRAM-POSITIVE AND GRAM-NEGATIVE ORGANISMS, THE MAIN DIFFERENCE BEING THE ADDITIONAL CELL MEMBRANE LAYER SURROUNDING THE PEPTIDOGLYCAN CELL WALL OF THE GRAM-NEGATIVE BACTERIA [62]

1.4.1 Inhibitors of cell wall synthesis.

The most common mode of action for antibacterials is inhibiting the synthesis of the bacterial cell wall, most bacterial cell walls contain a peptidoglycan layer within them, this layer provides the cell with strength and rigidity. The peptidoglycan layer is a mesh of peptide and glycan chains, cross-linked covalently by a family of transpeptidase enzymes. The more crosslinks, the higher the strength of the cell to withstand lysis by osmosis. Drugs like penicillin and Cephalosporins act as pseudosubstrate mimics, and bind to the transpeptidases, forming complexes [16]. This prevents the enzyme from undertaking it's

purpose of forming crosslinks, thus weakening the wall, and rendering the cell susceptible to osmotic lysis (Figure 3). The vancomycin group of antibacterials also inhibit cell wall synthesis, but instead of targeting the enzymes involved with the crosslinking, they target the substrate peptides. The vancomycin structure forms five hydrogen bonds with the dipeptide terminus of the pentapeptide side chain, effectively capping it. This prevents the enzymes from forming the cross links, and again renders the cell susceptible to osmotic lysis. Generally, Gram-negative bacteria are less susceptible to antibacterials that inhibit cell wall synthesis, as the compounds have difficulty crossing the cell wall.

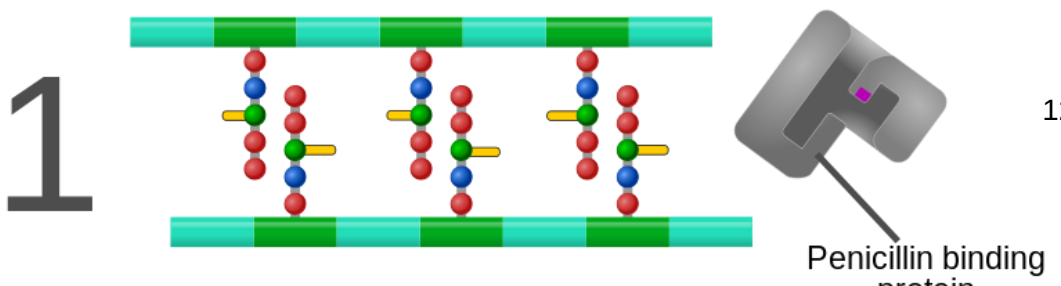

FIGURE 3 - MODE OF ACTION FOR ANTIBACTERIAL COMPOUNDS THAT INHIBIT CELL WALL SYNTHESIS (PENICILLIN IN THIS EXAMPLE)[63]
THE DRUG COMPOUNDS OCCUPY THE ACTIVE SITE OF THE ENZYMES, PREVENTING THE FORMATION OF THE PENTAGLYCINE CROSSLINK CHAINS

1.4.2 Inhibitors of protein synthesis

The main route of attack for antibacterials that inhibit protein synthesis is ribosomal inhibition. Ribosomal organelles are constructed from two ribonucleoprotein subunits, the 30s and 50s. The antibacterial compounds that inhibit protein synthesis will interact with either one of the subunits [17]. The drugs that inhibit the 50s subunit physically block the initiation of protein translation, halting the peptidyltransferase process that extends the peptide chain. Recent study has clarified the mode of action of these compounds, stating that the drug prevents the binding of peptidyl tRNAs to the subunit, and stopping the growth of the peptide chain. Macrolide and amphenicol families of antibacterials are amongst those that target the 50s subunit [18]. The compounds that target the 30s subunits have various modes of action; Tetracycline based compounds block the access of aminoacetyl tRNAs, and Aminocyclitols bind to sections of the rRNA causing protein mistranslation due to codons being altered. They can also corrupt the stability of tRNA when is binds to the ribosome. In the family of protein inhibiting antibacterials, the naturally produced aminoglycosides are the only ones that are mainly bactericidal. Macrolides, tetracyclines and chloramphenicols, are typically bacteriostatic, though some have exhibited bactericidal properties on isolated strains of microorganism.

1.4.3 Inhibitors of nucleic acid synthesis

Antibacterial compounds such as the quinolone and fluoroquinolone families target the enzymes involved in the synthesis of bacterial nucleic acids such as DNA gyrase and topoisomerases involved in the replication, cleaving, reattaching and coiling of the DNA strands [19]. Quinolone based antibiotics such as ciprofloxacin bind to the complex formed by the DNA gyrase enzyme, and the DNA strand itself. The antibacterial stabilises the complex, and prevents the enzyme from removing the positive supercoiling in the DNA strand, this causes the bacterial DNA to fragment. This fragmentation of the DNA triggers the SOS repair system in the bacteria, and will ultimately lead to cell death. (Figure 4) DNA gyrase (or topoisomerase II) is the primary target of quinolones and fluoroquinolones within

Gram-negative bacteria and topoisomerase IV is the primary target of these compounds within Gram-positive bacteria.

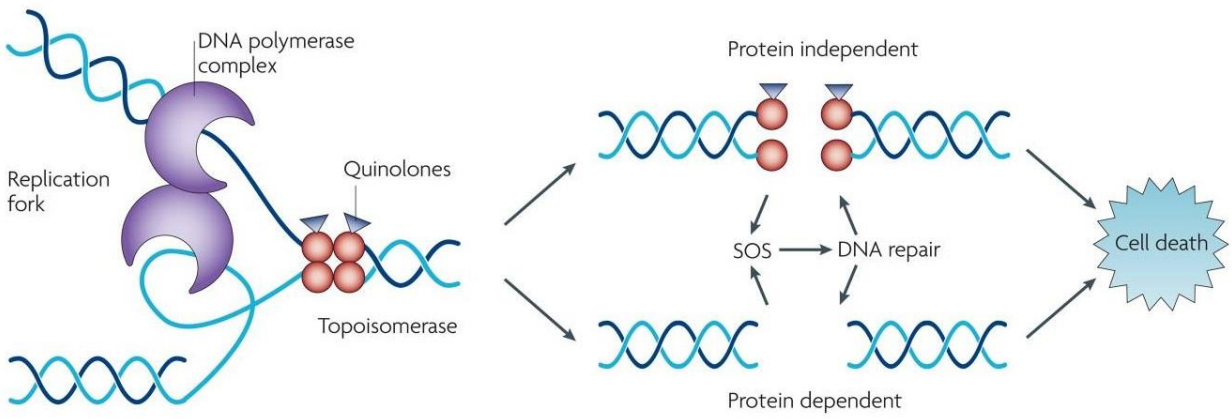

FIGURE 4 – THE MODE OF ACTION OF QUINOLONE BASED COMPOUNDS ON DNA GYRASE ENZYMES, CAUSING FRAGMENTATION OF THE DNA STRAND. THIS CAUSES THE CELL TO TRY AND REPAIR THE BROKEN STRANDS, AND AS THE DRUG IS STILL PRESENT WITHIN THE CELL PREVENTING THIS REPAIR, THE CELL EVENTUALLY TRIGGERS APOPTOSIS. [20]

1.5 Commercially Available Antibacterials

1.5.1 Penicillins

Penicillins were first discovered by Alexander Fleming in 1928. During experimentation on *Staphylococcal* bacterial strains, an inoculated plate was left out uncovered next to an open window. Upon revisiting it, Fleming discovered that it had been contaminated with mould spores. These mould spores appeared to have produced zones of inhibition on the bacterial lawn. Fleming isolated the mould and categorised it as a member of the Genus *Penicillium*, he extracted the excretion of the mould and tested it on various strains of bacteria. The new 'Penicillin' compound was found to be effective against all Gram-positive pathogenic organisms.

Later on, in 1940, Howard Florey and Ernst Chain took an interest in the Penicillin molecule and devised a method to mass produce it. This allowed Penicillin to be widely available for distribution during world war II [21].

Penicillin is produced as a secondary metabolite of the *Penicillium* fungus when its growth is halted by stress factors in its environment, like bacteria

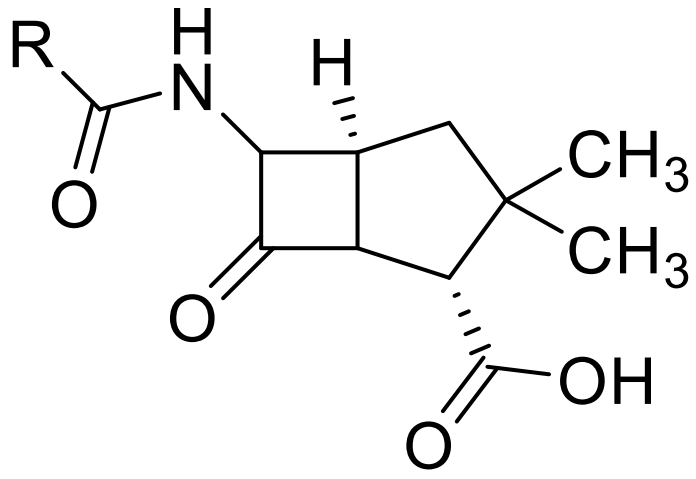

FIGURE 5 - CORE CHEMICAL STRUCTURE OF PENICILLIN BASED COMPOUNDS

All Penicillins contain a β-Lactam ring, a four membered functionality that provides the drug with its antibacterial properties. This ring is also bonded to a five membered thiazolidine ring, causing it to become much more reactive. (Figure 5) This increased reactivity is due

to the steric distortion placed on the β-Lactam amide bond. The mode of action for most Penicillins is targeting the formation of peptidoglycan crosslink formation within the bacterial cell wall. The drug binds to DD-Transpeptidase enzymes, preventing them from catalysing the reaction. This causes the cell wall synthesis to slow, and wall degradation to overtake, leading to cell death [22].

1.5.2 Cephalosporins

The first Cephalosporin based compounds were investigated during 1948 by Guiseppe Brotzu, he discovered a colony of *Acremonium strictum* growing at the outlet of a sewer pipe, finding that a metabolic filtrate of the mould colony produced inhibitive effects against the growth of *Staphylococcus* strains [23].

The compounds were further developed by Edward Abraham and Guy Newton, they were able to isolate three versions of the Cephalosporin base molecule; P, N and C. These molecules were not strong enough to be used as clinical antibacterials, but after further investigation, the removal of their side chains yielded molecules similar in structure to Penicillins. This allowed Cephalosporin analogues to be produced and developed into clinically available antibacterials.

Cephalosporins are β-Lactam based antibacterials like Penicillins, (Figure 6) so both compounds share similar modes of activity, targeting the cell wall synthesis of the bacteria, preventing peptide crosslinking and causing the cell to lyse due to osmosis [24].

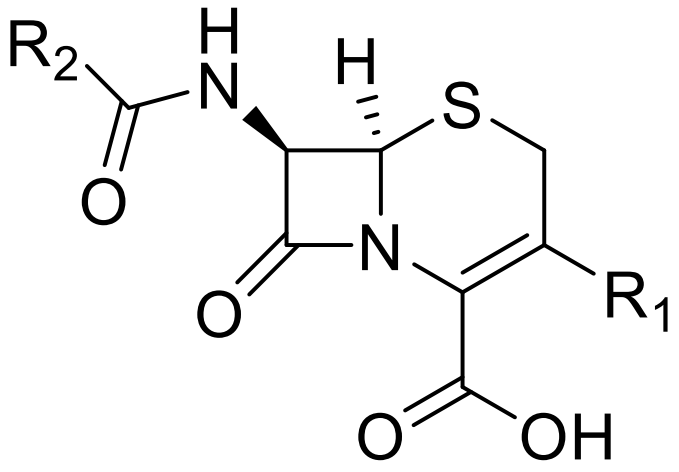

FIGURE 6 - CORE CHEMICAL STRUCTURE OF CEPHALOSPORIN BASED ANTIBACTERIALS

1.5.3 Carbapenems

In the late 1960s after it was observed that bacteria were producing β-Lactamase enzymes to counteract administered Penicillins. In 1976, researchers started developing compounds able to inhibit β-Lactamase [25]. One of the observed bacterial strains was *Streptomyces clavuligerus*, which secreted products that showed ability to inhibit these enzymes, Olivanic acid, and Clavulanic acid. Olivanic acid was initially investigated, but found to be too unstable, so Clavulanic acid was investigated and then developed into the first clinical β-Lactamase inhibitor. A different strain of *Streptomyces*, *S. cattleya*, was investigated, and found to produce the first Carbapenem, Thienamycin. This compound still bound to the penicillin binding proteins produced by the bacteria it was administered to, however, its broad spectrum of inhibitory activity against both Gram-positive and Gram-negative bacteria, it was widely used, and became the template for the next generation of more stable clinical Carbapenems. (Figure 7)

As with most β-Lactam antibiotics, Carbapenems target cell wall synthesis, inhibiting the formation of the peptide crosslinks, leading to cell death.

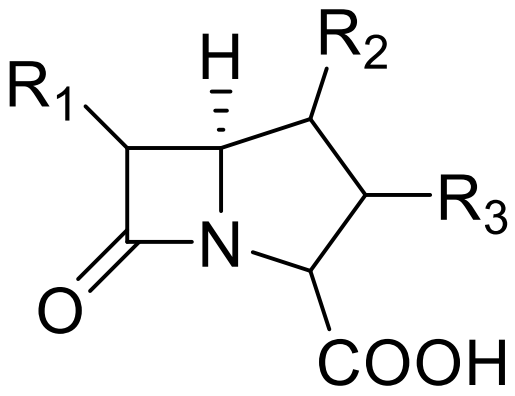

FIGURE 7 – CORE CHEMICAL STRUCTURE OF CARBAPENEM BASED ANTIBACTERIALS

1.5.4 Quinolones and Fluoroquinolones

Quinolones were first developed in the early 1960s by George Lesher and his research group. The compound was isolated in the by-product produced from the attempted synthesis of the antimalarial drug Chloroquine. This new compound, known as Nalidixic acid, was used to treat urinary tract infections. Over the following years, many more analogues were synthesised using Nalidixic acid as a structural template.

The core structure of quinolone antibacterials is an aromatic quinolone functionality, with various other functionalities attached to the structure, including a carboxylic acid functionality at position 3 of the aromatic ring. Later generations of the quinolone compounds produced had a Fluorine atom at position 6 of the ring structure [26]. (Figure 8)

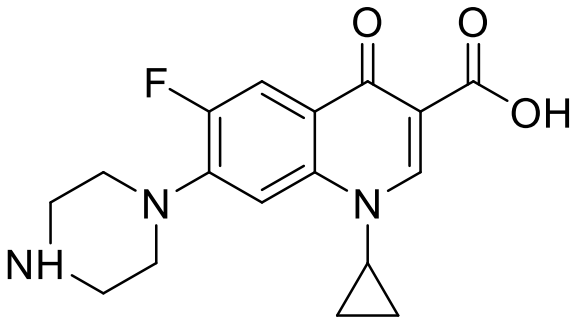

FIGURE 8 – CHEMICAL STRUCTURE OF CIPROFLOXACIN, A FLUOROQUINOLONE BASED ANTIBACTERIAL

Quinolones and Fluoroquinolones are effective against both Gram-positive and Gram-negative bacteria, making them 'broad spectrum antibacterials'. Whilst this is advantageous, use of all broad spectrum antibacterials can enhance the development of multidrug resistance within all strains of bacteria [27].

Quinolones and Fluoroquinolones are also recorded exhibiting serious adverse side effects in patients they have been prescribed to. These side effects are potentially disabling, being linked to problems in tendons, muscles, joints and the central nervous system. There have been a small number of tendon rupture and tendonitis cases linked to the ingestion of quinolone based medications, and some of the recorded nervous system side effects have been recorded as being insomnia, seizures and psychosis [28].

1.5.5 Tetracyclines

Tetracyclines are a class of antibacterial developed in the 1940's by Benjamin Minge Duggar. They exhibit antibacterial activity against a large range of organisms, including Gram-positive and negative bacteria, protozoans and mycoplasmas [29]. They inhibit the protein synthesis of micro-organisms by stopping charged tRNA attaching to its complimentary ribosome, halting the extension of the protein chain. Tetracyclines have few recorded harmful side effects, this beneficial factor, coupled with the large effective range of the compounds, has led to wide and extensive use in the treatment of infections in humans and animals. Tetracyclines are also used in malaria prevention, due to its minimal side effects and activity against the protozoans that are becoming resistant to the quinine based therapies that are available. In addition to being a therapeutic antibacterial, tetracyclines are also added to livestock foodstuffs in sub-critical concentrations to promote growth.

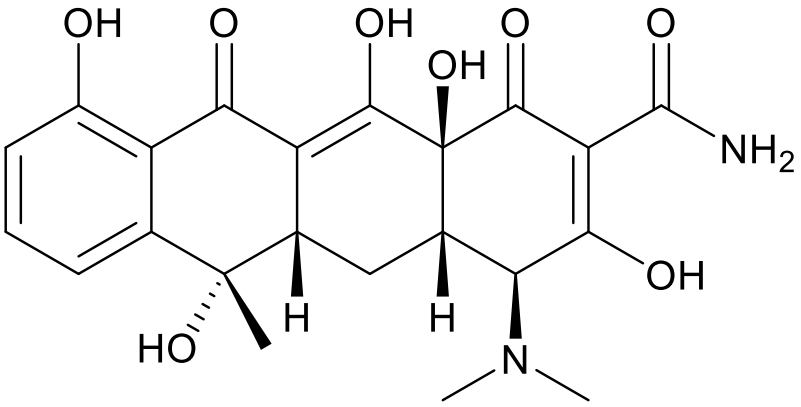

FIGURE 9 - BASIC CHEMICAL STRUCTURE OF TETRACYCLINE BASED ANTIBACTERIALS

All tetracyclines follow the structural pattern of a 4 piece, conjugated ring system – Naphthacene [30], (Figure 9) with several functional groups connected to it. This basic structure can be further modified with other functional groups, alkyl chains.

Tetracycline based drugs usually have a mode of action against the protein synthesis of the bacterial cell it is targeting.

1.6 Resistance Mechanisms

1.6.1 Modification of the antibiotic

Bacteria are able to resist the action of antibacterial compounds applied to them by targeting them and performing modifications to their structure with the help of enzymes. One such family of enzymes is the aminoglycoside modifying enzymes (AMEs) [31], these proteins have become the primary resistance mechanism for bacteria against antibacterials that target the protein and DNA synthesis of a bacteria. These enzymes will covalently alter the functional groups of antibacterials, like the amino and hydroxyl groups on the aminoglycoside molecule. Both Gram-positive and Gram-negative bacteria have exhibited production of these enzymes [32].

Another modification performed on antibacterials by bacteria is just to destroy the molecule by dismantling the part of the structure that provides the antibacterial functionality. The primary example of this mechanism is the development of β-Lactamase enzymes to combat β-Lactam molecules [33]. (Figure 10-11) These enzymes exist in several classes of differing structures, granting resistance to a wide range of β-Lactam based antibacterials like Penicillins, Carbapenems and Cephalosporins.

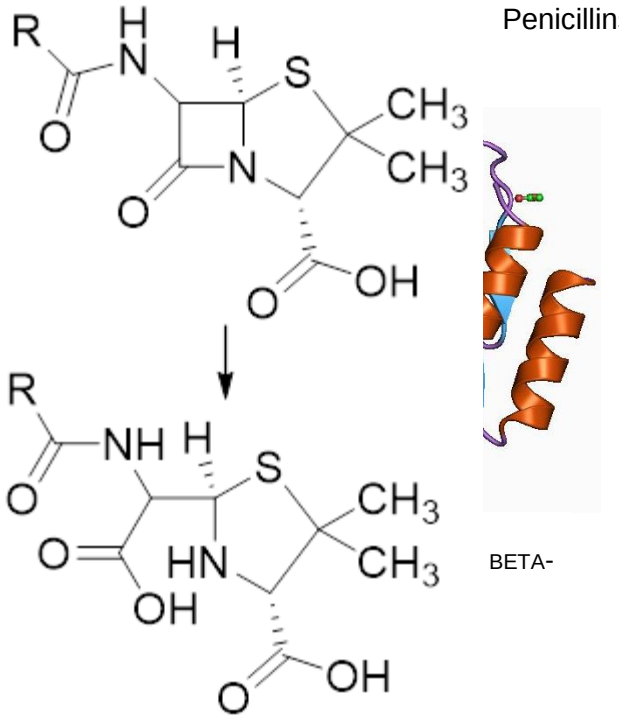

BETA-

FIGURE 11 (LEFT) – RING OPENING EFFECT OF BETA-LACTAMASE ENZYME ON A PENICILLIN MOLECULE

1.6.2 Efflux pumps and decreasing antibiotic penetration

A large proportion of antibacterial compounds are water soluble, containing hydrophilic functionalities. This helps them penetrate the outer membranes of target bacteria through water filled diffusion channel proteins known as porins [34]. As a resistance mechanism, bacteria have altered their genetic code to alter the characteristics of porin production within the cell, changing the size of the porin protein itself to prevent the influx of the compounds. The other modification to porin production within the cell is simply expressing less of the proteins, giving the antibacterial compounds less zones of access into the cell, slowing the mode of action.

In addition to slowing the influx of antibacterial drugs to the cell, bacterial have also developed ways of increasing the efflux. Using structured membrane proteins known as Efflux Pumps [35], (Figure 12) they rapidly remove compounds considered toxic to the cell. Efflux pumps have been observed within both Gram-positive and Gram-negative bacteria and exist in a multitude of classes, all of these pump proteins are active, so require a chemical power source, sources include ATP, positive ions and Protons. Bacterial efflux

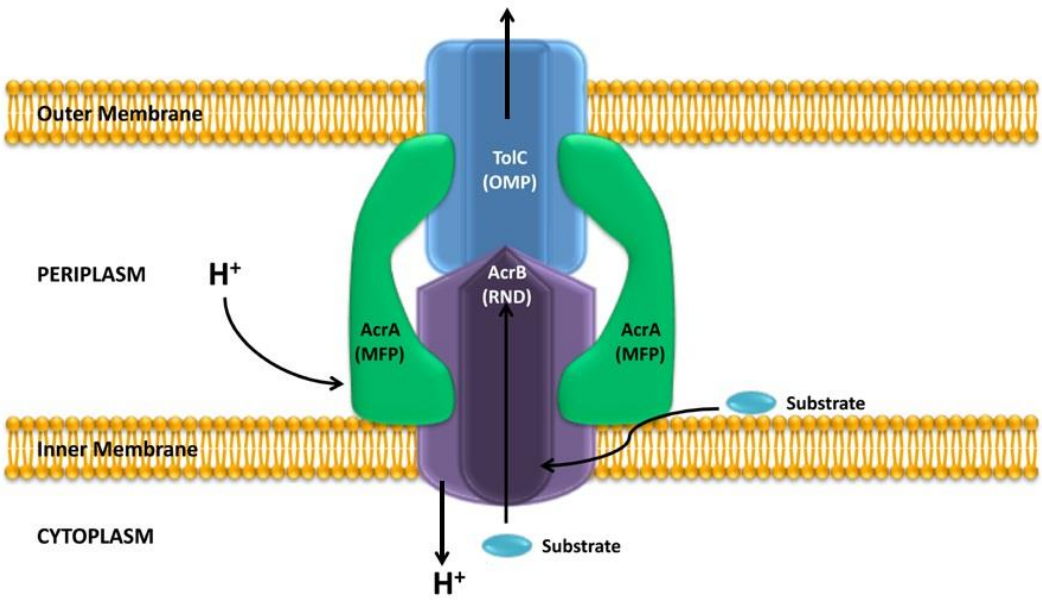

pumps, much like antibiotics, can be ‘broad spectrum’ targeting a multitude of toxic antibacterial compounds for removal, or they can be specifically synthesised to target one family of compounds, for example, Tet efflux pumps solely target compounds from the tetracycline family [36].

1.6.3 Changing target sites

Another resistance strategy that bacterial cells employ is modifying the site that the antibacterials target. There are two main methods of site modification, protection and modification, these are caused by the modification of proteins contained within the target and

FIGURE 12 – CROSS SECTION OF AN *E. COLI* CELL MEMBRANE, SHOWING THE STRUCTURE AND FUNCTION OF AN RND EFFLUX PUMP, SHOWING HOW THEY USE PROTONS AND SUBSTRATE MOLECULES. [65]

binding sites by mutations in the cell’s genetic code. These mutations are caused by multi-generational selection pressures from various sources like the environment, and applied antibiotics.

Target protection usually occurs against compounds that inhibit protein and DNA synthesis, for example, Tetracycline resistance observed in strains of *Campylobacter and Streptococcus* produces the proteins Tet(M) and Tet(O), these proteins are able to unbind Tetracycline from its target rRNA and halt its action. The Tet(M) [37] also modifies the geometry of the binding site within the rRNA, prevent further interaction from the drug molecule. Tet(O) has a similar mode of action, but attacks the drug molecule itself, changing the structure of the molecules active site, and preventing binding with the rRNA substrate.

Modifications of the microbial target sites are very common resistance mechanisms employed by bacteria. These target modifications can exist as; point mutations in the genes that code for the target sites, modification of the binding site itself via enzymes, or total replacement and bypassing of the original target site.

Point mutations in the genetic code of the target site cause the expression of different proteins at various points along the peptide that makes up its structure [38]. This will slightly alter the superstructure of the site, meaning that it is no longer a conformational fit for the antibacterial molecule, rendering it ineffective.

Enzymatic modification of the target sites can also occur, for example, *erm* genes (Erythromycin Ribosomal Methylation) [39] cause macrolide resistance within aerobic, anaerobic, Gram-positive and Gram-negative bacteria by bonding one or two methyl groups onto an adenine residue contained within the 50s subunit of cell's ribosomes. This prevents the drugs from being able to form complexes with the ribosome subunits to inhibit the cells protein synthesis.

The most common example of complete target replacement is resistance within *MRSA* strains, they have been able to develop analogues of the old target sites that perform similar intracellular functions. Another antibacterial bypass is overexpression of the target sites within the cell, this meant that the antibacterial compound will still bind to its target sites, but due to the large number of targets produced, the cell will be able to continue its processes unhindered [32].

1.7 Membrane Differences

Both bacteria and eukaryotes contain glycerol as the chief component in their phospholipids [40]. The phospholipids usually contained within bacterial cells: *(PS) - Phosphatidylserine*, *(PE) - Phosphatidylethanolamine*, and *(PG) - Phosphatidylglycerol*, are also contained within eukaryotes. *PG* is a large component of Gram-positive bacterial cell membranes, and another (smaller) component of Gram-negative bacterial cell membranes (Figure 13)

(It is also a main component in mammalian pulmonary surfactant). Mammalian Cell membranes contain a similarly structured 'alternative' to the PG phospholipid - *(PC)* – *Phosphatidylcholine* [41–43].

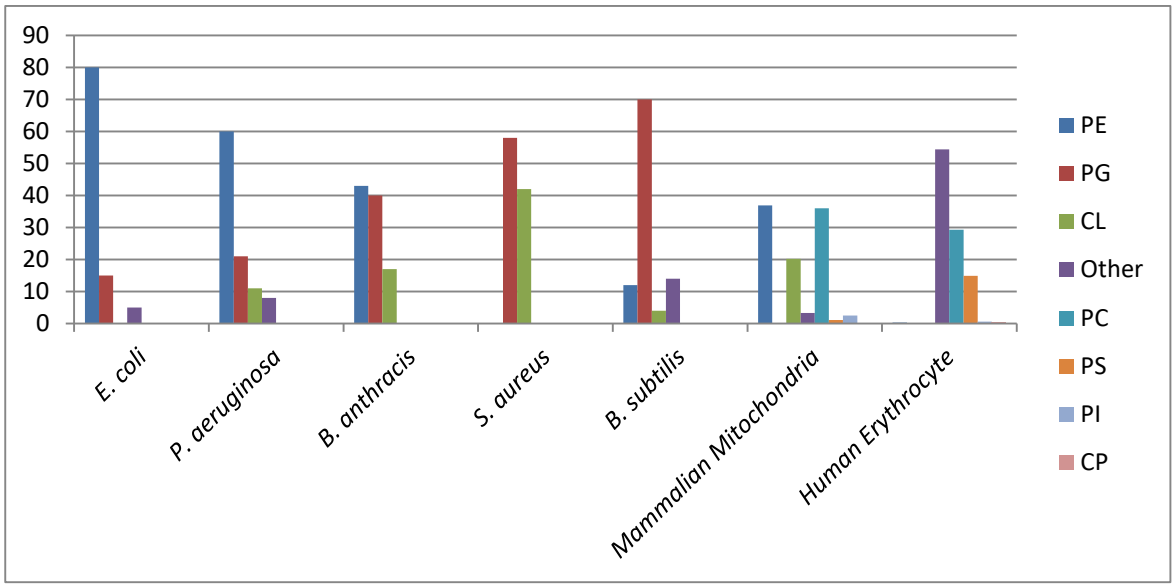

FIGURE 13 - CHART COMPARING MEMBRANE COMPOSITION OF VARIOUS CELLS (KEY - (PE) - PHOSPHATIDYLETHANOLAMINE, (PG) - PHOSPHATIDYLGLYCEROL, (CL) CARDIOLIPIN, (PC) PHOSPHATIDYLCHOLINE, (PS) PHOSPHATIDYLSERINE, (PI) PHOSPHATIDYLINOSITOL, (CP) CHOLINE PHOSPHOLIPIDS)

1.8 Current Antibacterial Testing Methods

Generally, the current methods of screening novel antibacterials are based around diffusion [44]. The literature standard method of primary screening novel antibacterials is the Kirby Bauer disc diffusion method. The other diffusion based protocol is the well diffusion screen. These methods of antibacterial screening are effective for compounds that diffuse freely through materials, compounds that don't diffuse as readily have severe problems with false negatives. For example, compounds like the ones being tested in this thesis that readily form hydrogen bonds during processes like self-assembly do not diffuse through agar, or off cellulose filter paper discs. This is because agarose and cellulose are materials rich in hydrogen bond forming functionalities, the potential antibacterials are forming hydrogen bonds with the materials in preference to diffusing off/through it. The disc diffusion assay is described in literature as the reliable testing method for screening antibacterials [45–47], however, tests carried out last year by a third year project student showed its ineffectiveness in screening certain compounds. (Figure 14)

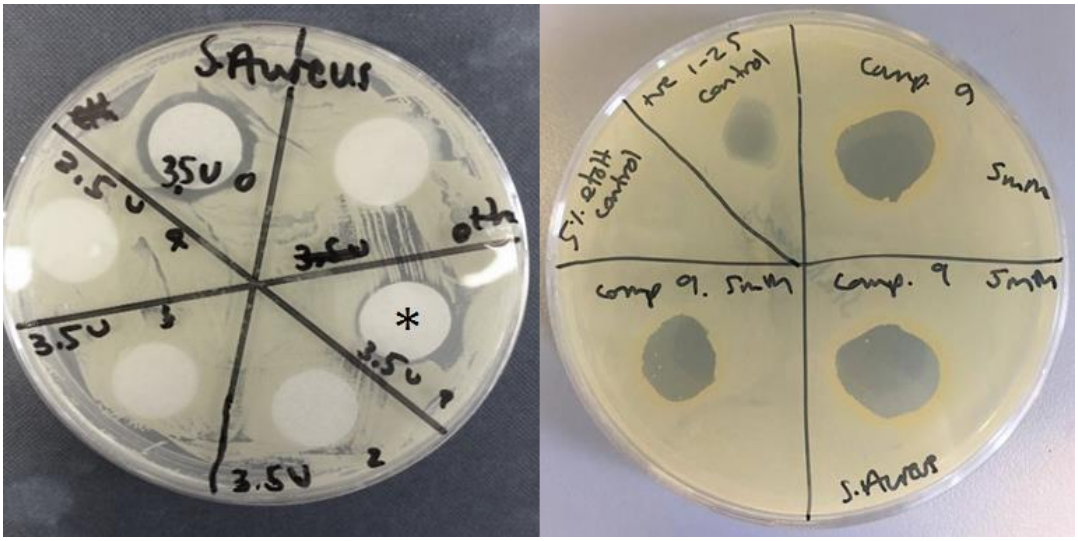

FIGURE 44 - RESULTS OF EXPERIMENT SHOWING FALSE NEGATIVES PRODUCED BY KIRBY BAUER DISC DIFFUSION TEST, THE COMPOUND MARKED WITH THE ASTERISK IS THE SAME COMPOUNDS THAT IS BEING DROP TESTED ON THE RIGHT-HAND PLATE. THE DISC ASSAY PRODUCED NEGLIGIBLE RESULTS, WHEREAS THE DROP TEST ASSAY SHOWED THAT THE COMPOUND WAS VERY EFFECTIVE.

1.8.1 Kirby Bauer Disc Diffusion

To perform this assay, an agar plate is inoculated with a standardised volume of bacterial strain, the bacteria is spread with a sterile bar, and the plate is left to dry in sterile conditions. Once the plate is dry, sterile discs of filter paper impregnated with the test compounds are placed onto the plate surface before the plate is incubated [48,49]. The zones of inhibition produced after incubation are measured and recorded.

1.8.2 Well Diffusion

To perform this assay, the molten agar is inoculated with a standardised volume of bacterial strain. The agar is then poured into a sterile petri dish. After the agar has set, a cutter is used to remove plugs of agar material to create wells. A standard volume of drug solution is added to each well, and the plate is incubated [50,51].

1.9 Development of New Screening Method

The propensity of current antibacterial testing methods to produce false negatives has led to a need for the development of a new screening procedure, taking and adapting methodology from existing assays. The drop test assay was produced, the sterile agar plate is inoculated with a standardised volume of bacterial strain, the bacteria is spread with a sterile bar, and the plate is left to dry in sterile conditions. After the plate has dried, a 10µl droplet of compound solution is administered to the plate using a micropipette or a Hamilton syringe. This assay eliminates the diffusion element of the standard antibacterial screens by placing the compound in direct contact with the bacterial lawn. The drawbacks of the assay are that it is very difficult to produce completely uniform repeatable droplets manually, this could lead to exaggerated antibacterial effects shown if the droplet spreads out too far during application.

1.10 The compounds

The compounds tested within this thesis belong to a family of novel supramolecular amphiphilic salts, first discussed by J. Hiscock *et al* in 2016 [52]. These salts consist of a hydrogen bond donating functionality, bookended either side by a lipophilic and a hydrophilic functionality. This is the part of the compound that provides the functionality. In addition to this structure, a countercation consisting of a tetraalkylammonium balances out the charge (Figure 15).

Urea Base

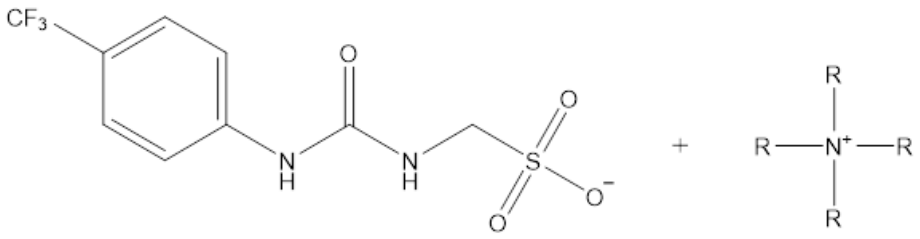

Thiourea Base

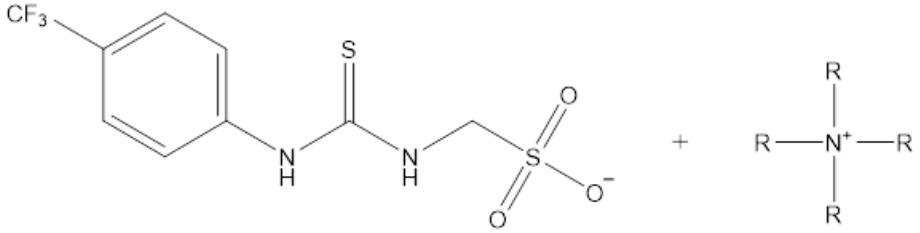

R- Groups

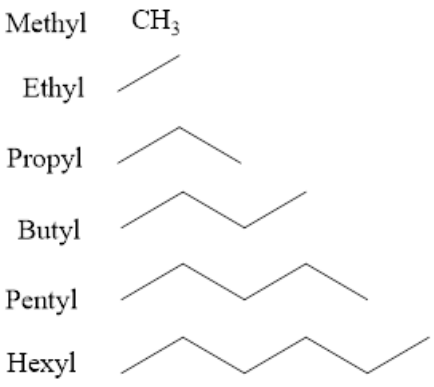

FIGURE 15 – STRUCTURE OF THE ANTIBACTERIAL COMPOUNDS TESTED WITHIN THIS THESIS

These compounds readily form and receive hydrogen bonds, allowing them to interact with each other. These interactions allow them to self-assemble, forming structures such as dimers, tapes, and two modes of stacking, *Anti* and *Syn.* (Figure 16) These binding modes cannot all exist at the same time, leading to a 'frustrated system'. The mode of binding that is exhibited by a system relies on the balance of all the other binding modes existing within the contained solvent system.

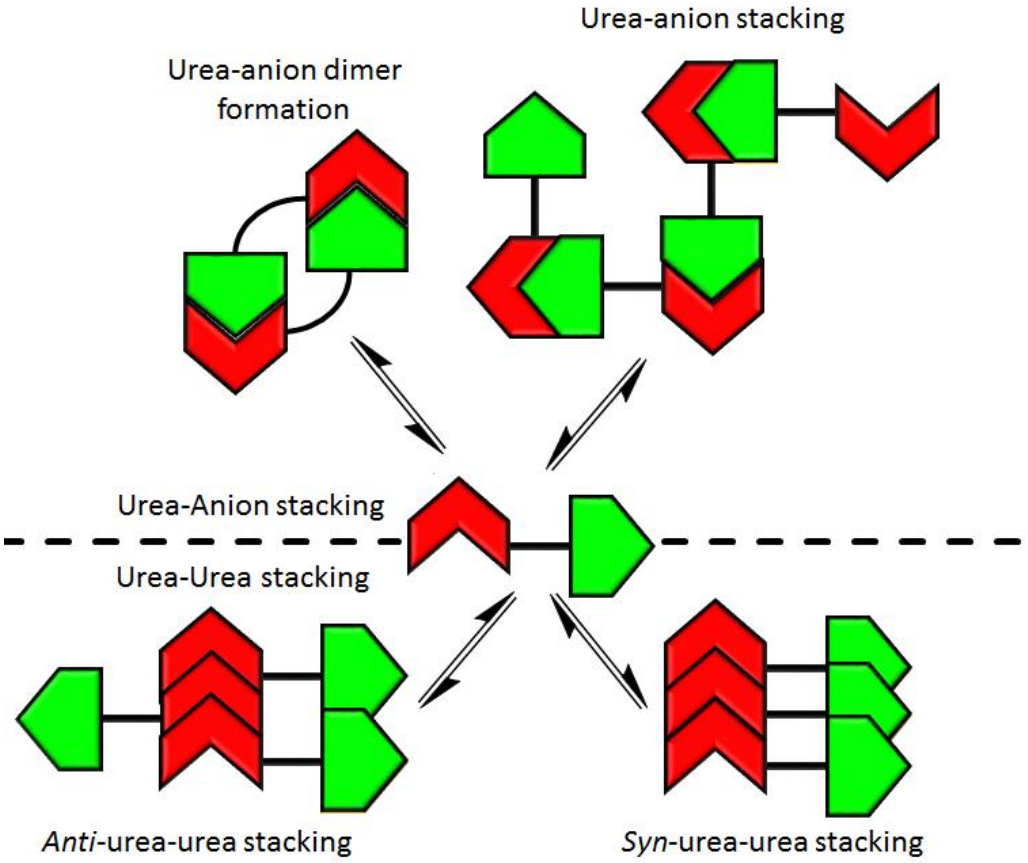

FIGURE 16 - DIGITAL RENDERING OF DIFFERENT BINDING MODES FORMED BY THE COMPOUNDS TESTED WITHIN THIS THESIS

1.11 Novel Amphiphillic Antibacterials

Amphiphilic compounds have been recently investigated as antibacterial agents with lower probability of placing selection pressures on bacteria, causing the development of resistance. Membrane-targeting antibacterials have this reduced probability, as it would require a multi-generational timeframe for bacteria to recalibrate their complete membrane structure [53].

In recent studies, amphiphillic compounds containing polar head groups and hydrophobic functionalities, have been investigated as novel antibacterials. Amphiphilic compounds are able to self-associate through stabilising supramolecular interactions; forming hydrogen bonds that link monomers into a nanostructure. Interactions between these amphiphilic compounds and bacterial cell membranes have been alluded to the interactions of membranes and surfactant detergents [54]. In polar solvents, these amphiphiles can self-associate to form micelles and bilayers. These aggregate structures have been proposed to interact with and disrupt cellular membranes, causing lysis, and eventually, complete cell death.

Recent studies have developed several different families of amphiphile based compounds that have been shown to interact with bacterial cell membranes and cause cell lysis [53–56]. These compounds are the closest in structure and theoretical action to the compounds tested within this thesis

1.13 MIC

The MIC of a compound is the Minimum Inhibitory Concentration. This refers to the percentage of bacterial growth that is susceptible to inhibition from the compounds [44]. This assay is considered the 'gold standard' of antibacterial susceptibility testing, and is used to confirm activity of novel compounds, especially when diffusion methods such as Kirby Bauer and Etesting aren't compatible with the mode of activity. The standard method of calculating the MIC of a compound is the broth microdilution method. The procedure for this assay involves placing serially diluted concentrations of the drug being tested into sterile tubes. The tubes are then inoculated with a set volumes of standardised bacterial suspension. These drug and bacterial suspensions are then used to inoculate fresh agar plates. The plates are then incubated overnight to promote bacterial lawn growth, and the MIC value of the compound is calculated from the plates on which the bacterial lawn has not grown [57]. There is also an assay for determining MIC by broth microdilution [58]. Whilst not a 'gold standard' of susceptibility testing, it is still widely used within microbiology. Using this method would overcome the diffusion issues posed by other methods, however, the newly developed plate reader assay has several advantages over it. These are time and the raw results produced. The broth dilution assay is incubated for 24 hours before the plates are examined, whereas the plate reader assay is run for a period of 15 hours, with most of the results being produced well before, and up to the 12-hour mark, making it twice as quick as the broth assay. The results produced by the plate reader assay can then be processed and plotted to form quantifiable graphs, whereas, the broth microdilution results are collected by looking at bacterial colony growth by eye, and no electronic data is produced.

2 Materials and Methods

2.1 Bacterial Cultures:

Cultures of *S. aureus* and *E. coli* were stored at -80 °C in glycerol. The freezer stocks of bacteria were prepared by adding 0.85 mL of bacterial culture to 0.15 mL of autoclave sterilised glycerol, to produce a final concentration of 15%. The culture and glycerol solution was then vortexed to produce an even mixture, before being transferred to a storage tube. The tube was then labelled and frozen in liquid nitrogen, and moved into -80 °C freezer for storage. Bacterial strains were streaked out onto fresh LB agar plates (5 g Yeast Extract, 10 g Tryptone, 10 g Sodium Chloride, 15g Agar, 1 L deionised water) in sterile conditions to isolate single colonies. Under sterile conditions, these colonies were picked with a sterile pipette tip, and transferred into a universal tube the bacteria cell cultures were then grown using standard lab protocols in 37°C incubators.

2.2 Testing methods:

The structure and composition of the compounds being tested gives rise to moieties that can donate and accept hydrogen bonds. This allows the compounds to form hydrogen bonds with itself, creating structures such as micelles, vesicles and tapes. This characteristic forming of hydrogen bonds means that the literature standard testing methods such as Kirby Bauer disc diffusion and well diffusion are not effective methods of screening the compounds referred to in this thesis. The Kirby Bauer and well tests use cellulose based filter papers and agarose agar respectively, and these two materials contain many hydrogen bond donating functionalities. The compounds aren't able to diffuse properly off the paper and through the agar, leading to an inaccurate result showing antibacterial activity. These false negative results lead to the development of a new assay, drop testing, and an automated way of carrying out the testing, the Rapid Antibacterial Susceptibility Screener – R.A.S.S.

2.3 Drop Test solution preparation:

The solution for the drop testing assay was prepared by dissolving a set mass of compound in 5% in either 2.5, 5 or 10ml of 5% ethanol solution (5ml ethanol and 95ml deionised water). The solutions were then vortex mixed to ensure the solid was dissolved and the vials were then Parafilmed® to prevent evaporation of the solution. It should be noted that neither the urea or the thiourea tetrapentylammonium compounds were able to dissolve in any of the biocompatible solutions tested.

2.4 Drop testing:

200µl of bacterial culture were pipetted onto a fresh agar plate, spread with a sterile glass spreader bar, and allowed to dry, as per the standard literature method. The compound solutions were then dropped onto the dry plate using a 50 µL Hamilton® syringe; needle size 22s ga (bevel tip), needle L 51 mm (2 in.) The plates were placed into an incubator and incubated at 37°C overnight to allow growth of the bacterial lawn, and theoretical antibacterial action of the compounds producing a zone of inhibition. After incubation, the size of the zone of inhibition is measured and recorded.

2.5 McFarland Standard Solution Preparation

The McFarland solutions (Figure 17) for calibration and standardisation of the spectrophotometers were prepared by adding volumes of 1% sulphuric acid to 1% barium chloride. (Table 1)

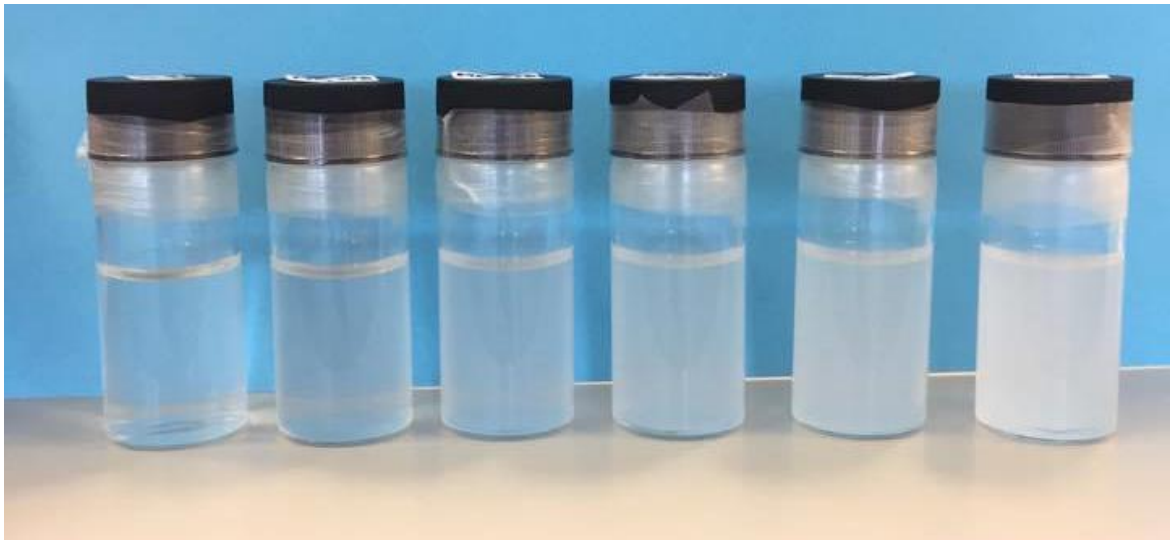

FIGURE 17 - SET OF SYNTHESISED MCFARLAND STANDARDS, SHOWING THE GRADIENT OF OPTICAL DENSITIES PRODUCED

McFarland Standard No.	**0.5**	**1**	**2**	**3**	**4**	**5**	**6**
1.0% Barium chloride (ml)	0.05	0.1	0.2	0.3	0.4	0.5	0.6
1.0% Sulphuric acid (ml)	9.95	9.9	9.8	9.7	9.6	9.5	9.4

TABLE 1 - MCFARLAND STANDARD DILUTION TABLE

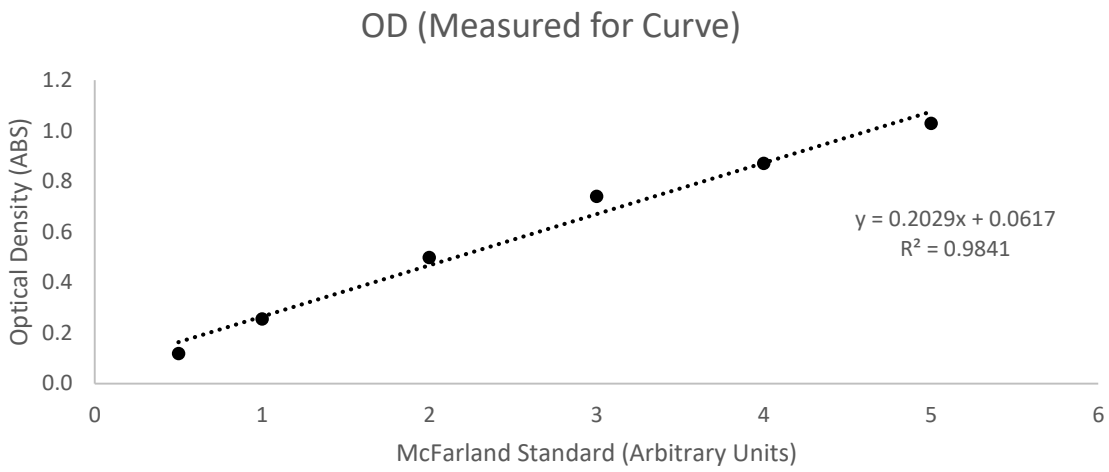

FIGURE 18 - GRAPH SHOWING THE MEASURED VALUES FOR THE MCFARLAND STANDARD SPECTROPHOTOMETER CALIBRATION ASSAY

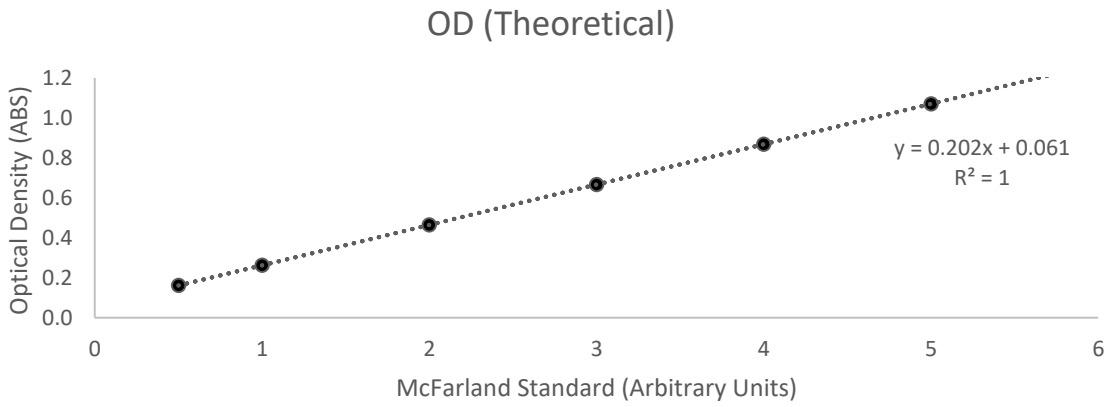

FIGURE 19 - GRAPH SHOWING THE THEORETICAL VALUES FOR THE MCFARLAND STANDARD SPECTROPHOTOMETER CALIBRATION ASSAY

The prepared McFarland Standards were scanned at 595nm on a spectrophotometer to produce calibration curves for the standardisation of the optical density of the bacterial suspension used in assays. (Figure 18-19)

2.6 MIC_{50} Assay – 96 well plates:

Bacteria was cultured in Luria Broth (LB) media and incubated at 37ºC until in mid-log phase. The culture was then diluted to an optical density of 0.75 ABS using a spectrophotometer calibrated using the McFarland standards. The MIC_{50} assay was

prepared by adding 50µl of the cell culture in media to each well of a sterile 96 well F-bottom Greiner UV-Star® plate using a HandyStep® Electronic Repeating Pipette. After the culture was added, 10µl of the drop test solutions were added to each well. (Figure 20) The plates were then Parafilmed® to prevent evaporation of the solution. The plates were then placed into the spectrophotometer (Thermo Scientific™, Multiskan™ GO Microplate Spectrophotometer), and optical density readings were taken at 595nm, at a time interval of 15 minutes, over a total time period of 16 hours.

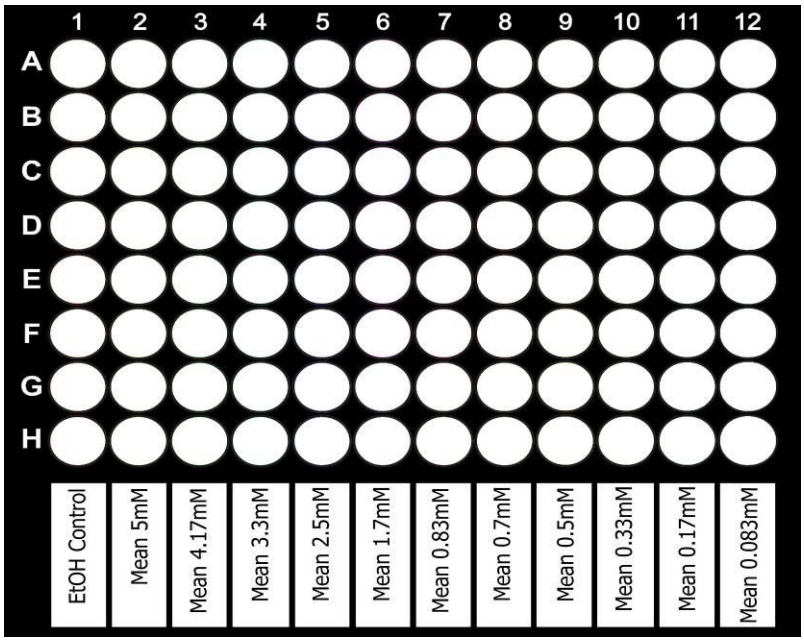

FIGURE 20 - 96 WELL PLATE LAYOUT USED FOR ASSAY.

2.7 Tetraalkylammonium activity screen

The tetraalkylammonium compounds were tested using exactly the same procedures as the MIC_{50} assay described above, using solutions of the four tetraalkylammonium hydroxide compounds

2.8 NMR Spectroscopy

The NMR spectroscopy for the compounds synthesised was carried out on a Jeol ECS-400 spectrometer. All chemical shifts were reported in parts per million (ppm), and the spectra were calibrated to the peak produced by a deuterated solvent (Deuterated solvents

purchased from Cambridge Isotope Laboratories Inc.). The spectra were analysed using ACD/NMR Processor Academic Edition. (Version 12.01)

2.9 3D Design of Robot Parts

The parts for the R.A.S.S. system were designed within Sketchup Make 2017 [59] (Version 17.2.2555 64-bit copyright Trimble Inc. 2016) using the 3D printing mm template. After a component was finished, is was exported from Sketchup as a Sterolithography file (.stl). The .stl file was then imported in CURA [60] (Version 2.3.1 Copyright Ultimaker B.V. 2017) and optimised for printing. Once the model had been sliced, checked and optimised in CURA, it was exported from the program as a G-Code file. The G-code file was then transferred to an SD card, which was then inserted into the 3D printer.

2.10 3D Printing and Assembly of Robot Parts

Once the SD card was inserted into the printer, the component file was selected in the on-board menu and the print was executed. All components were printed on an Ultimaker 2+ with a layer height of 0.1mm, a wall thickness of 1.0mm, a top and bottom wall thickness of 1.0mm, an infill density of 20%, a print speed of 60mm/s, a travel speed of 120mm/s, cooling enabled, the fan speed manually set to 75%, and a build plate adhesion skirt printed to secure the model. The plastic used was RS Pro black PLA 1.75mm, purchased from RS components. The cage assembly was constructed from lengths of RS Pro Aluminium Alloy Strut 20 x 20, 5mm Groove (4x500mm and 8x200mm), fastened together with Countersunk Head Machine Screws, M5 x 40mm, Bright Zinc Plated, Clear Passivated Steel. Loctite universal superglue was used to weld components together.

2.11 Incorporation of Lego Parts

The actuator and motor components are manufactured by The Lego Group, the linear actuator (Part number 61927c01) was sunk into the syringe block and glued into place, with a Mindstorms NXT motor (Part number 53787) glued into place on the bottom of the stage and coupled up to the actuator. A small LEGO Technics rail was glued to the top of the

stage assembly and a medium Mindstorms EV3 motor (Part number 99455) was attached to it. This motor was coupled to a LEGO Technic 24 tooth gear wheel (Part number 24505). This tooth gear was coupled to the 3D printer tooth rail part of the lowering mechanism assembly. The lowering and syringe drop mechanism was then attached to a frame consisting of two T-profile geared rails and endcaps. This whole assembly was attached to the X-Movement structure via two geared interfaces (consisting of a large EV3 motor – Part number 95658, and two more 24 tooth gear wheels joined by a LEGO Technic axle), this created the Y-Movement assembly. The X-Movement structure was powered by two more Mindstorms NXT motors. The wiring was constructed by taking the stock LEGO Mindstorms connector cables (Part number bb601), stripping them to expose the 6 core wires, and extending the wires by splicing in lengths of Ethernet cable core, this allowed the wires to reach from the Mindstorms controller bricks to the far end of the robot's metal frame. (Figure 21)

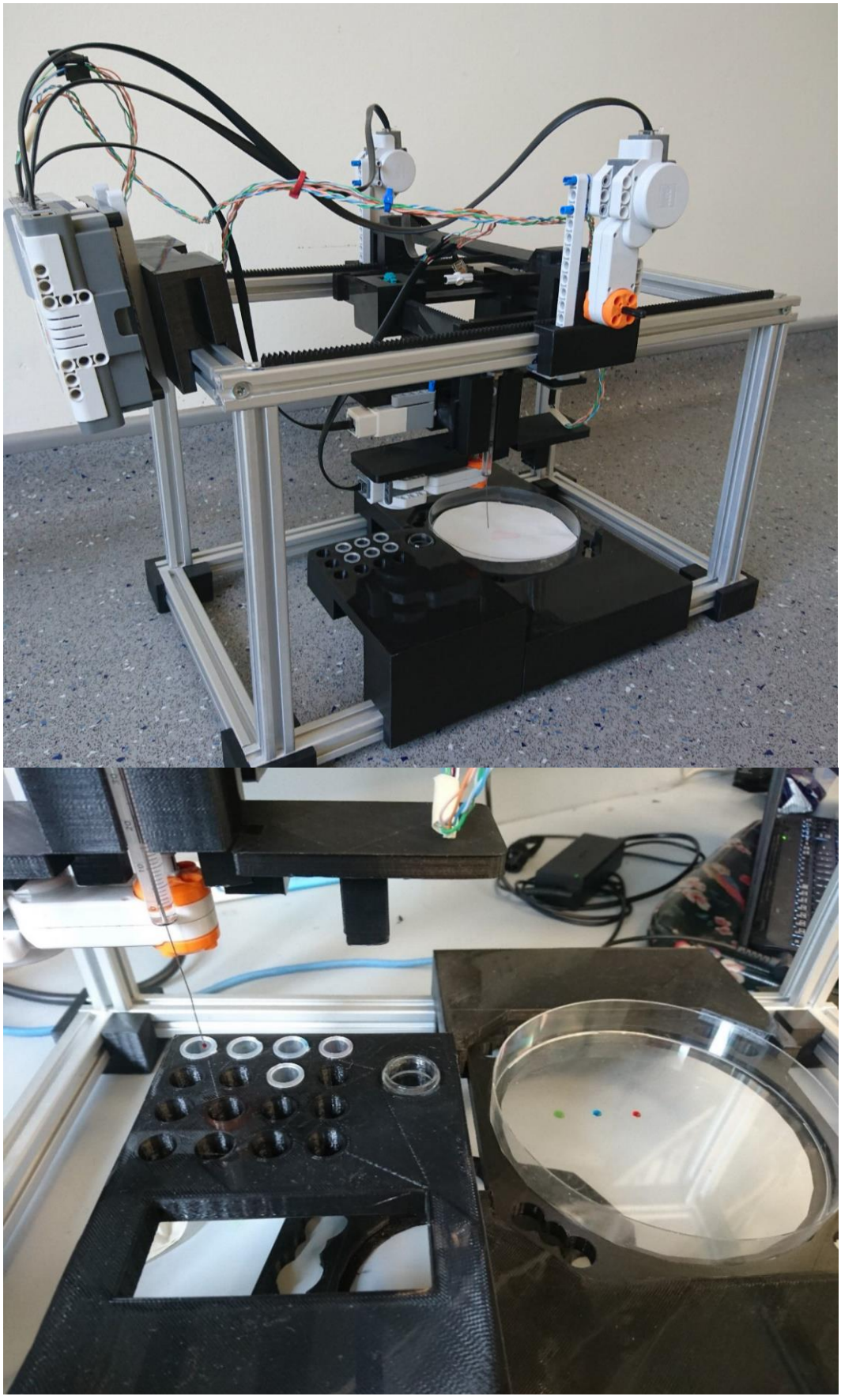

FIGURE 21 - THE R.A.S.S. SYSTEM

2.12 Robot Code

The program for the robotic testing system was executed by two LEGO Mindstorms controller bricks, one NXT and one EV3 (Part numbers 9841 and 45500). The EV3 brick controlled the Y movement, the stage lowering, and the syringe plunger actuator. The NXT brick controlled the X movement of the whole assembly.

The program was written in the LEGO Mindstorms EV3 home edition [61](Version 1.2.2 Build 20161007.4 Copyright The Lego Group 2013) with one file containing the program for controlling the X movement loaded onto the NXT brick, and another file containing the program for controlling all of the other processes. The problem faced with these two programs was that since the NXT brick is from a previous generation of hardware, the EV3 brick wasn't able to communicate with it. This lead to the two separate programs being developed, with the process commands separated by time delay buffers. This allowed both programs to be executed without interfering with each other and causing damage to the dropping mechanism, as failed programs bent the dropping needle by starting the X movement whilst it was still sunk into a well.

2.13 Setting up the Sampling Rack and Loading a Plate

The sample rack attached to the frame of the robot is loaded with 15 samples and an ethanol wash. The liquids were contained within 2.0ml Eppendorf tubes, with the ethanol tube loaded into the (1,1) co-ordinate of the rack, as that is where the needle assembly will home to at the end of each drop cycle. A squat glass vial is loaded into the waste disposal section of the sample rack. The plate stage interface has 3 interchangeable plate caddies, fitting standard 95mm petri dishes, large diameter 200mm petri dishes, and 96 well plates.

2.14 Pyridinium Salt

4-(Trifluoromethyl) phenyl isocyanate (0.268g) was added to a stirring solution of aminomethanesulfonic acid (0.416) in anhydrous pyridine (15 mL) under an inert

atmosphere. The mixture was heated to 60 °C for four hours. The pyridine was then removed by filtration. Yield: 0.378g (55%)

2.15 Tetrapentylammonium Salt

Solution of tetrapentylammonium hydroxide (1.8ml) was added dropwise to pyridinium Salt (0.360 g) in chloroform (10 mL) and washed with water (50 mL). The organic fraction was then taken to dryness to give the pure product as a white solid. Yield: 0.276g (76%)

2.16 Tetrahexylammonium Salt

Solution of tetrapentylammonium hydroxide (1.9ml) was added dropwise to pyridinium Salt (0.360 g) in chloroform (10 mL) and washed with water (50 mL). The organic fraction was then taken to dryness to give the pure product as an oil. Yield: 0.257g (71%)

2.17 Analysis of False Negative Disc Assay Results

The Kirby Bauer disc diffusion assay was not used for the compounds tested in this thesis. A third year project student performed an analysis of the assay, measuring the diffusion of the compound off of the filter paper discs. The results obtained show the hydrogen bonding association between the paper discs and the compounds has an adverse effect on the ability of the compounds to diffuse off of them and cause zones of inhibition, needing a greater concentration of compound contained within the disc to produce the zone of inhibition that would be observed with a lower concentration without the disc hindrance. This leads to false negative results when performing the assay.

These false negatives were the reason that the drop testing assay was developed, removing the need for the filter paper interface, and therefore removing the diffusion hindrance. This allowed the compounds to be applied directly to the bacterial lawn, allowing the potential antibacterial effect to be observed more accurately. (Research Credit to Tom Runacres)

2.18 Validation of growth curve assay with clinically available antibacterials

MIC values of compounds were calculated using the growth curve assay developed during this project. This assay measured the optical density of bacterial suspensions contained within sterile 96 well plates every 15 minutes for a total of 17 hours. Each numerical column on the plate was a series of 8 repeats of varying concentrations of the compound being tested. After the data was collected, it was copied into a spreadsheet that split the concentration repeats, plotting them into 12 separate graphs. This allowed the data to be analysed and outliers to be removed. The remaining data was then averaged and the final growth curve could be plotted. The endpoint optical densities were then taken from the time of 15 hours (900 mins).

The assay described above for calculating the MIC_{50} values of antibacterials was validated by another Masters project student within the group, performing it with commercially

available drugs, and comparing the resultant values with literature values. The antibacterials used were Ampicillin and Vancomycin, and as with the novel compound testing, the bacteria used were *S. aureus* and *E. coli*. Exactly the same procedure was used on the established antibacterials, and the novel compounds. All solutions were dissolved within 5% ethanol.

The MIC_{50} values of vancomycin were calculated against *S. aureus* in stationary growth phase at the seven hour (420 min) (Figure 22) This is where the compound exhibited its antibacterial activity. Using the growth curve assay the MIC_{50} value of Vancomycin was calculated to be around 0.99 µg/ml which is in between the literature values of 0.5-2.0 µg/ml. (Research Credit Laura Blackholly)

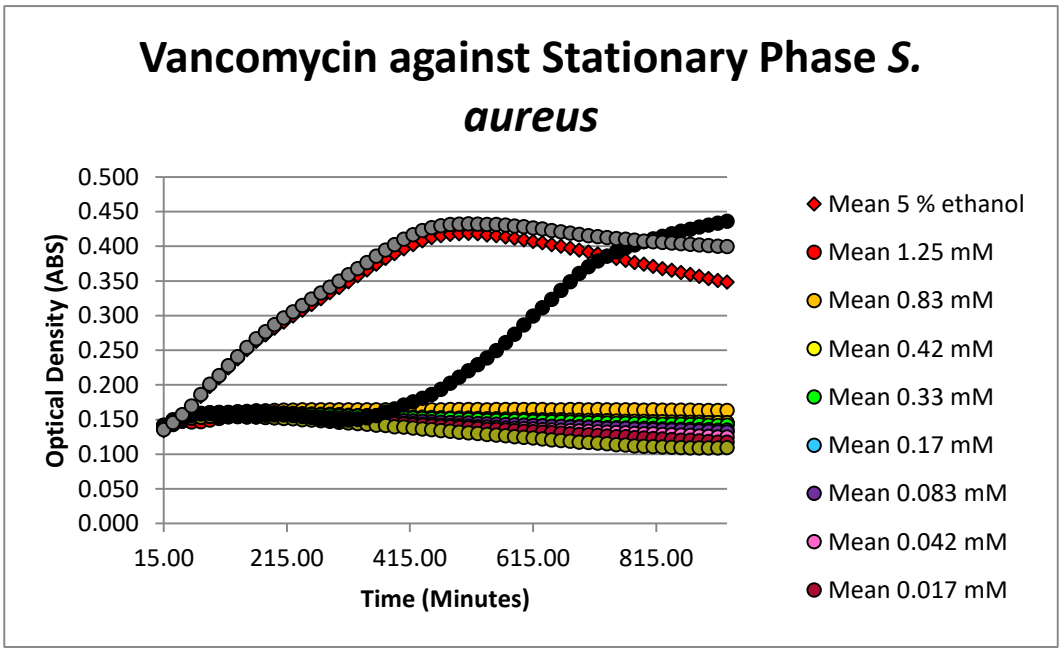

FIGURE 5 - GROWTH CURVE VALIDATION ASSAY WITH VANCOMYCIN

3 Results

3.1 ^{1}H NMR spectrum of Tetrapentylammonium Compound

Once the tetrapentylammonium compound was synthesised, it was dried and analysed by NMR spectroscopy. This analysis produced the spectrum visible below, showing the compound was present, clean and in the correct ratios.

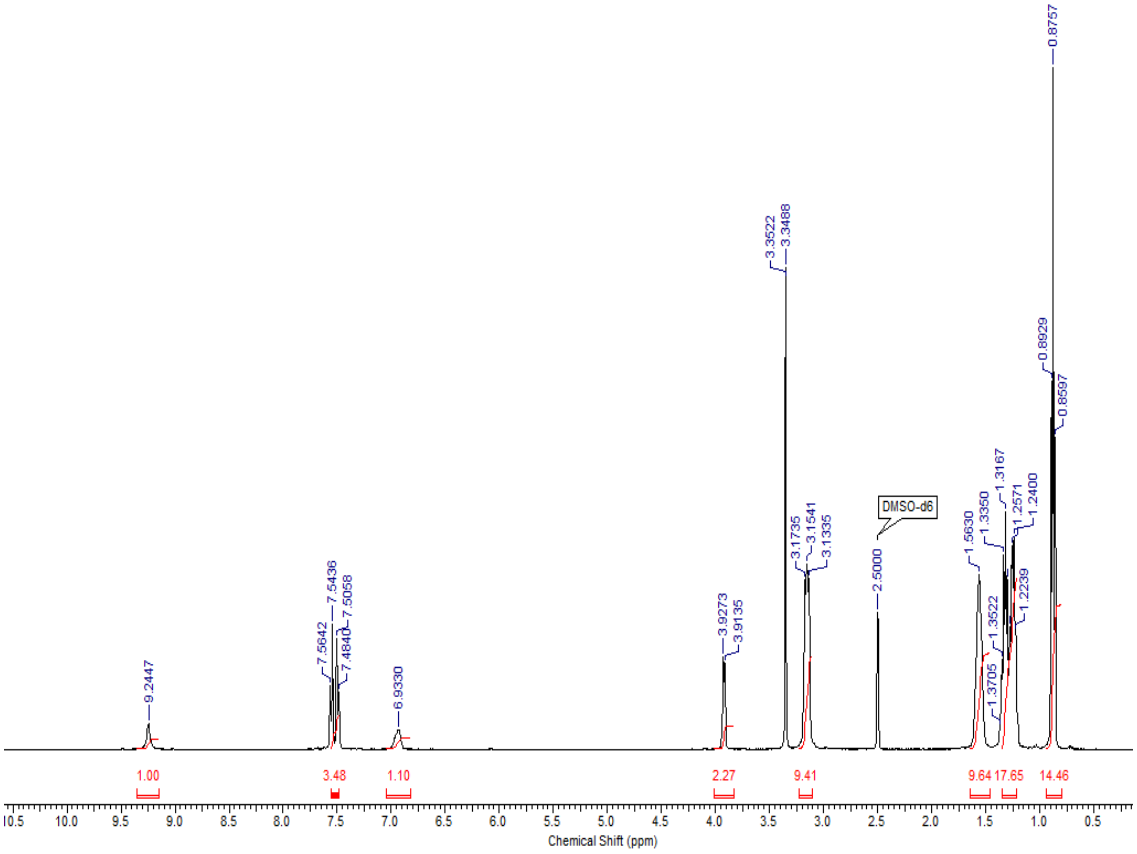

Full characterisation data for this compound are located on the appendix of this thesis.

3.2 ^{1}H NMR spectrum of Tetrahexylammonium Compound

Once the tetrapentylammonium compound was synthesised, it was dried and analysed by NMR spectroscopy. This analysis produced the spectrum visible below, showing the compound was present, clean and in the correct ratios.

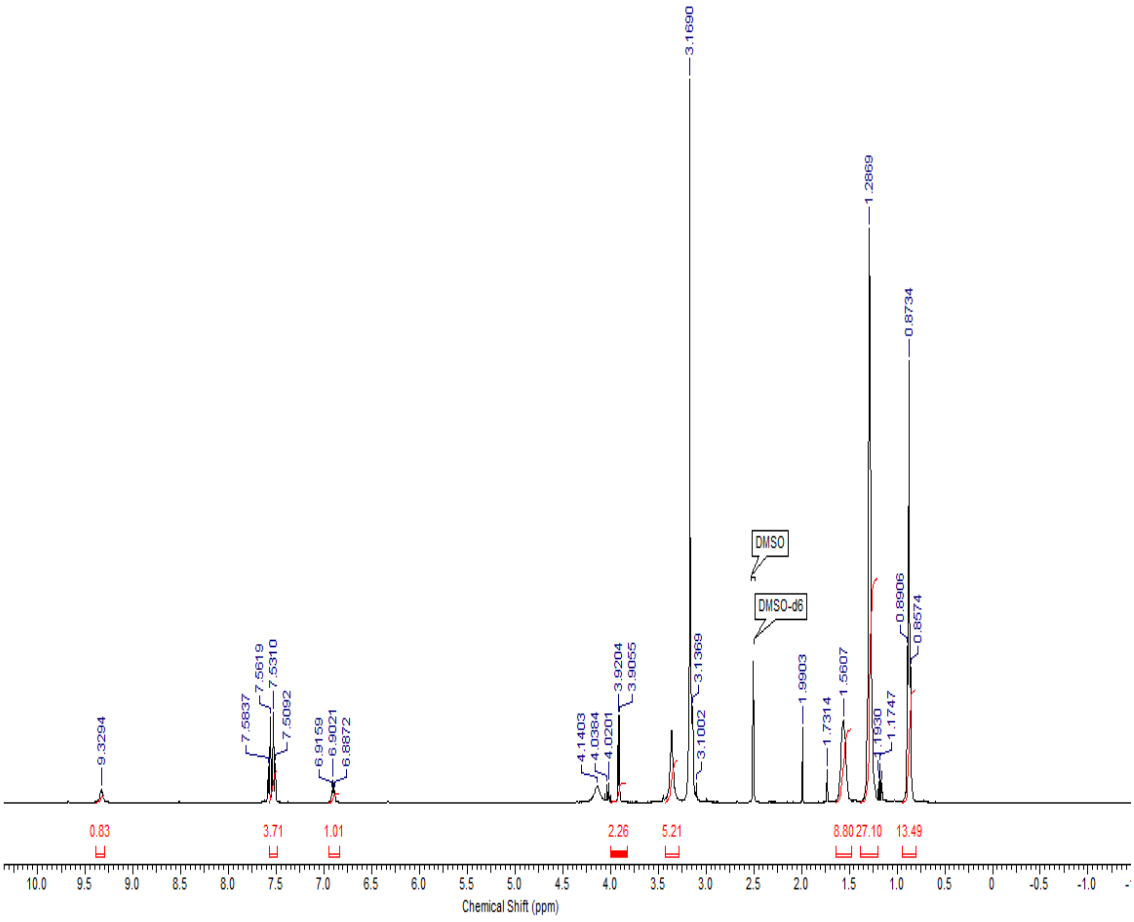

Full characterisation data for this compound are located on the appendix of this thesis.

3.3 MIC_{50} Assay Results

All of the MIC_{50} results were collected and analysed within a Microsoft Excel worksheet, this produced the raw growth curve graphs (These are the coloured graphs). The endpoint optical densities at 900 minutes were then taken for each concentration of compound and entered into Origin. These values were then plotted and fitted (These are the red-lined graphs). The data for the compounds producing antimicrobial effects against Gram-Positive bacteria were fitted with sigmoidal curves, with the cutoff in the graph giving the MIC_{50} values. The data for the compounds producing antimicrobial effects against Gram-Negative bacteria were fitted with linear curves, with the midpoint of the graph giving the MIC_{50} values.

The MIC values calculated from these datasets was collated, producing the table at the end of this section

The compounds were assayed against bacteria in different phases of growth, logarithmic (log) and stationary. During log phase the bacteria are rapidly reproducing, so the population exponentially increases, and during stationary phase, the growth rate of the bacteria levels out, producing a stable population. In addition to this, the morphology of the cell wall changes, so testing during this phase is needed, as the results will be different to those of the log phase tests.

3.3.1 Urea Based compound family with Log *S. aureus*

These compounds were found to be the most effective against the Gram-positive *S. aureus* bacteria, with all variants tested producing results. All of the Origin plots showed sigmoidal fits.

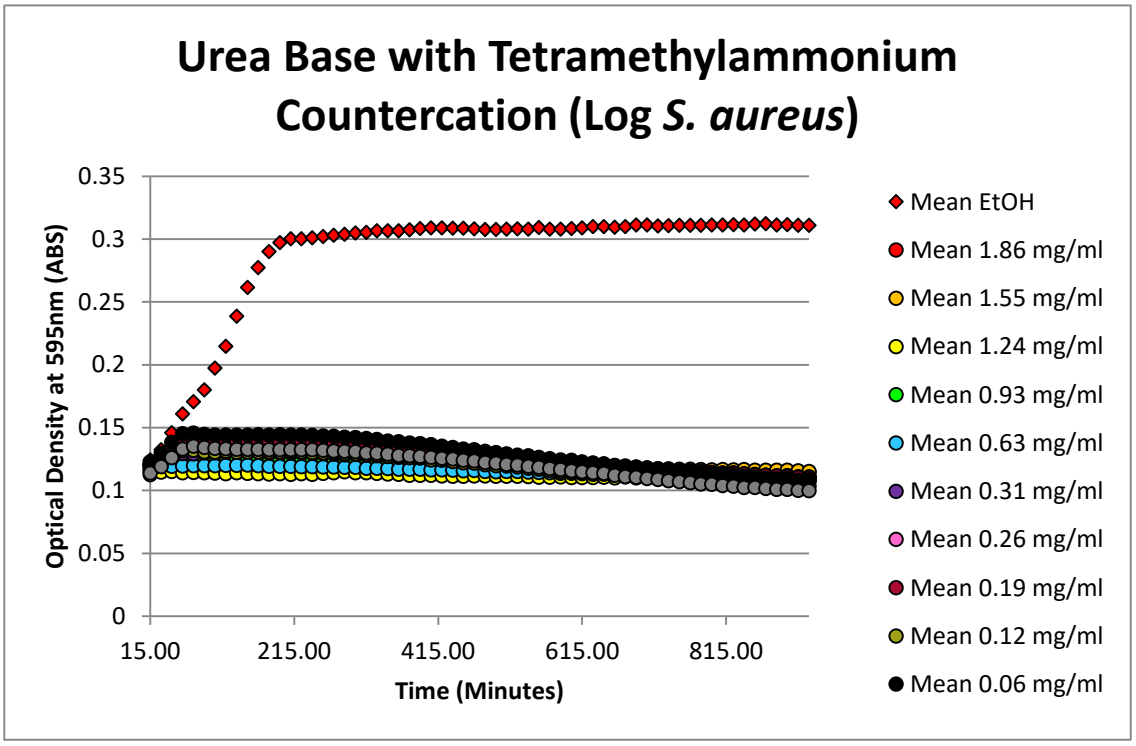

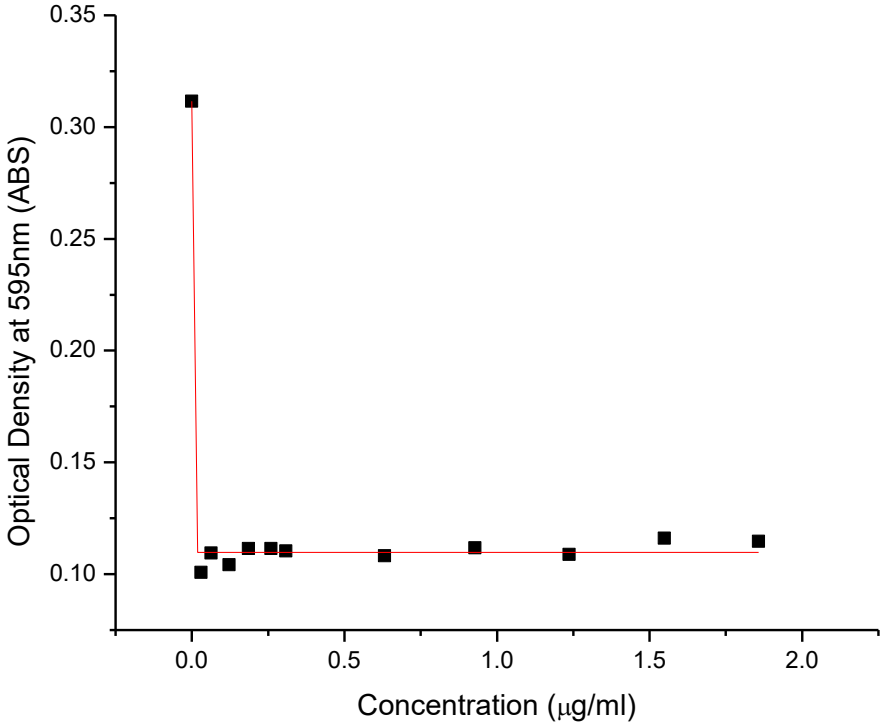

FIGURE 23 – GROWTH CURVE AND ORIGIN MIC PLOT FOR UREA BASED TETRAMETHYLAMMONIUM COMPOUND AGAINST LOG *S. AUREUS*

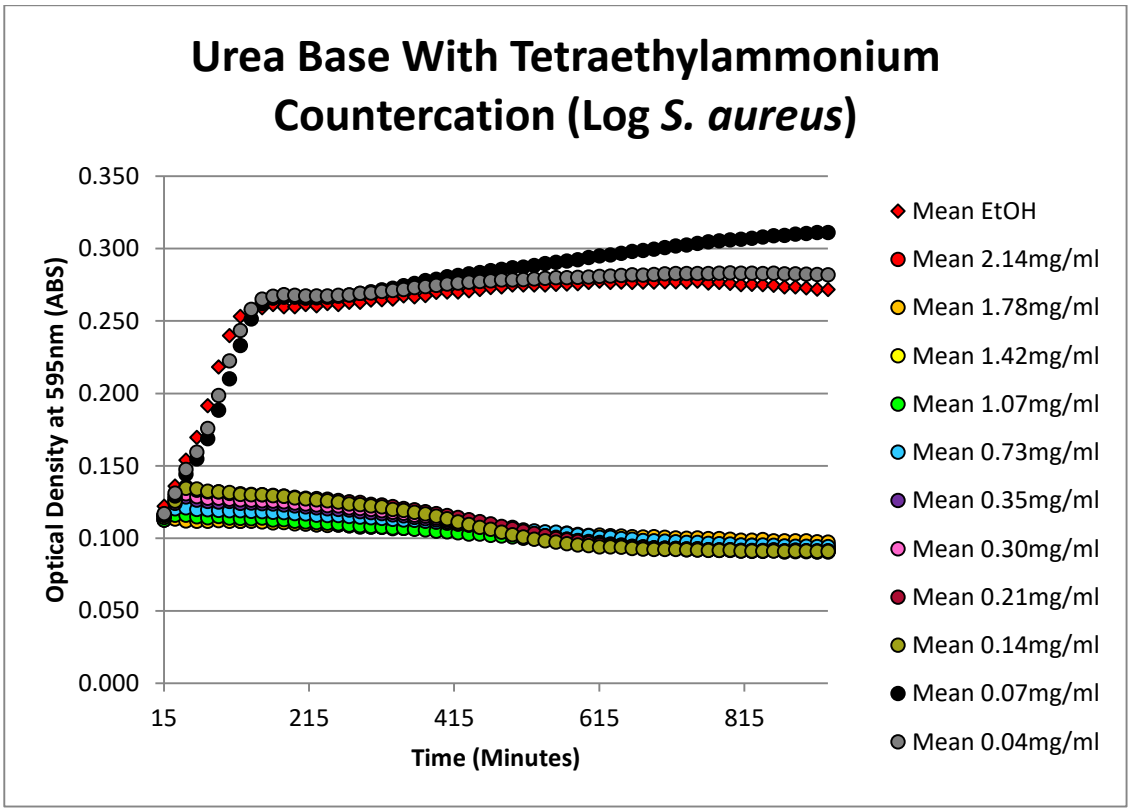

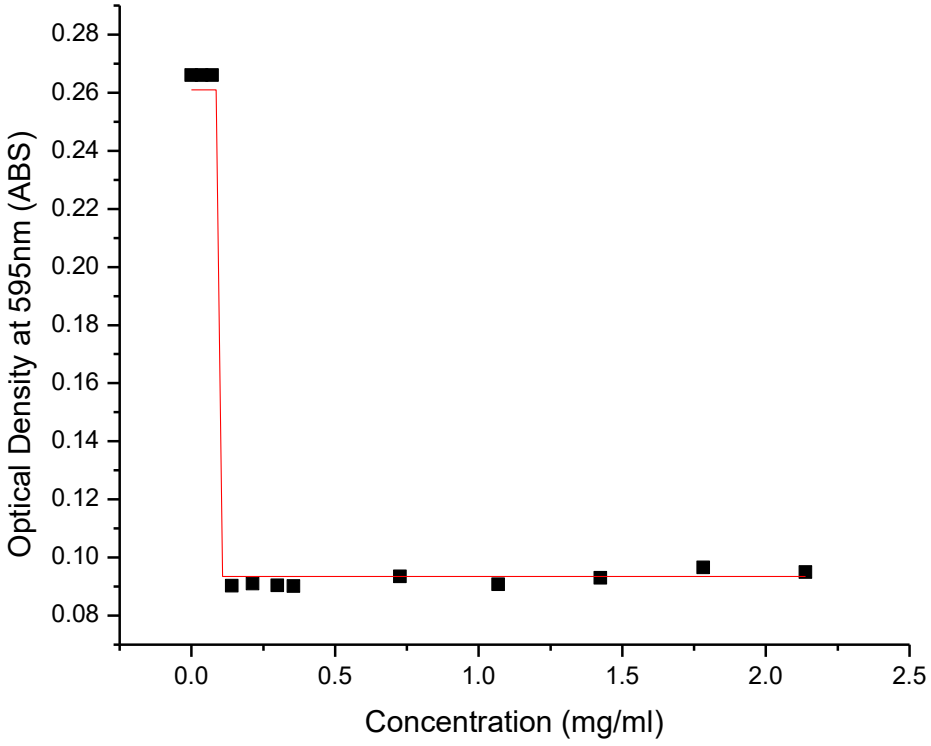

FIGURE 24 - GROWTH CURVE AND ORIGIN MIC PLOT FOR UREA BASED TETRAETHYLAMMONIUM COMPOUND AGAINST LOG *S. AUREUS*

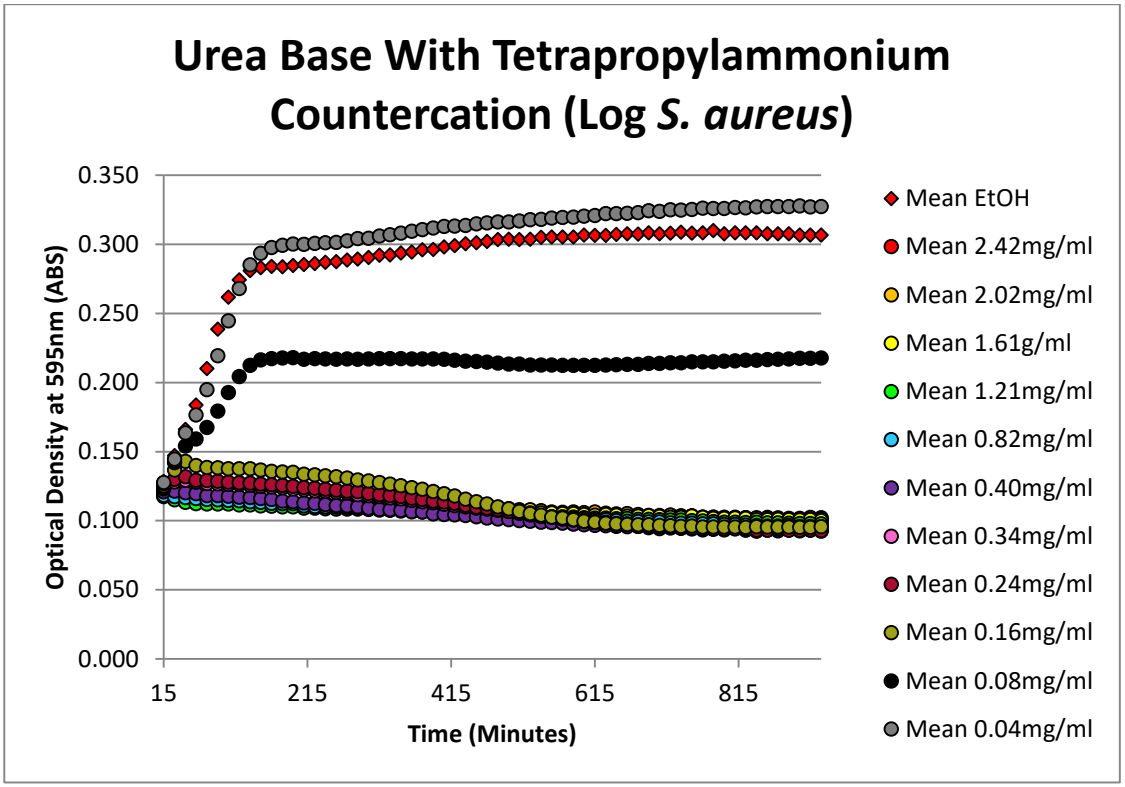

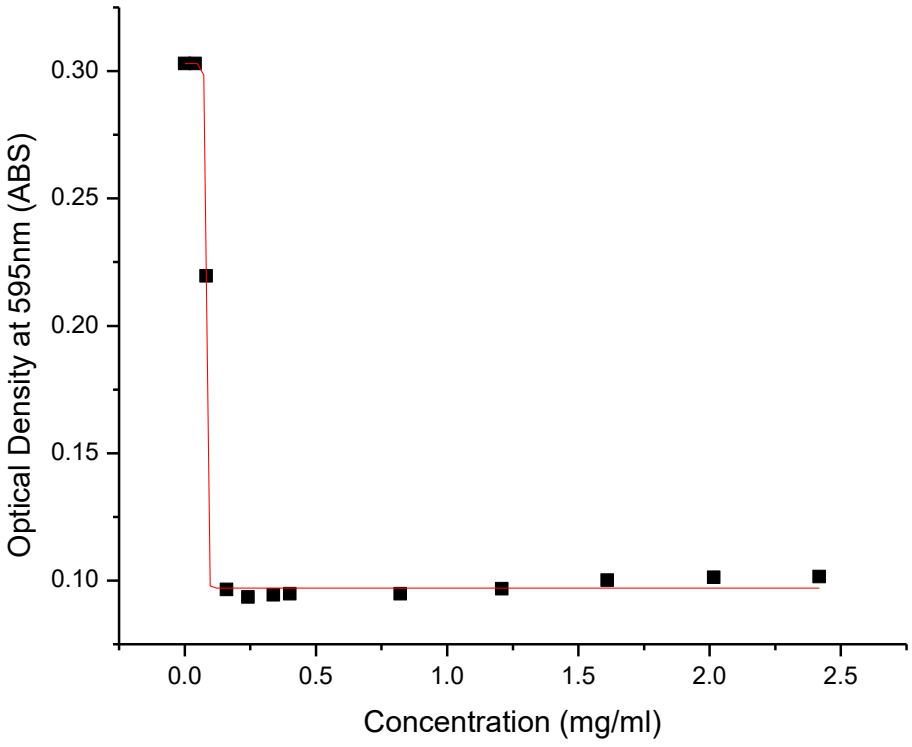

FIGURE 25 - GROWTH CURVE AND ORIGIN MIC PLOT FOR UREA BASED TETRAPROPYLAMMONIUM COMPOUND AGAINST LOG *S. AUREUS*

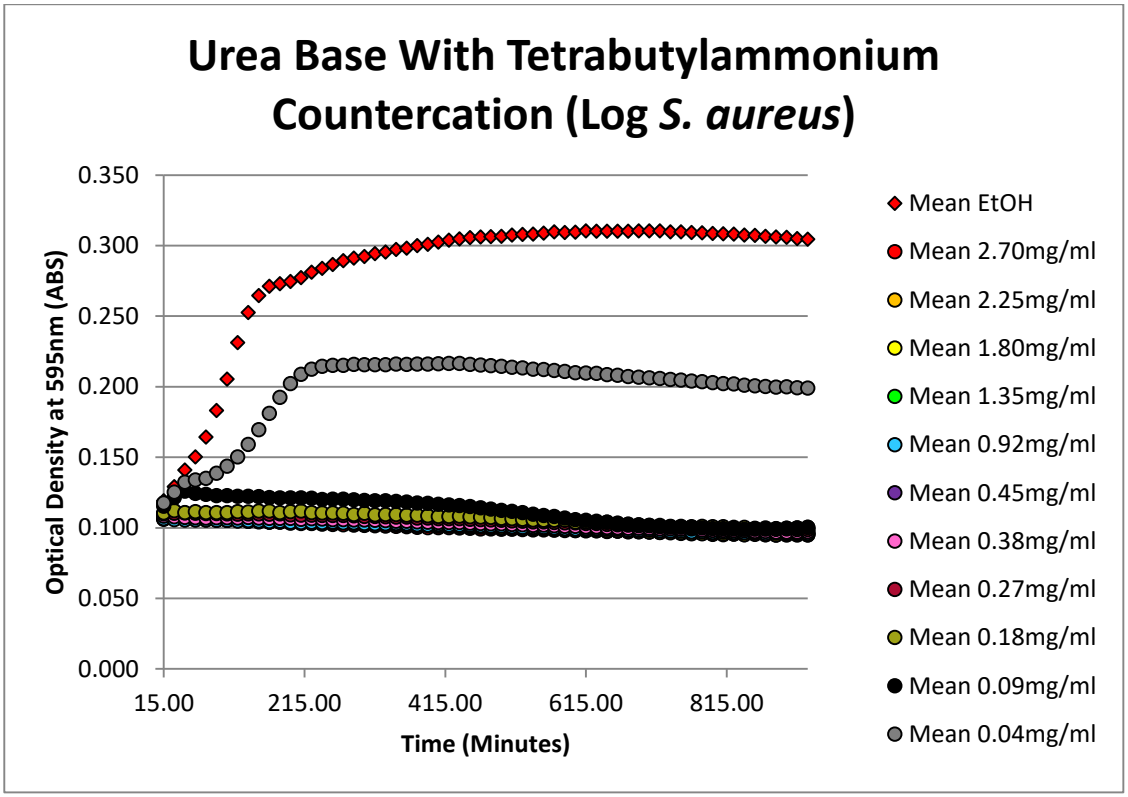

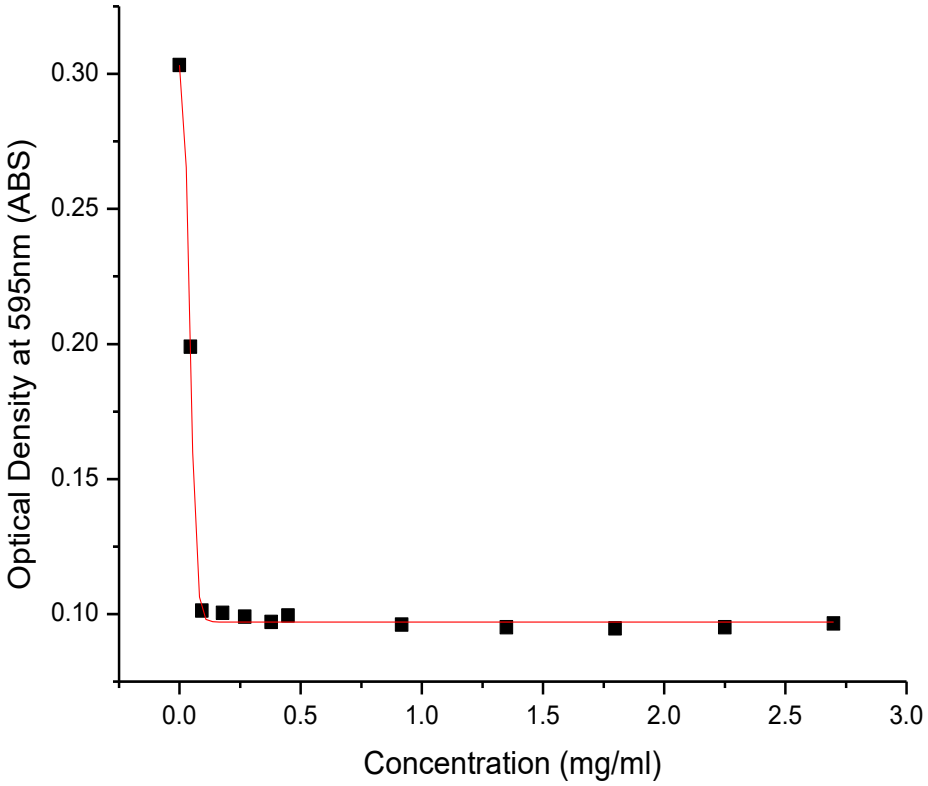

FIGURE 26 - GROWTH CURVE AND ORIGIN MIC PLOT FOR UREA BASED TETRABUTYLAMMONIUM COMPOUND AGAINST LOG *S. AUREUS*

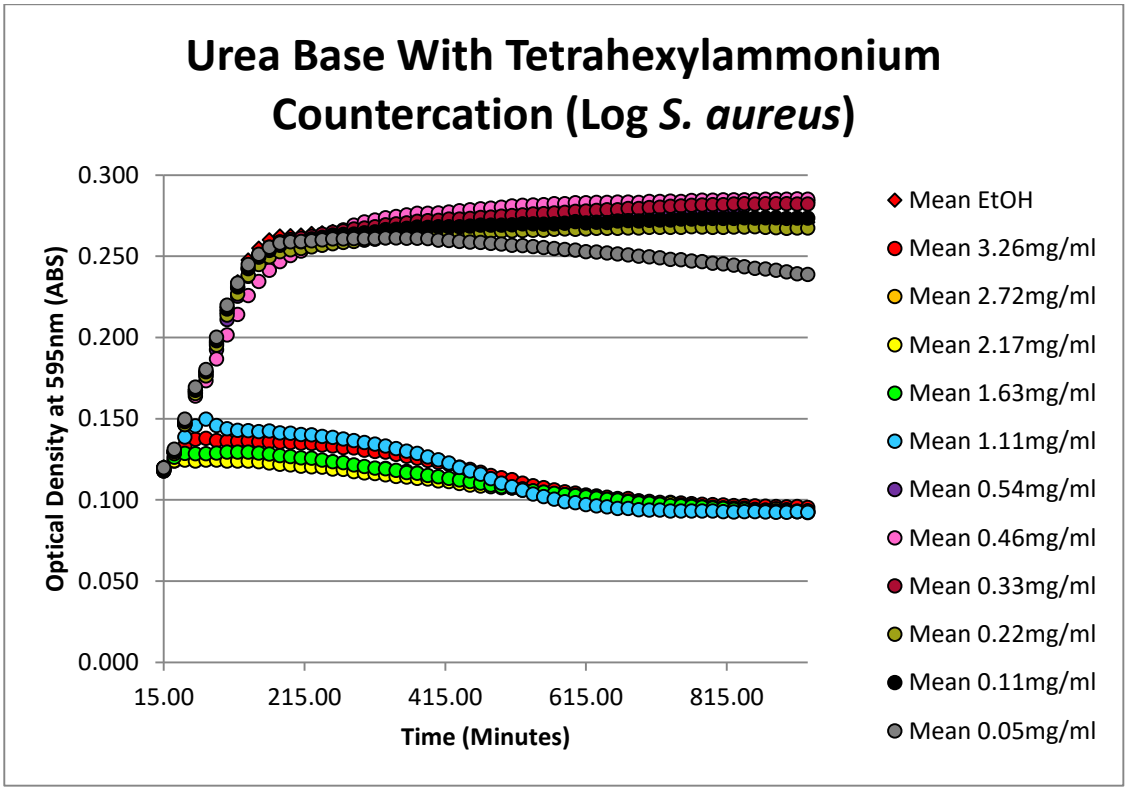

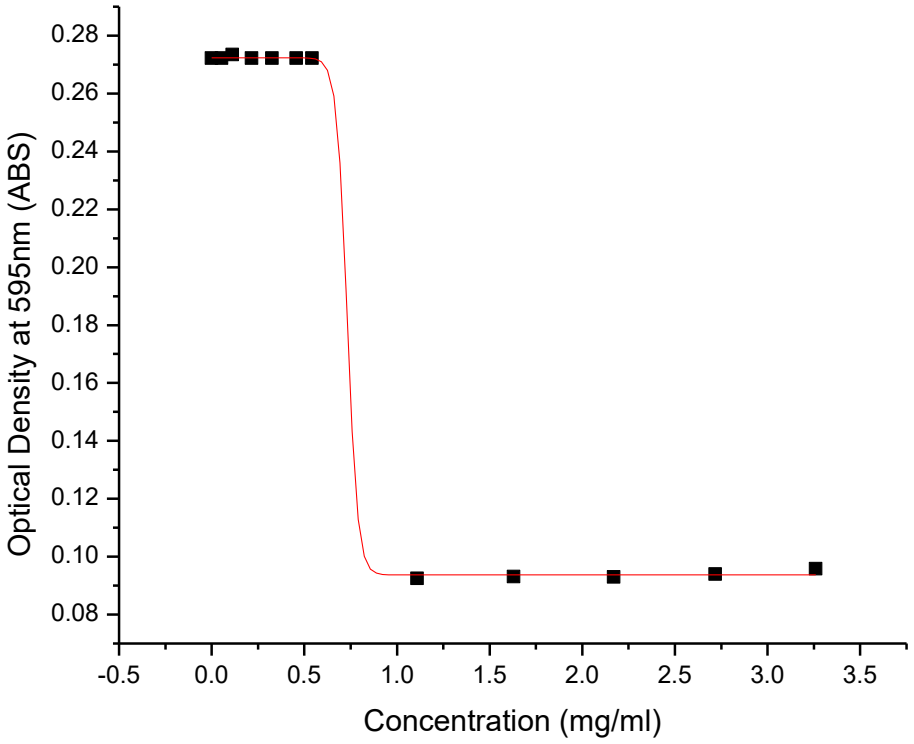

FIGURE 27 - GROWTH CURVE AND ORIGIN MIC PLOT FOR UREA BASED TETRAHEXYLAMMONIUM COMPOUND AGAINST LOG *S. AUREUS*

3.3.2 Thiourea Based compound family with Log *S. aureus*

These compounds were found to be ineffective against the Gram-positive *S. aureus* bacteria, with only the tetrabutylammonium variant tested producing a result. The Origin plot showed a sigmoidal fit.

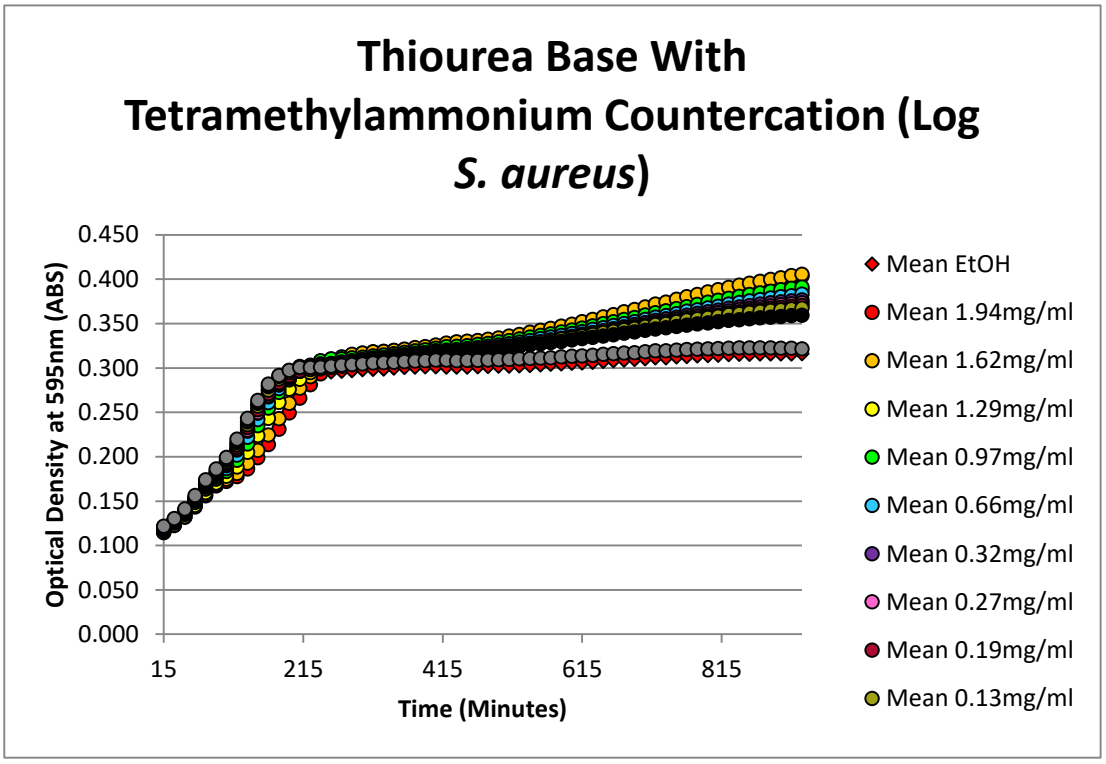

FIGURE 28 - GROWTH CURVE FOR THIOUREA BASED TETRAMETHYLAMMONIUM COMPOUND AGAINST LOG *S. AUREUS*

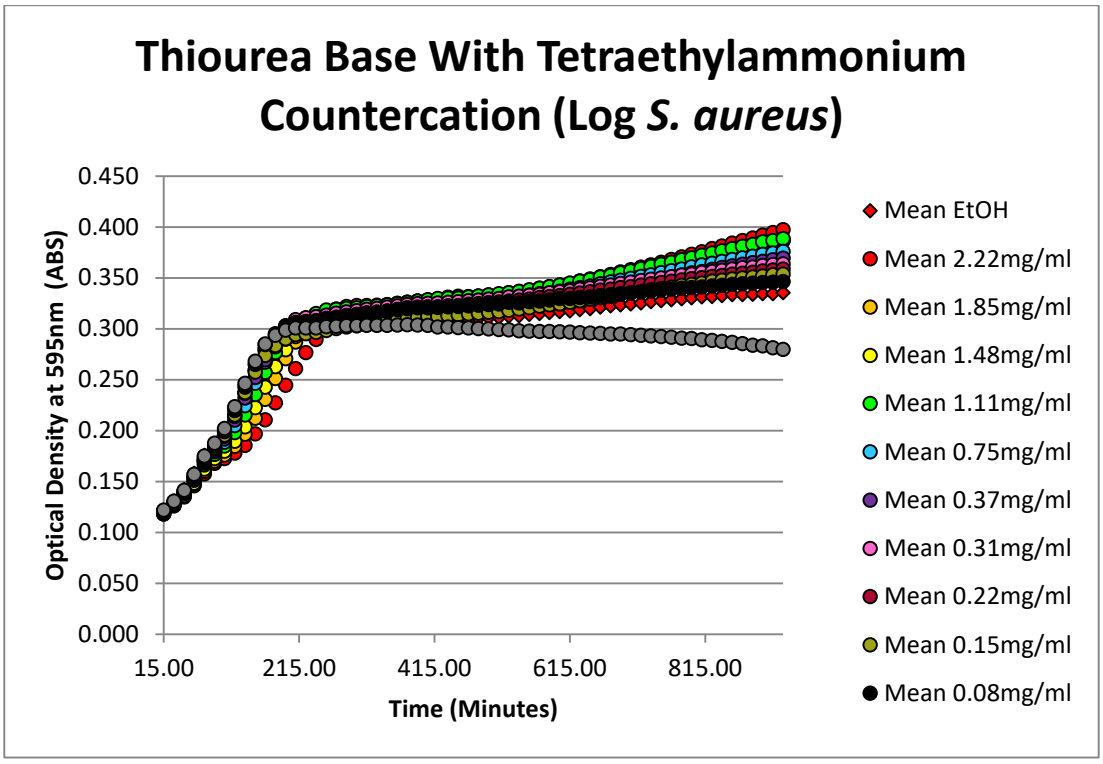

FIGURE 29 - GROWTH CURVE FOR THIOUREA BASED TETRAETHYLAMMONIUM COMPOUND AGAINST LOG *S. AUREUS*

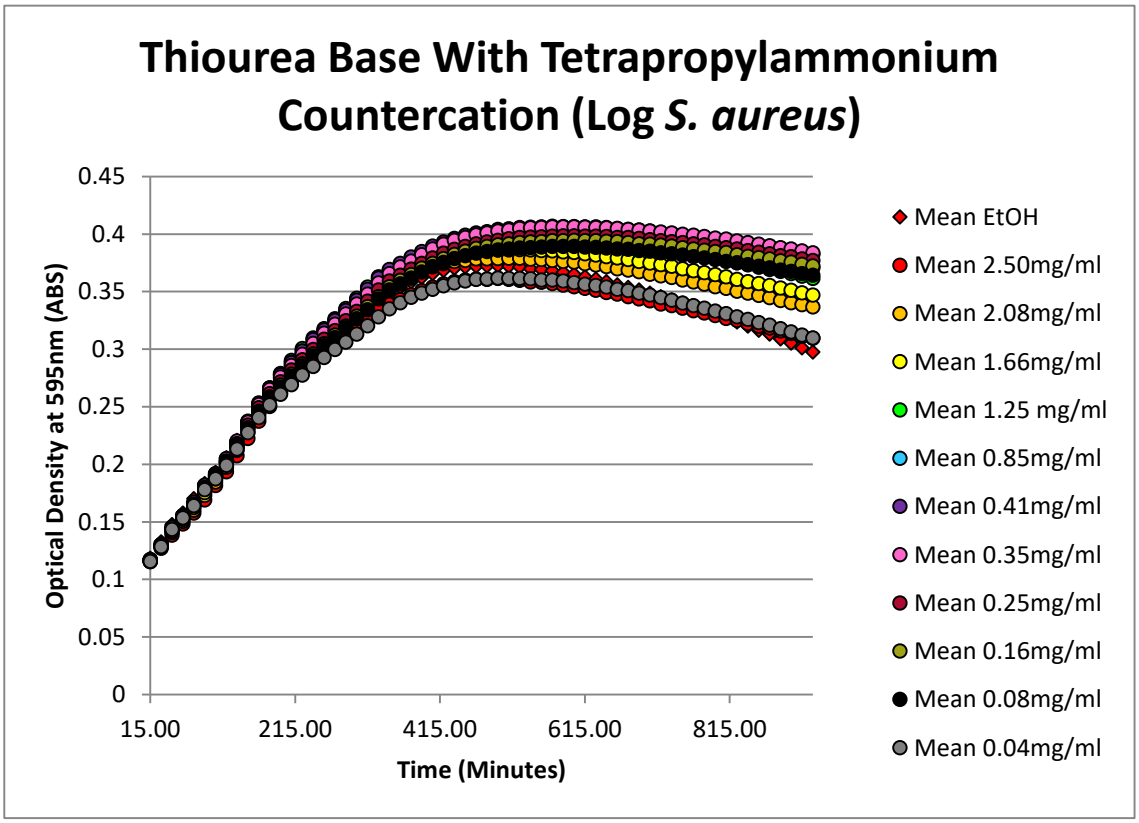

FIGURE 30 - GROWTH CURVE FOR THIOUREA BASED TETRAPROPYLAMMONIUM COMPOUND AGAINST LOG *S. AUREUS*

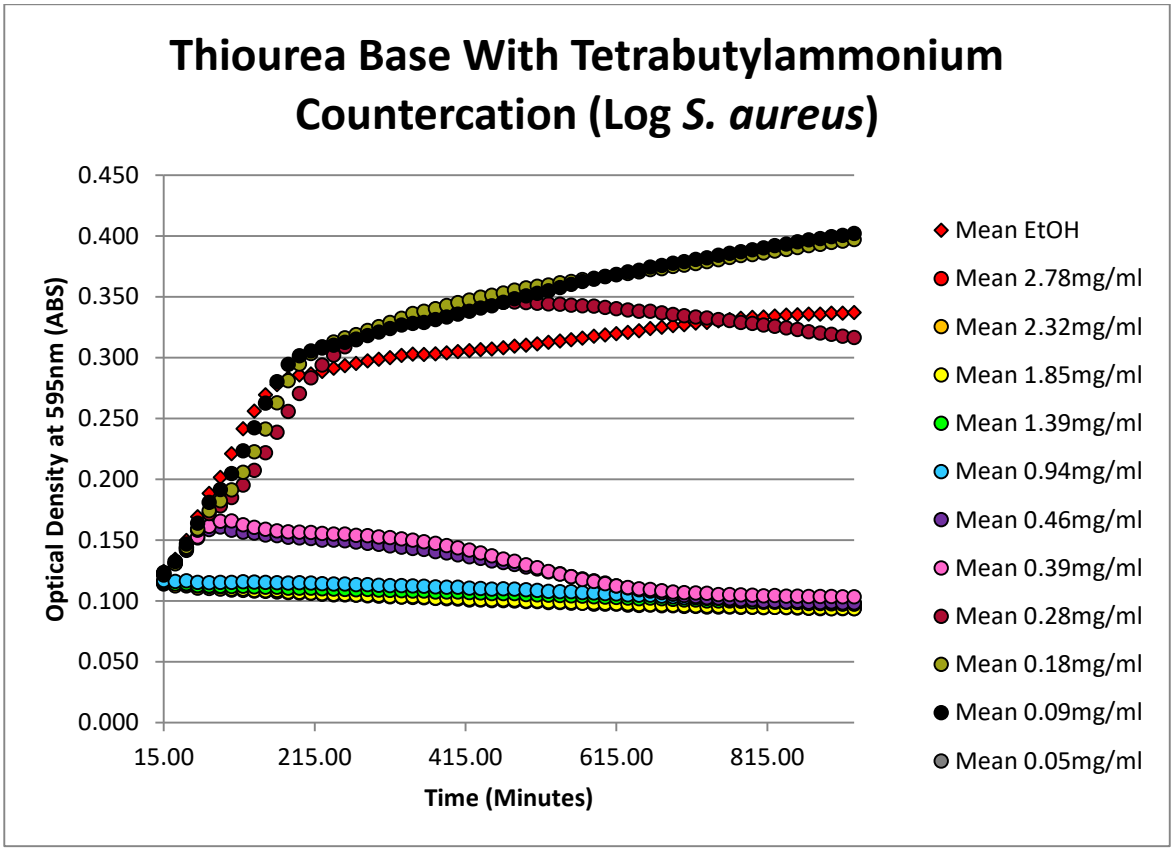

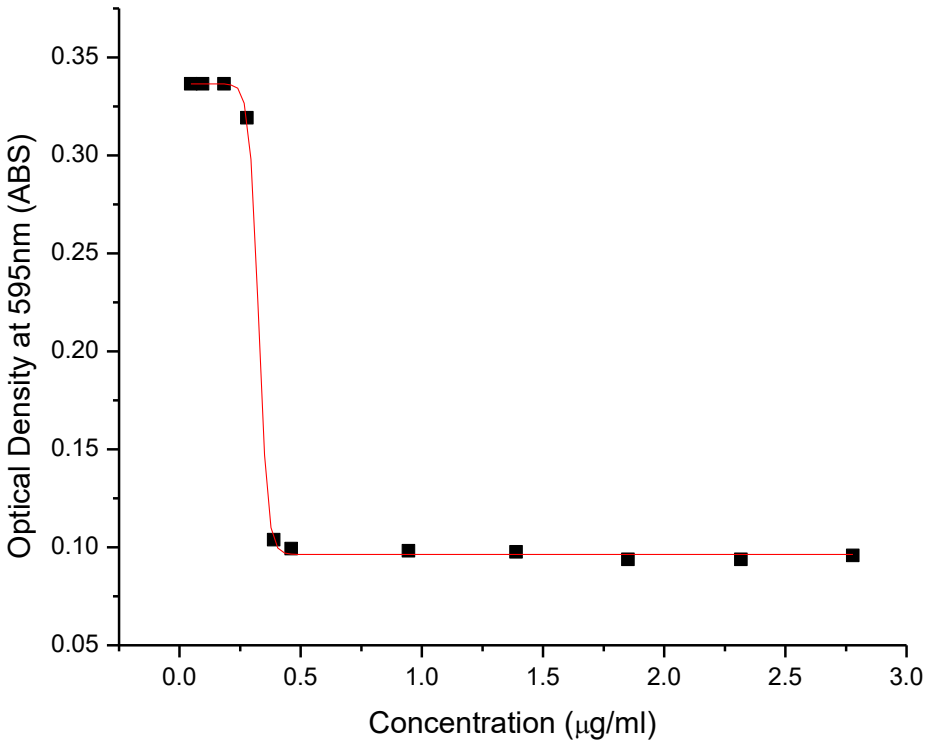

FIGURE 61 - GROWTH CURVE AND ORIGIN MIC PLOT FOR THIOUREA BASED TETRABUTYLAMMONIUM COMPOUND AGAINST LOG *S. AUREUS*

3.3.3 Urea Based compound family with Log *E. coli*

These compounds were found to be ineffective against the Gram-negative *E. coli* bacteria, with only the tetrahexylammonium variant tested producing a result. The Origin plot showed a linear fit.

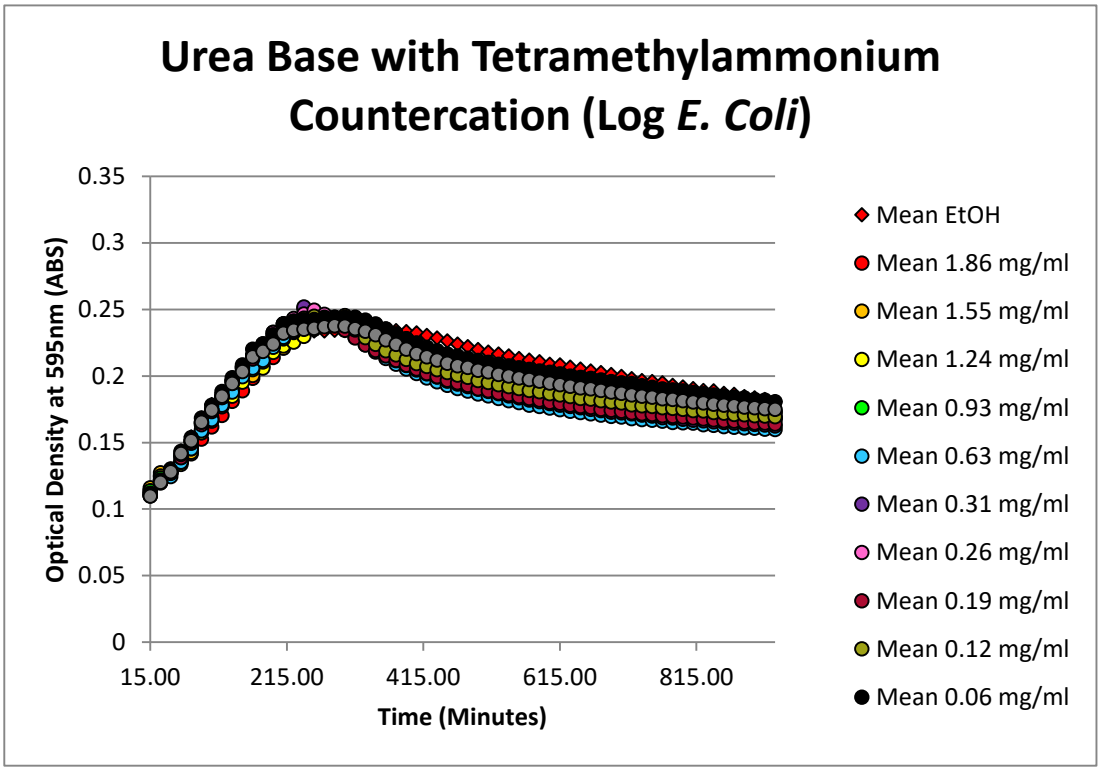

FIGURE 32 - GROWTH CURVE FOR UREA BASED TETRAMETHYLAMMONIUM COMPOUND AGAINST LOG *E. COLI*

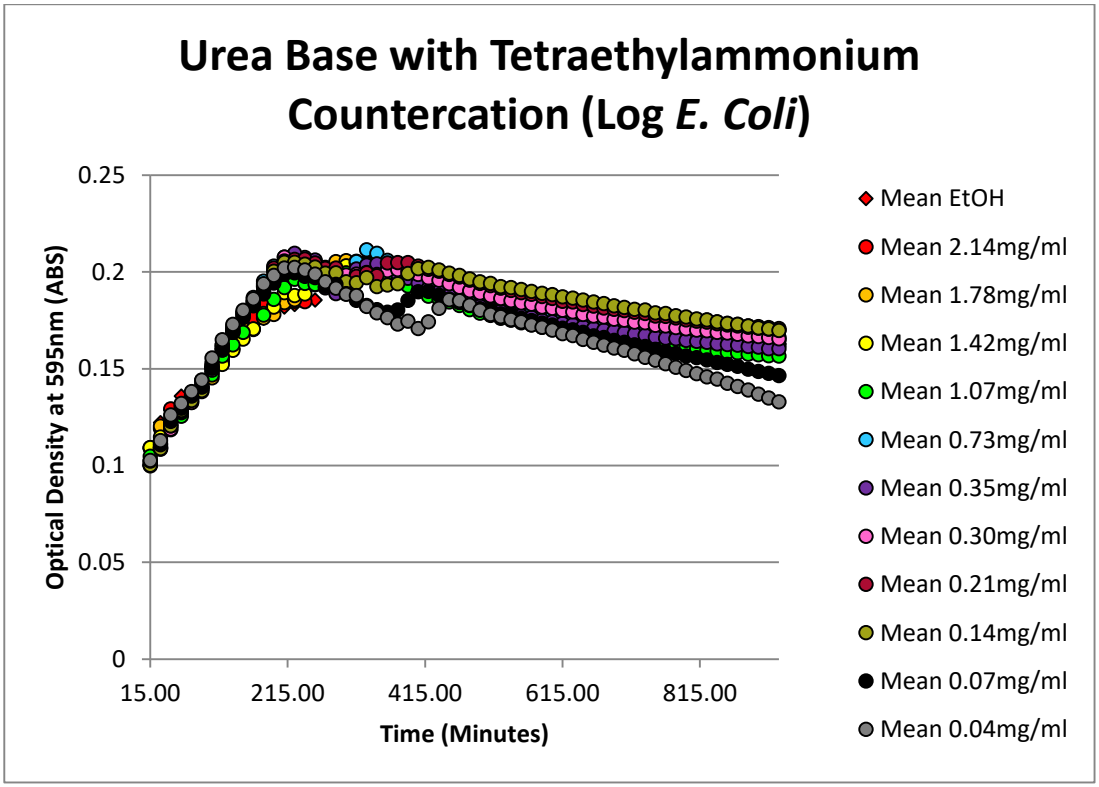

FIGURE 33 - GROWTH CURVE FOR UREA BASED TETRAETHYLAMMONIUM COMPOUND AGAINST LOG *E. COLI*

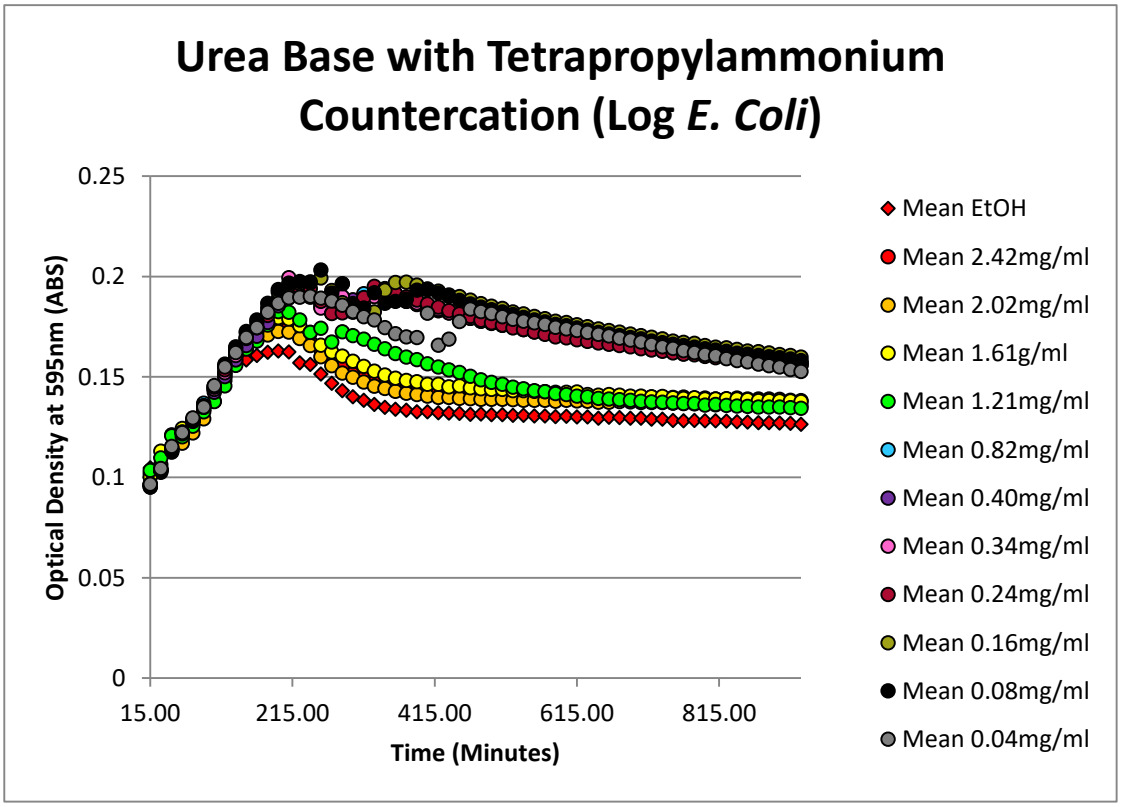

FIGURE 34 - GROWTH CURVE FOR UREA BASED TETRAPROPYLAMMONIUM COMPOUND AGAINST LOG *E. COLI*

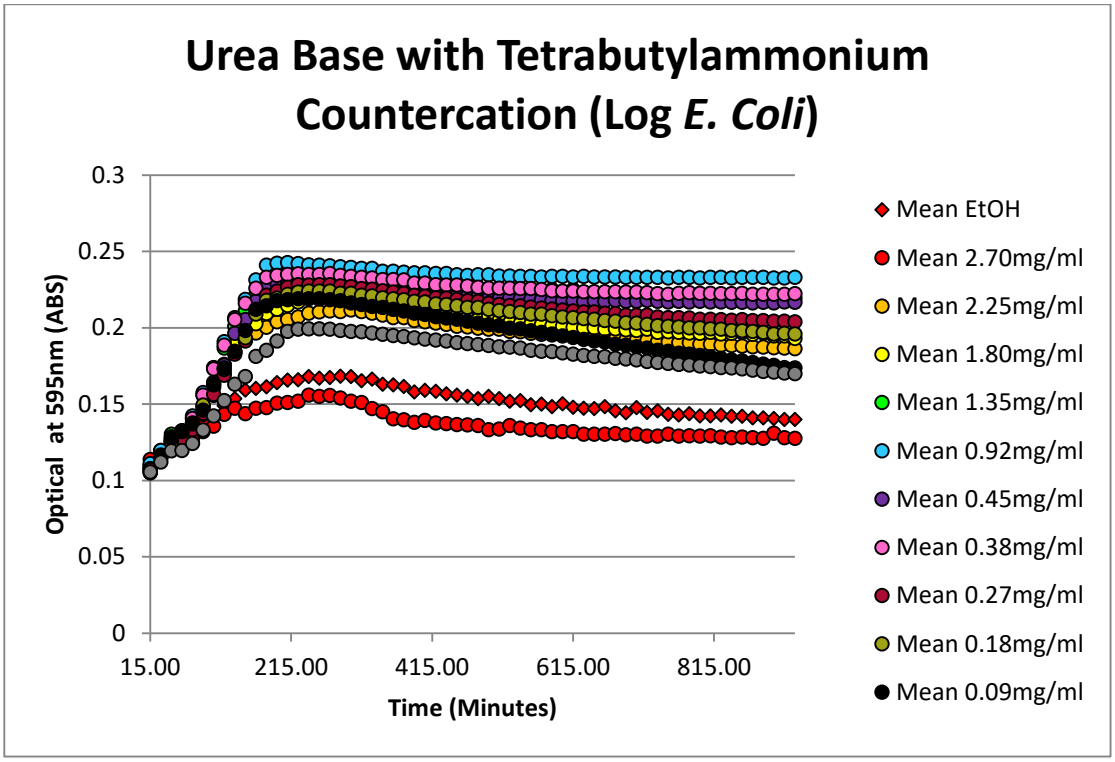

FIGURE 35 - GROWTH CURVE FOR UREA BASED TETRABUTYLAMMONIUM COMPOUND AGAINST LOG *E. COLI*

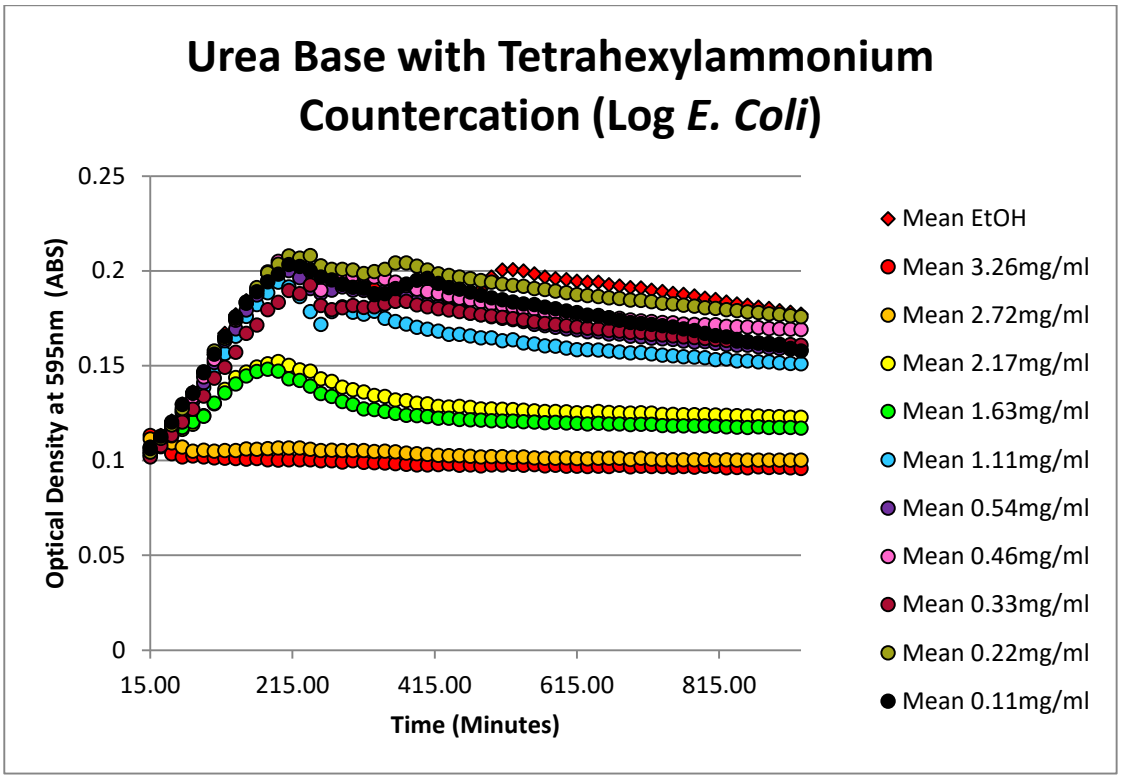

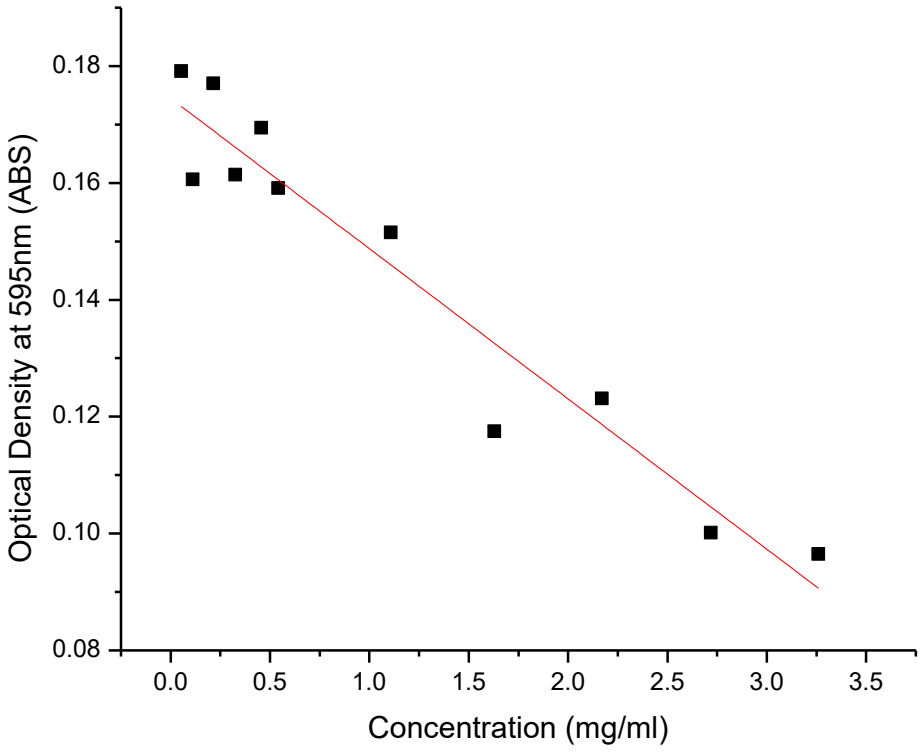

FIGURE 36 - GROWTH CURVE AND ORIGIN MIC PLOT FOR UREA BASED TETRAHEXYLAMMONIUM COMPOUND AGAINST LOG *E. COLI*

3.3.4 Thiourea Based compound family with Log *E. coli*

These compounds were found to be ineffective against the Gram-negative *E.coli* bacteria, with none of the variants tested producing a result. No Origin plots were needed for these results

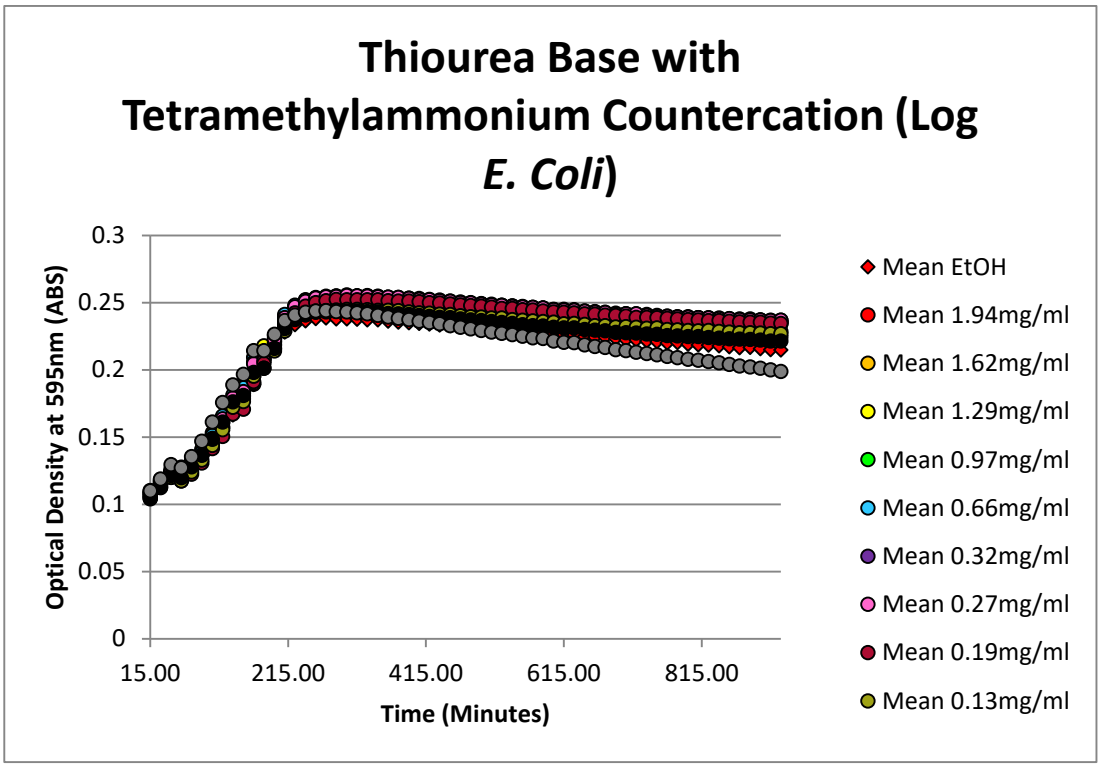

FIGURE 37 - GROWTH CURVE FOR THIOUREA BASED TETRAMETHYLAMMONIUM COMPOUND AGAINST LOG *E. COLI*

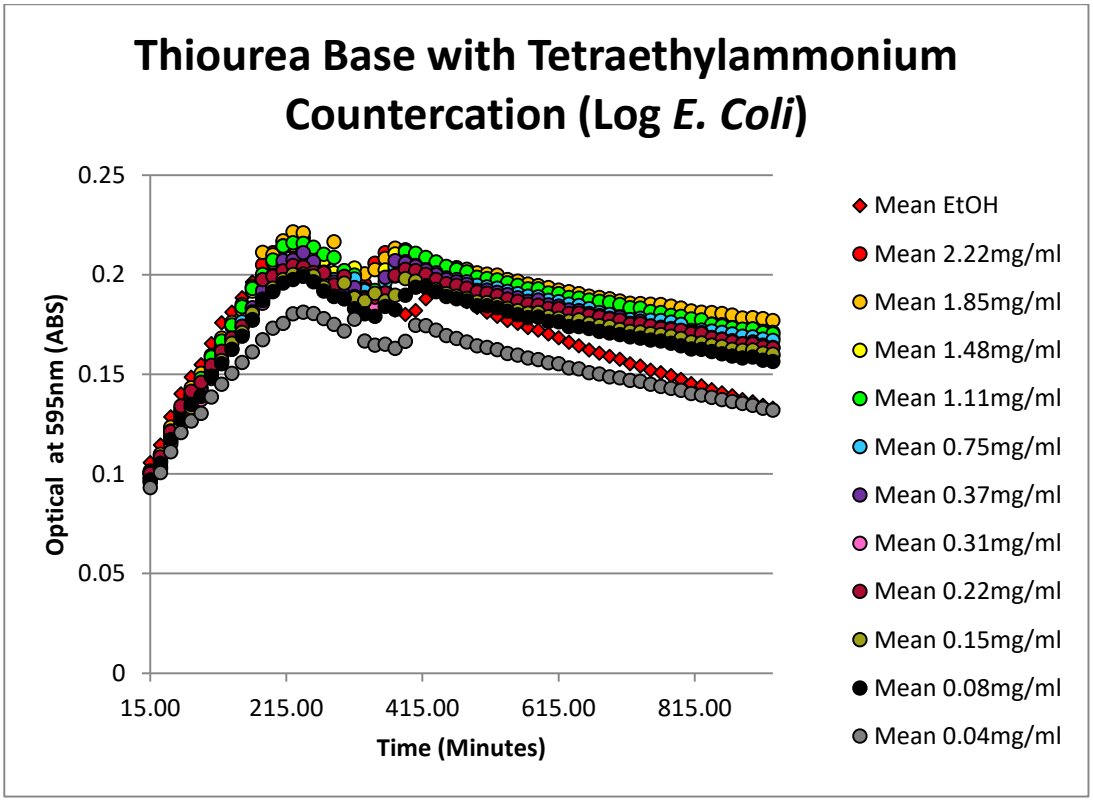

FIGURE 38 - GROWTH CURVE FOR THIOUREA BASED TETRAETHYLAMMONIUM COMPOUND AGAINST LOG *E. COLI*

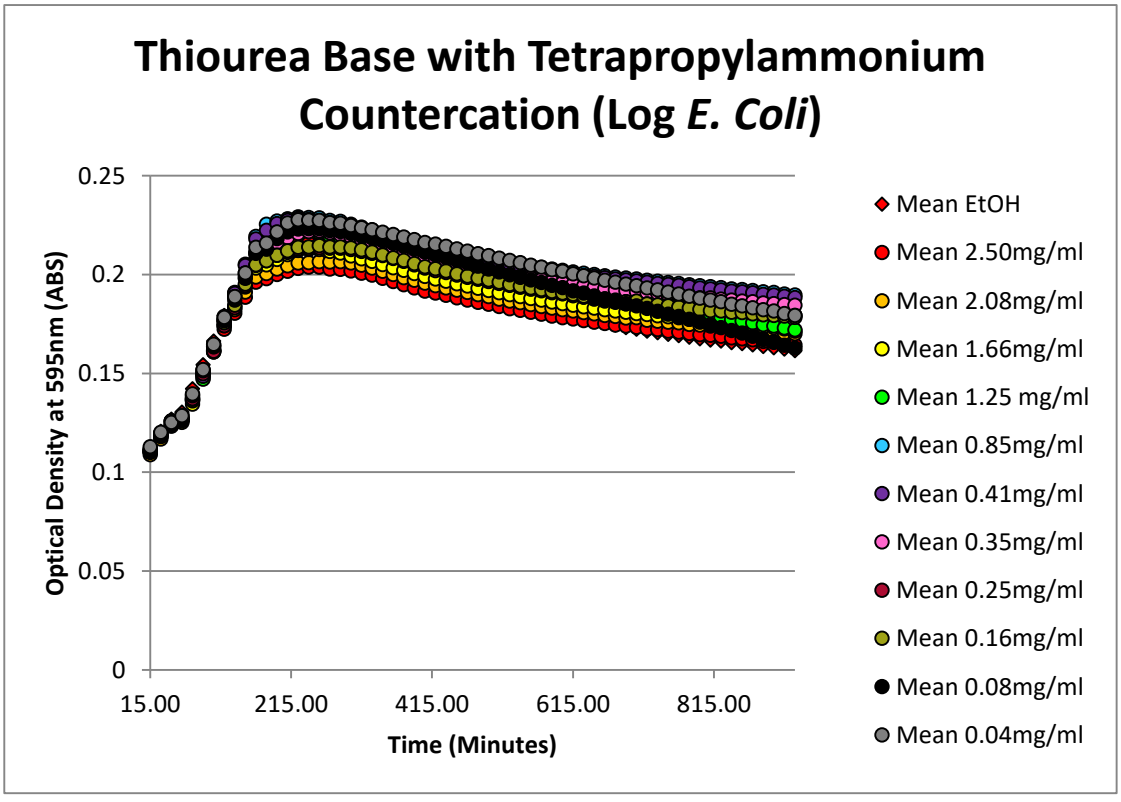

FIGURE 39 - GROWTH CURVE FOR THIOUREA BASED TETRAPROPYLAMMONIUM COMPOUND AGAINST LOG *E. COLI*

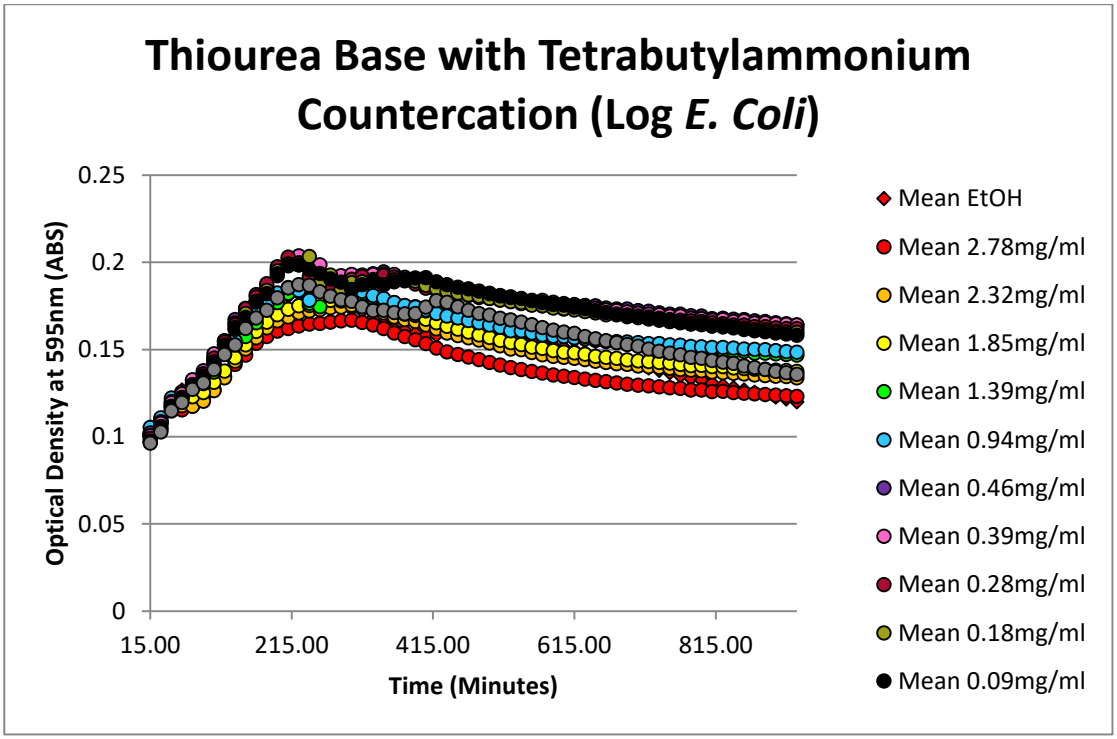

FIGURE 40 - GROWTH CURVE FOR THIOUREA BASED TETRABUTYLAMMONIUM COMPOUND AGAINST LOG *E. COLI*

3.3.5 Urea Based compound family with Stationary *S. aureus*

These compounds were found to be the most effective against the Gram-positive *S. aureus* bacteria, with all variants tested producing results. All of the Origin plots showed sigmoidal fits.

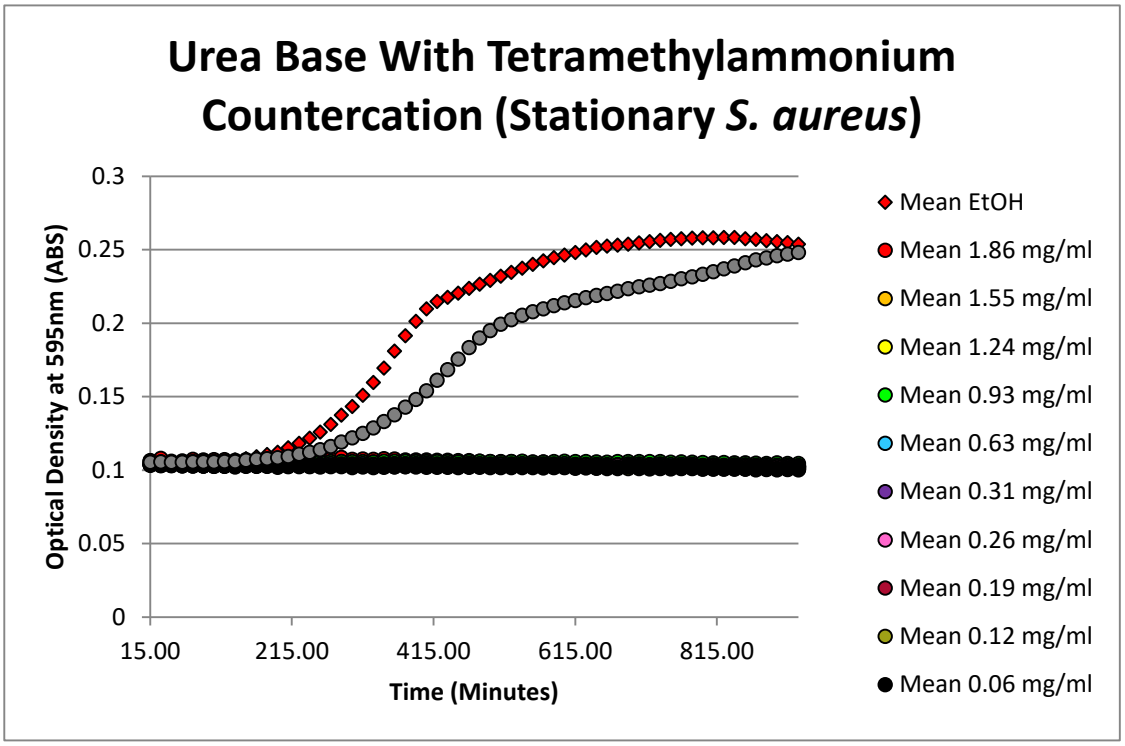

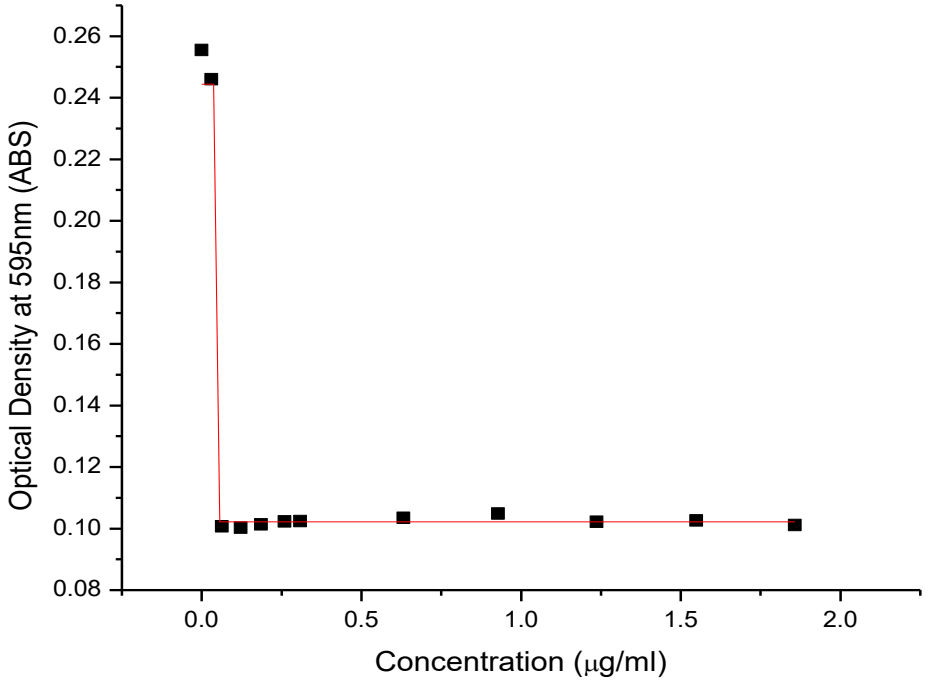

FIGURE 41 - GROWTH CURVE AND ORIGIN MIC PLOT FOR UREA BASED TETRAMETHYLAMMONIUM COMPOUND AGAINST STATIONARY *S. AUREUS*

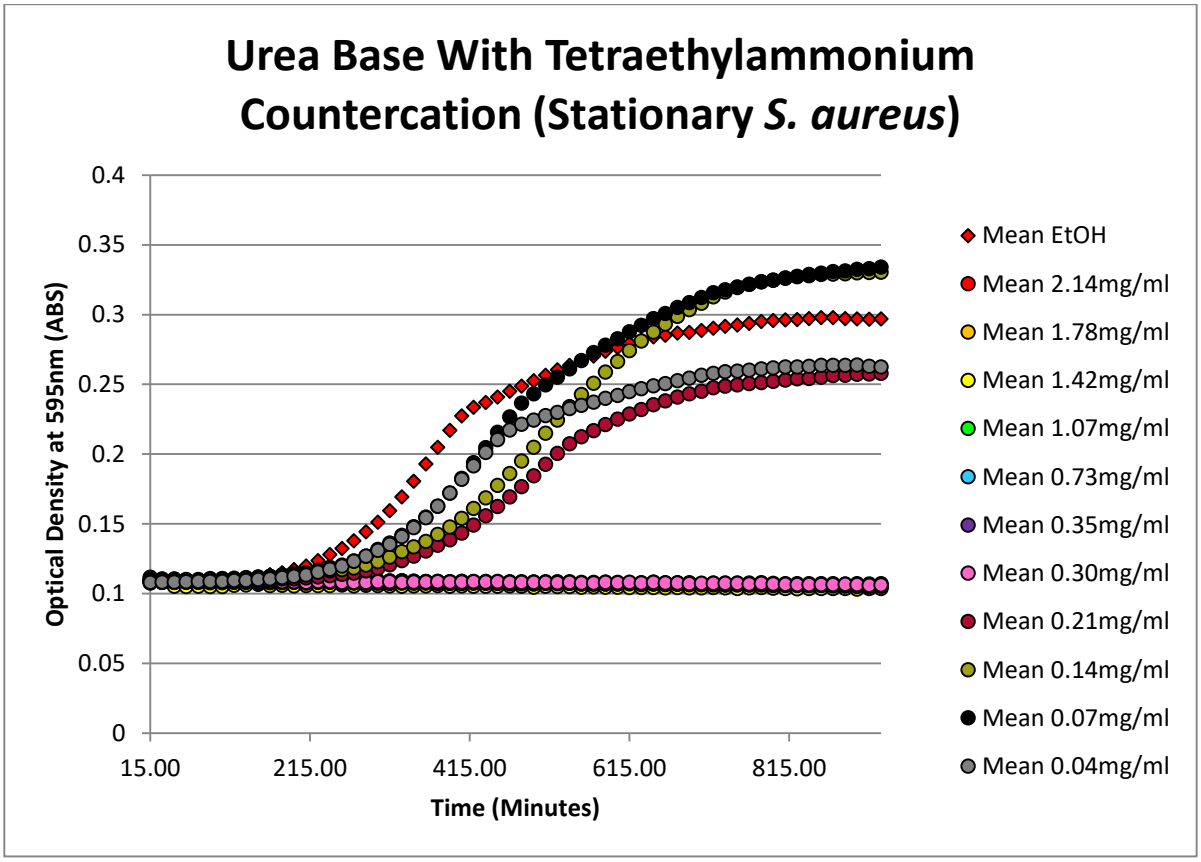

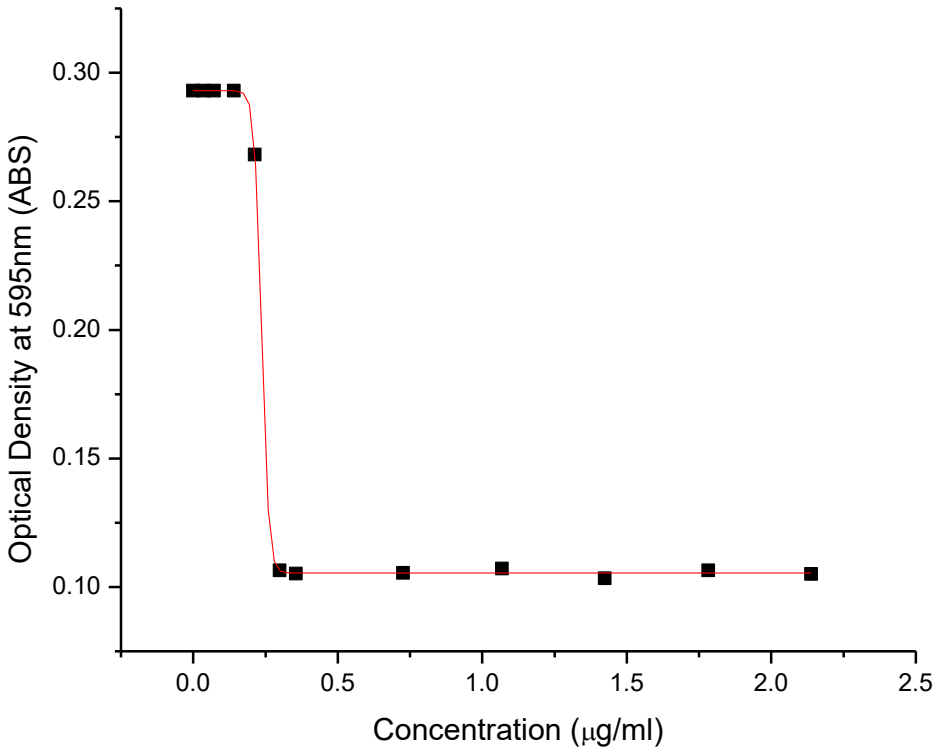

FIGURE 42 - GROWTH CURVE AND ORIGIN MIC PLOT FOR UREA BASED TETRAETHYLAMMONIUM COMPOUND AGAINST STATIONARY *S. AUREUS*

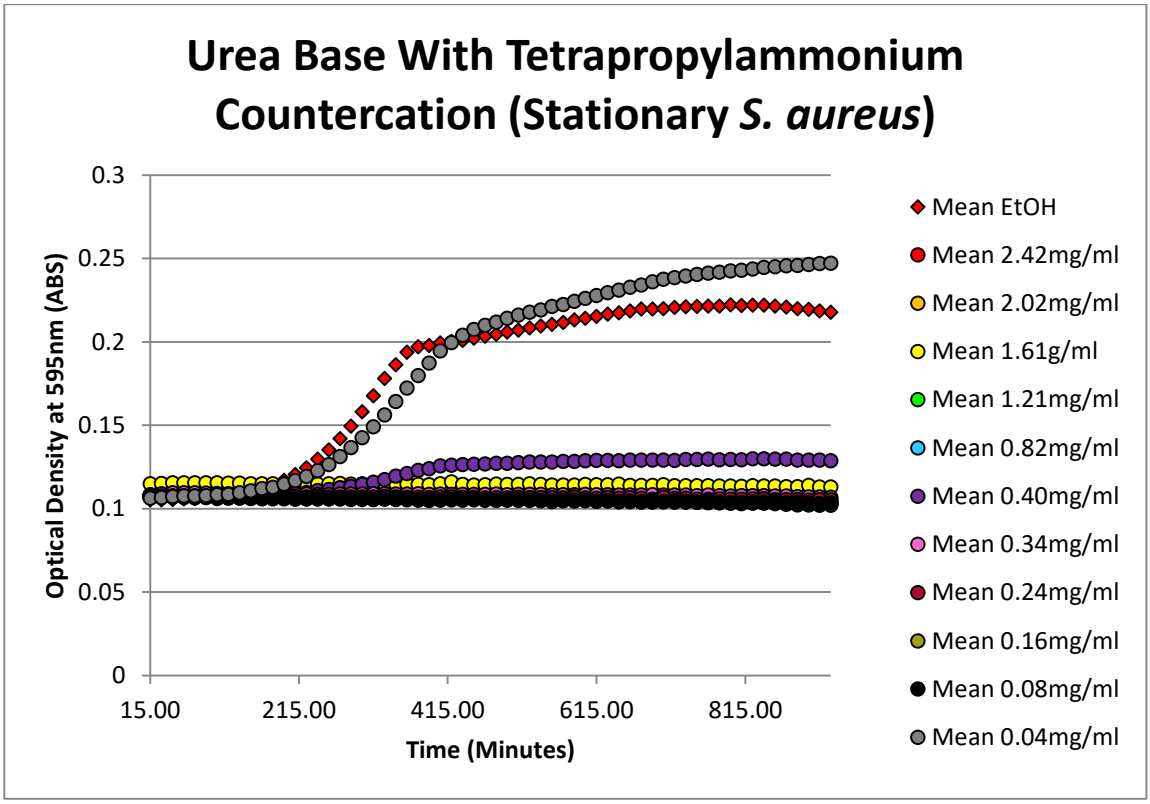

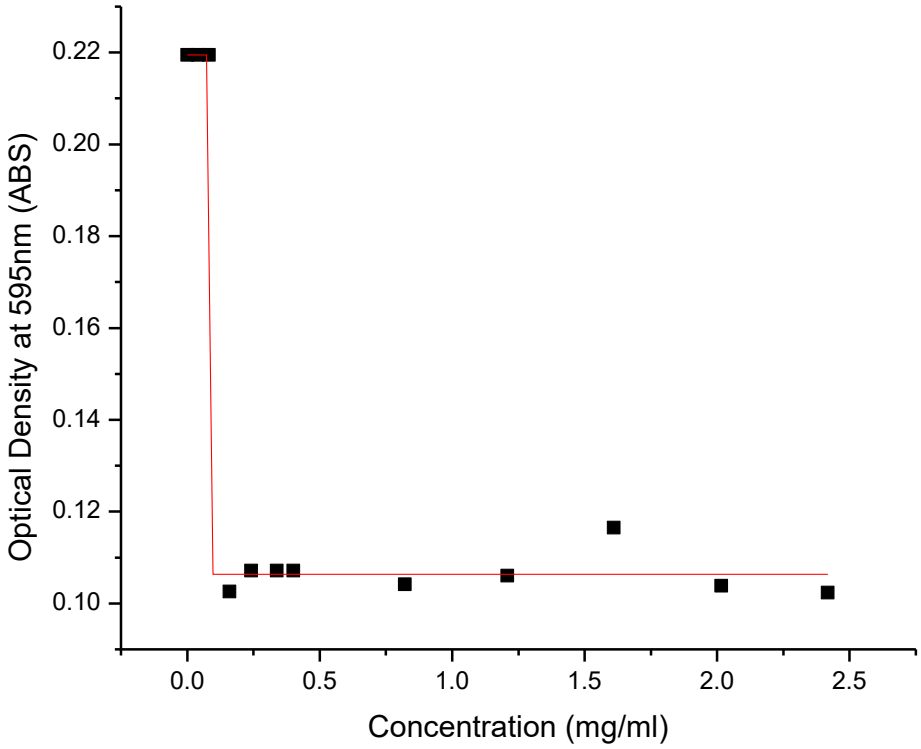

FIGURE 43 - GROWTH CURVE AND ORIGIN MIC PLOT FOR UREA BASED TETRAPROPYLAMMONIUM COMPOUND AGAINST STATIONARY *S. AUREUS*

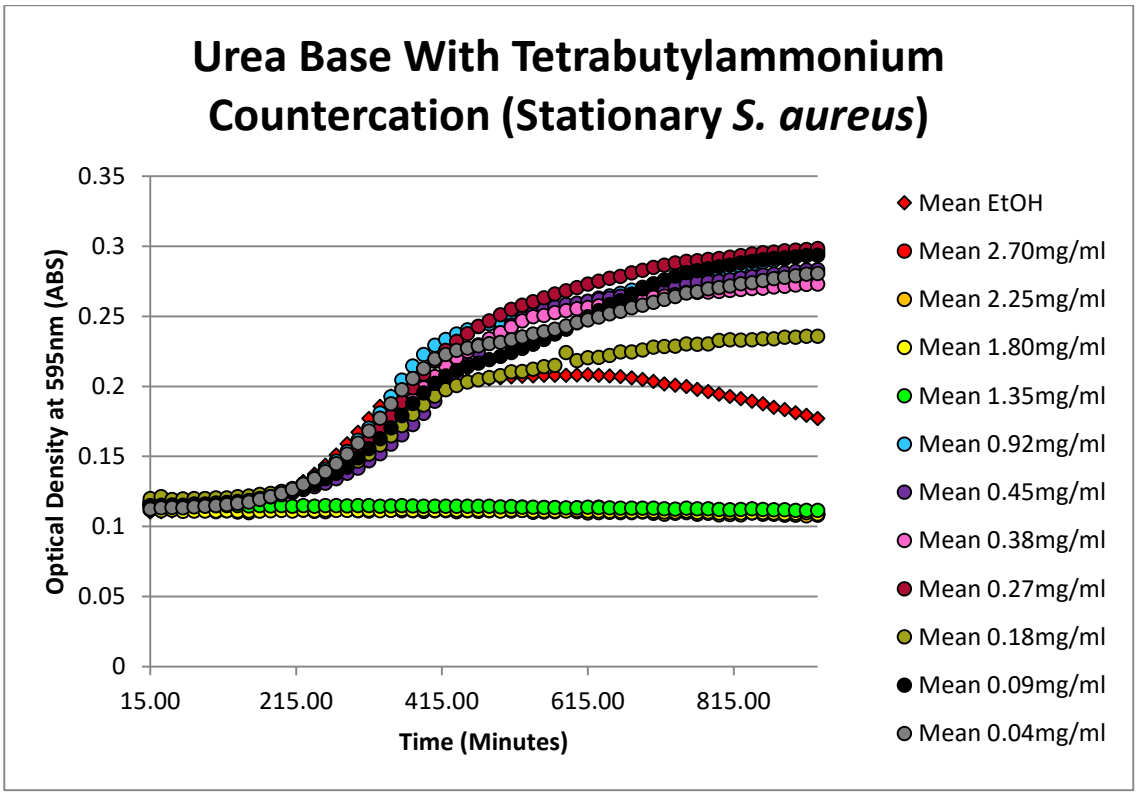

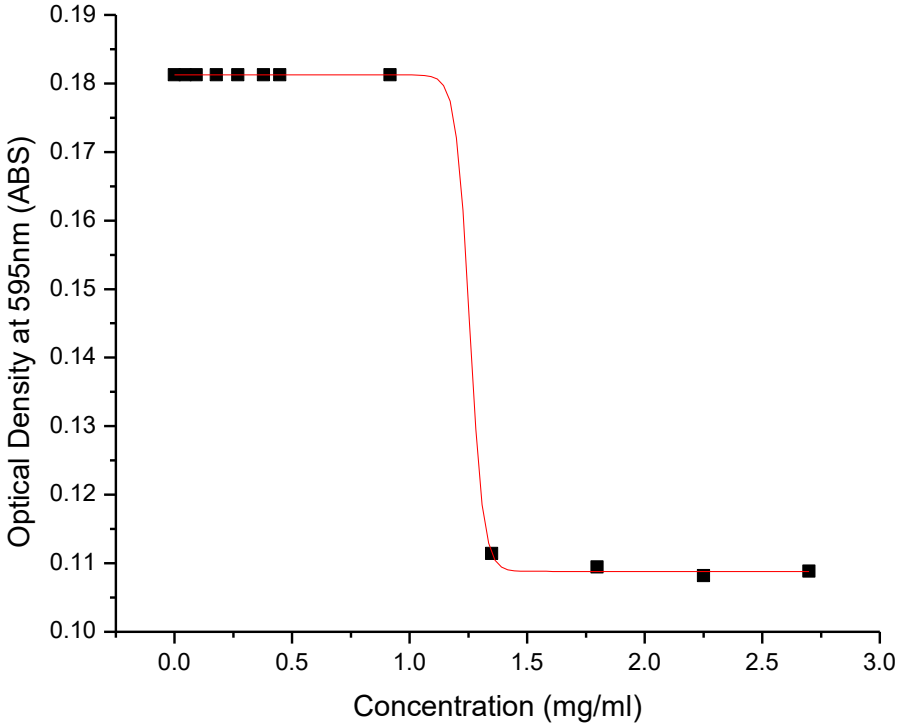

FIGURE 44 - GROWTH CURVE AND ORIGIN MIC PLOT FOR UREA BASED TETRABUTYLAMMONIUM COMPOUND AGAINST STATIONARY *S. AUREUS*

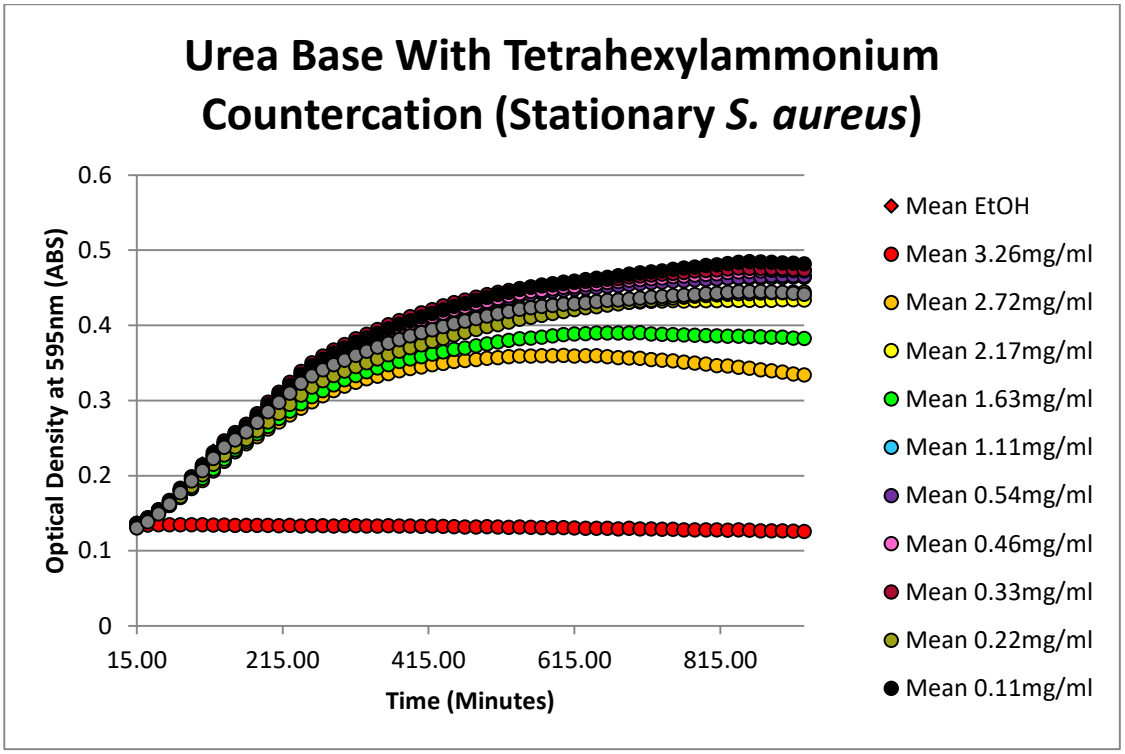

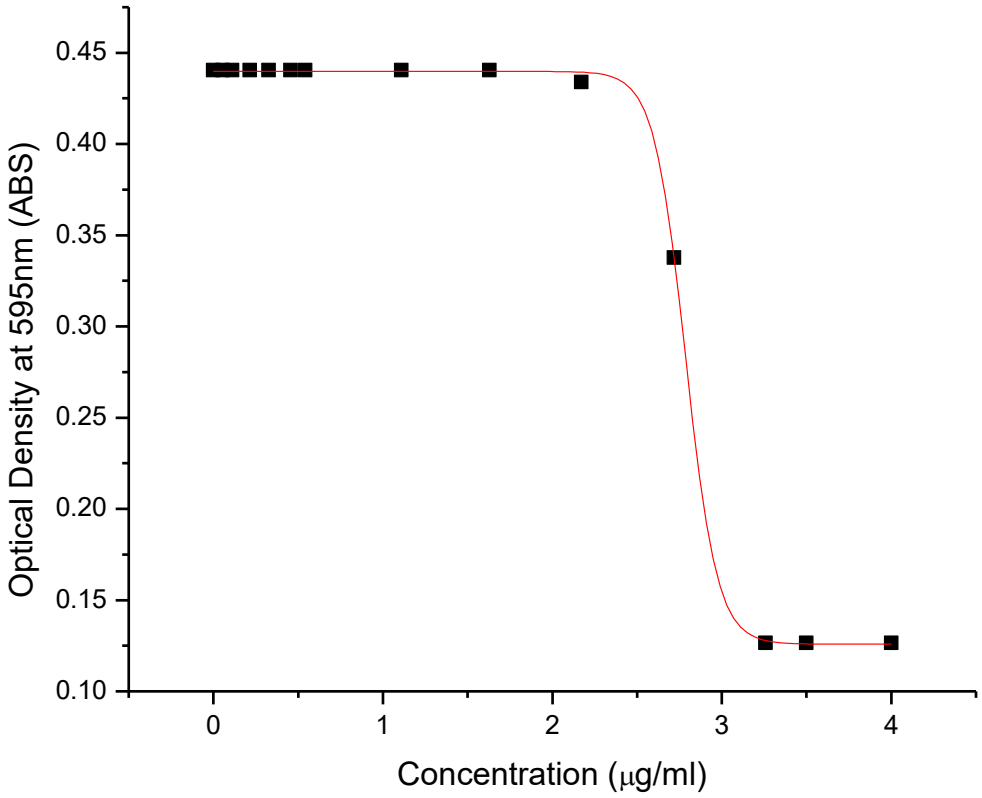

FIGURE 45 - GROWTH CURVE AND ORIGIN MIC PLOT FOR UREA BASED TETRAHEXYLAMMONIUM COMPOUND AGAINST STATIONARY *S. AUREUS*

3.3.6 Thiourea Based compound family with Stationary *S. aureus*

These compounds were found to be ineffective against the Gram-positive *S. aureus* bacteria, with none of the variants tested producing results. No Origin plots were needed

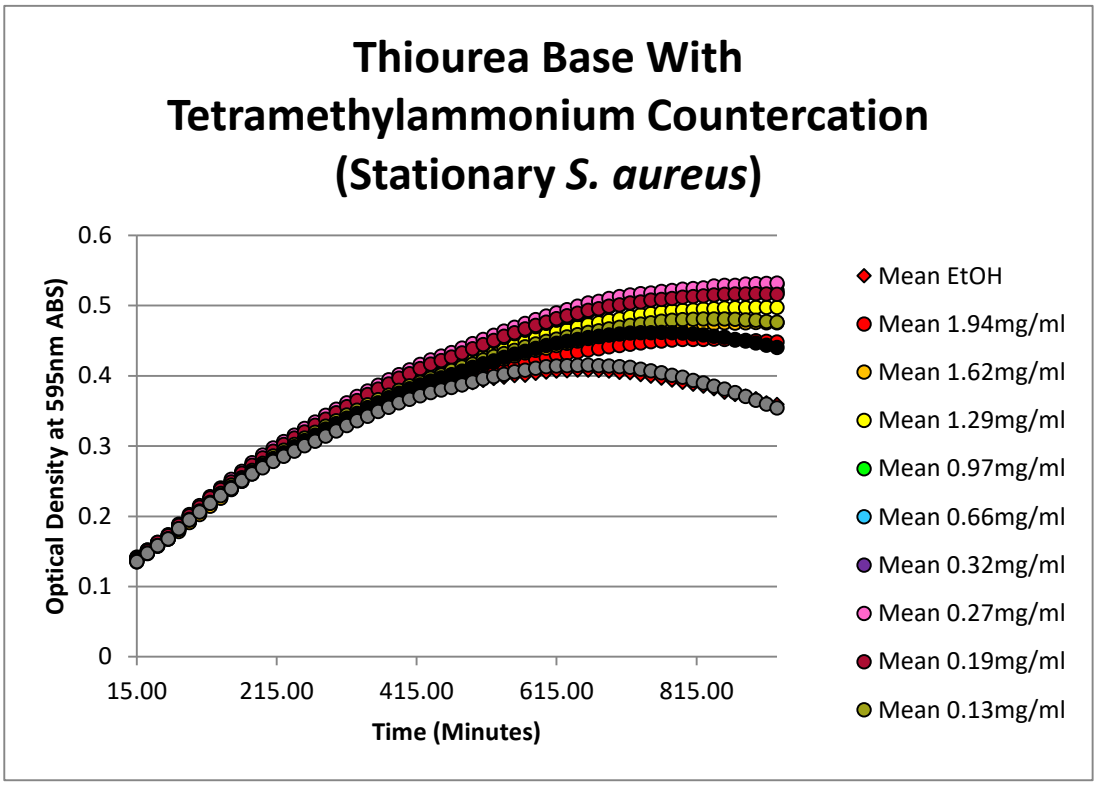

FIGURE 46 - GROWTH CURVE FOR THIOUREA BASED TETRAMETHYLAMMONIUM COMPOUND AGAINST STATIONARY *S. AUREUS*

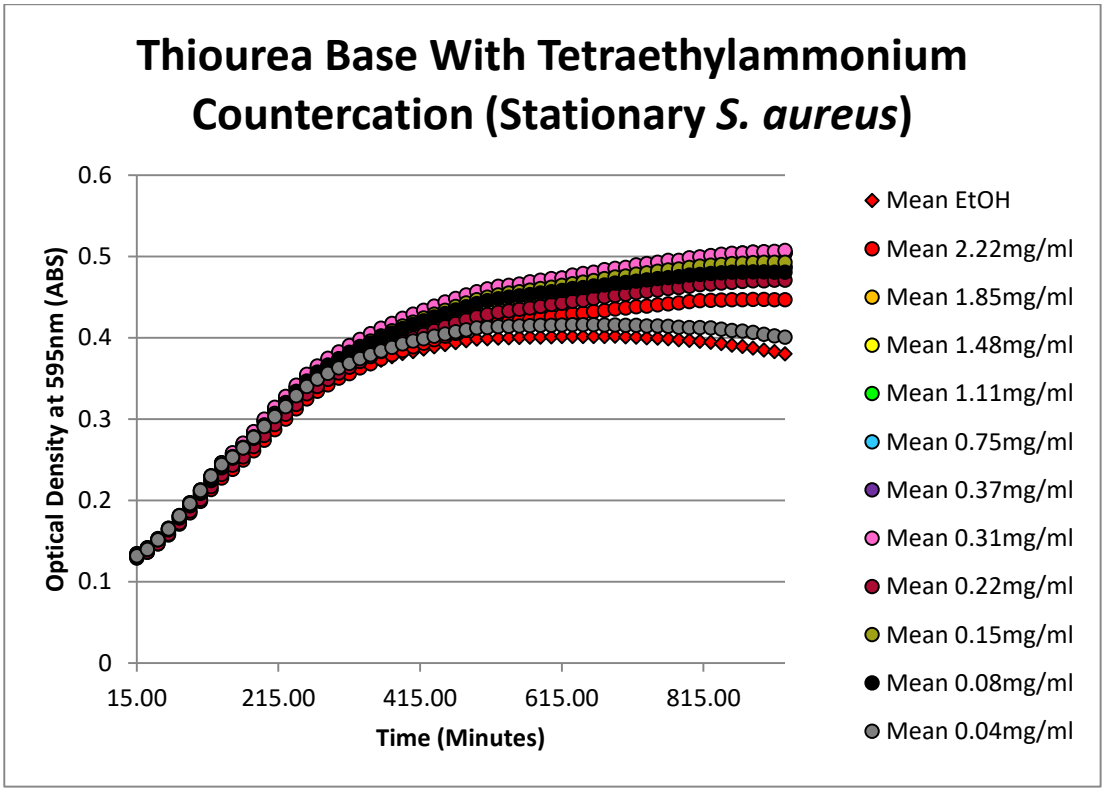

FIGURE 47 - GROWTH CURVE FOR THIOUREA BASED TETRAETHYLAMMONIUM COMPOUND AGAINST STATIONARY *S. AUREUS*

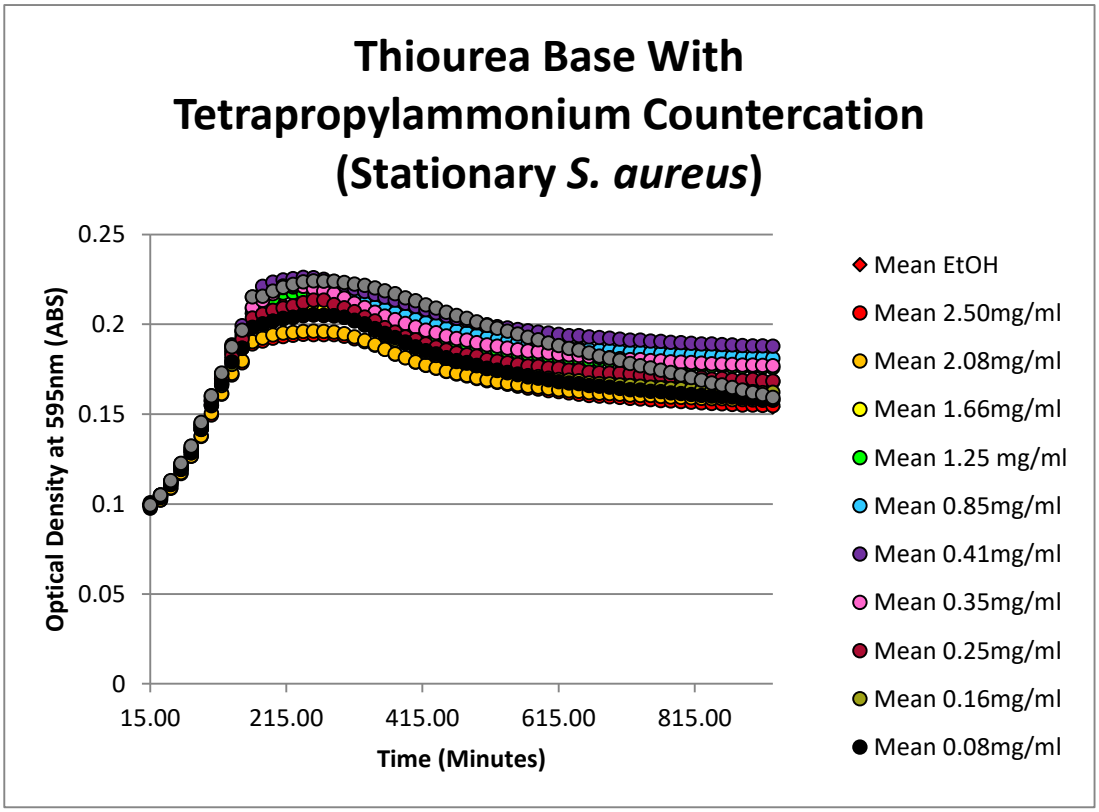

FIGURE 48 - GROWTH CURVE FOR THIOUREA BASED TETRAPROPYLAMMONIUM COMPOUND AGAINST STATIONARY *S. AUREUS*

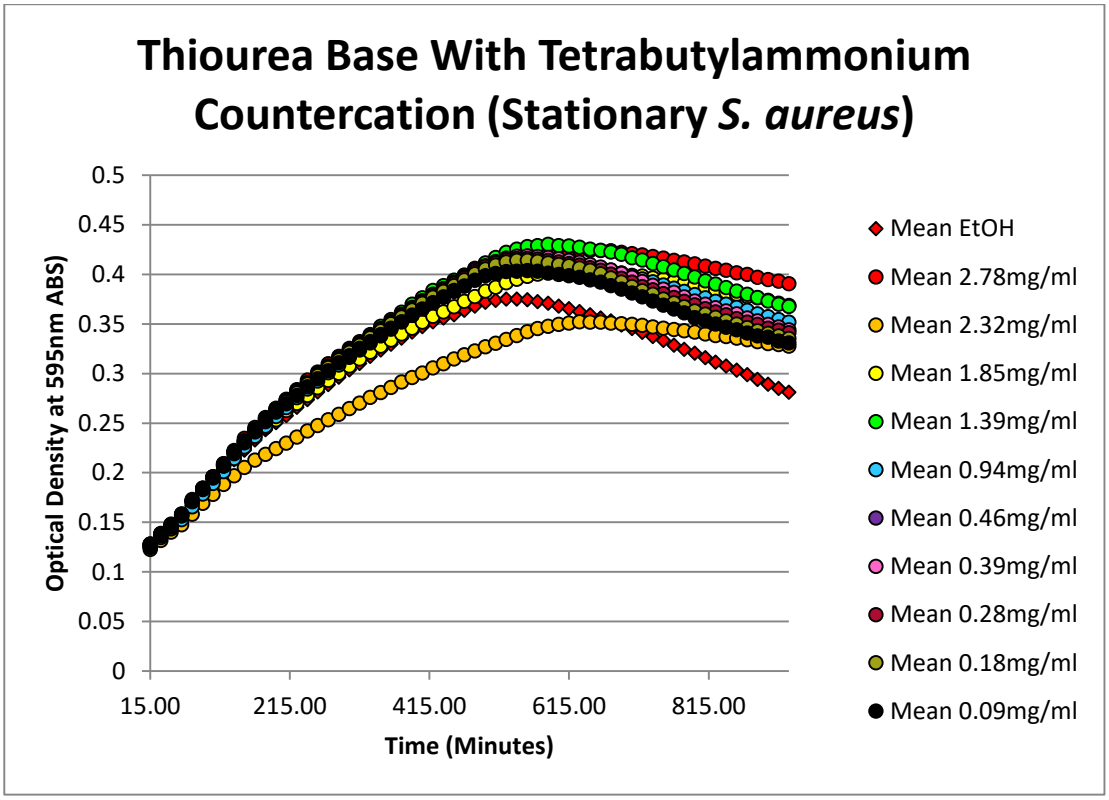

FIGURE 49 - GROWTH CURVE FOR THIOUREA BASED TETRABUTYLAMMONIUM COMPOUND AGAINST STATIONARY *S. AUREUS*

3.3.7 Urea Based compound family with Stationary *E. coli*

These compounds were found to be ineffective against the Gram-negative *E. coli* bacteria, with only the tetrabutylammonium variant tested producing a result. The Origin plot showed a sigmoidal fit.

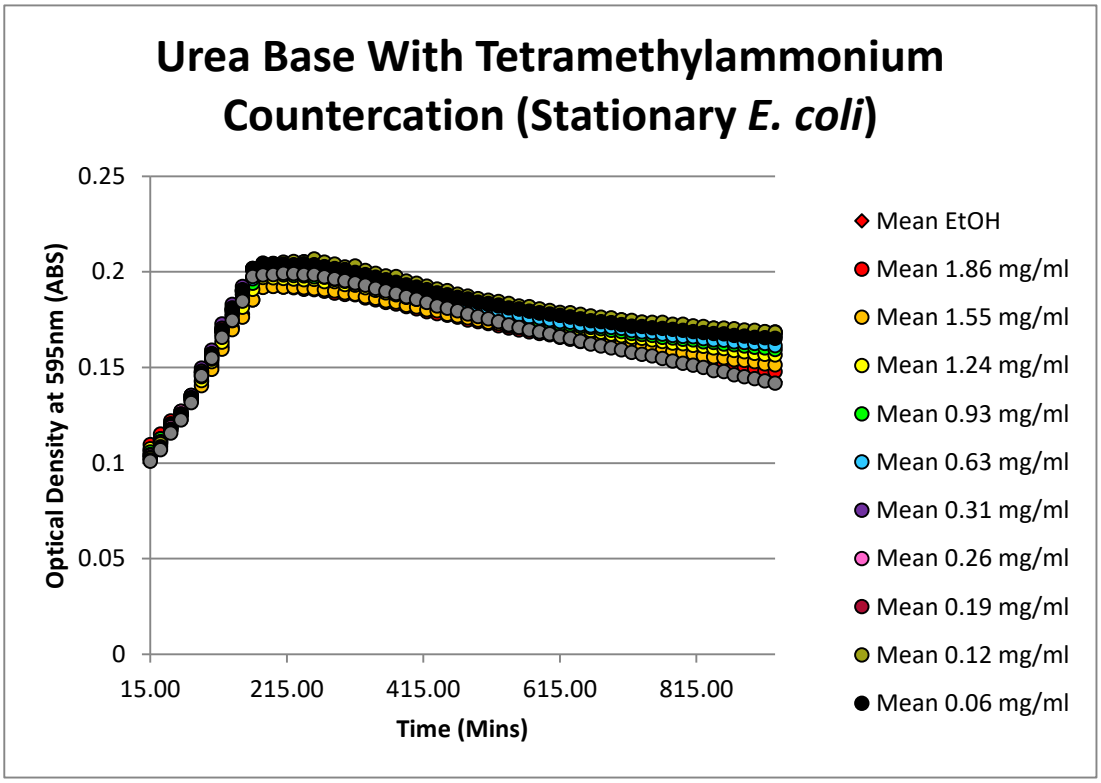

FIGURE 50 - GROWTH CURVE FOR UREA BASED TETRAMETHYLAMMONIUM COMPOUND AGAINST STATIONARY *E. COLI*

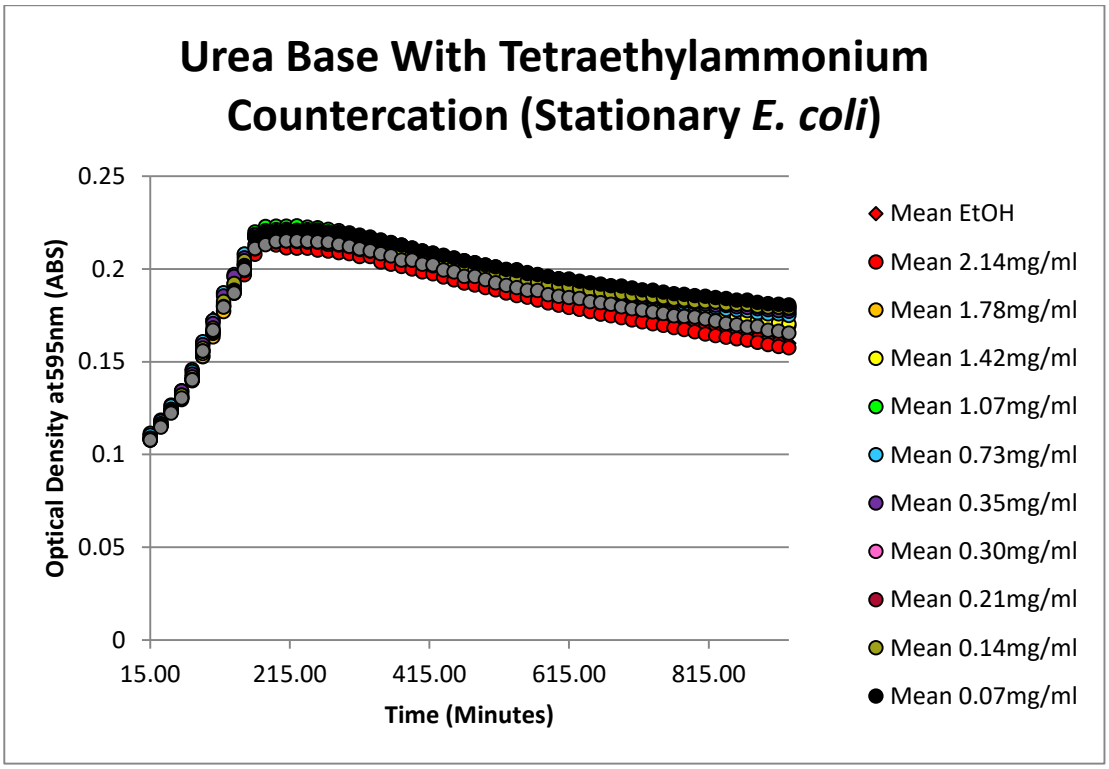

FIGURE 51 - GROWTH CURVE FOR UREA BASED TETRAETHYLAMMONIUM COMPOUND AGAINST STATIONARY *E. COLI*

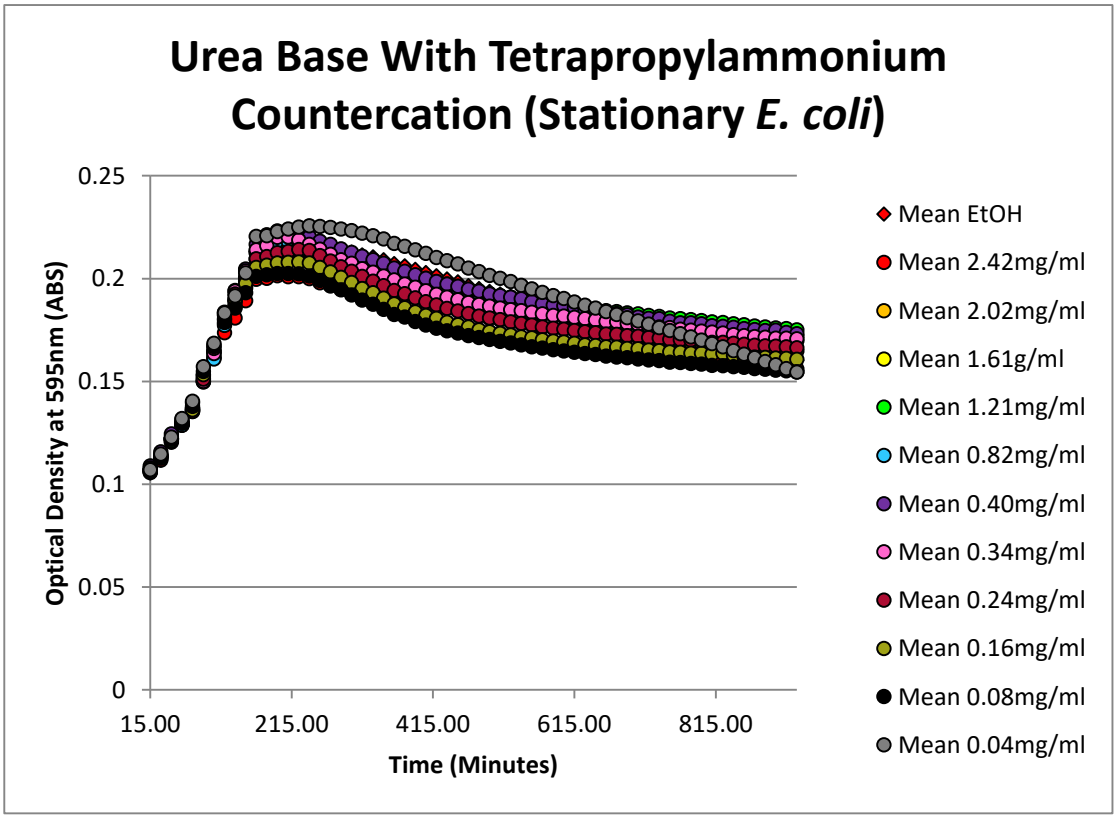

FIGURE 52 - GROWTH CURVE FOR UREA BASED TETRAPROPYLAMMONIUM COMPOUND AGAINST STATIONARY *E. COLI*

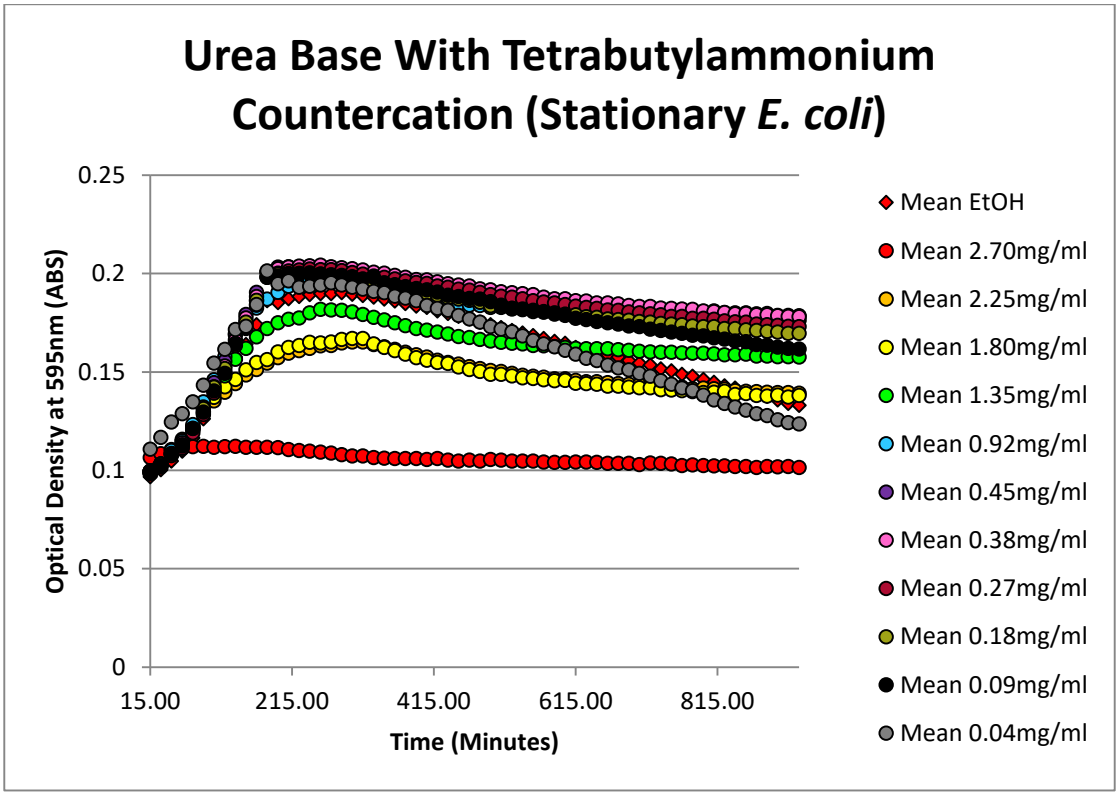

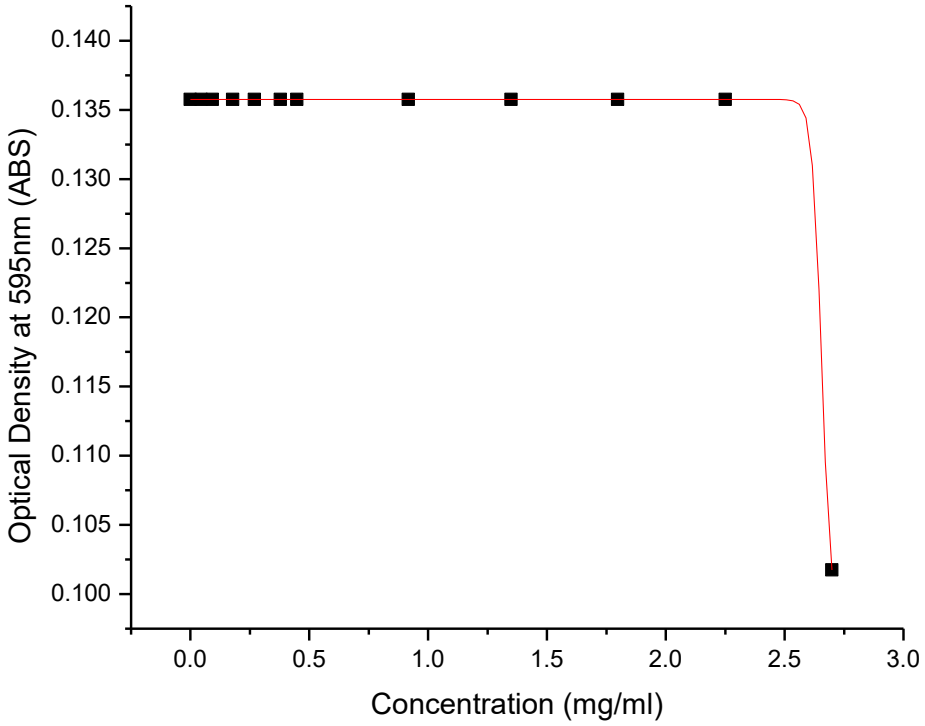

FIGURE 53 - GROWTH CURVE AND ORIGIN MIC PLOT FOR UREA BASED TETRABUTYLAMMONIUM COMPOUND AGAINST STATIONARY *E. COLI*

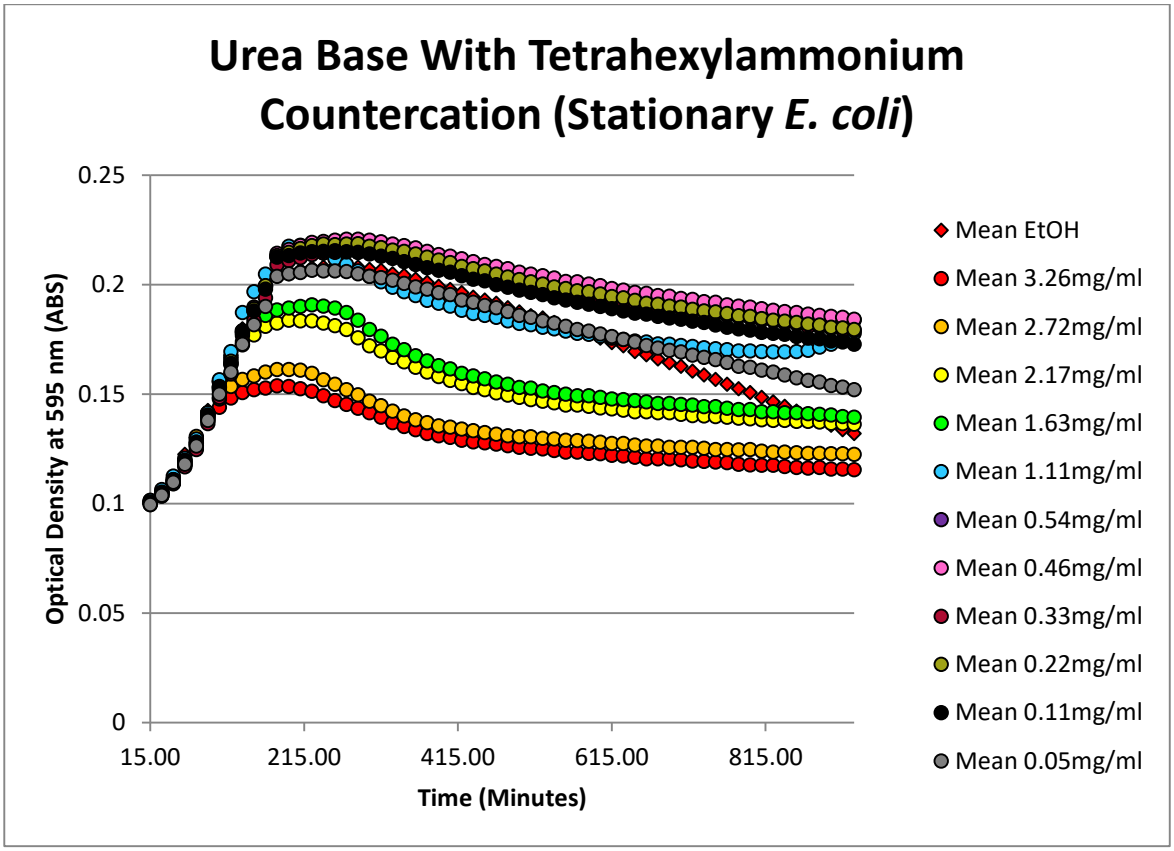

FIGURE 54 - GROWTH CURVE FOR UREA BASED TETRAHEXYLAMMONIUM COMPOUND AGAINST STATIONARY *E. COLI*

3.3.8 Thiourea Based compound family with Stationary *E. coli*

These compounds were found to be ineffective against the Gram-negative *E.coli* bacteria, with none of the variants tested producing a result. No Origin plots were needed for these results

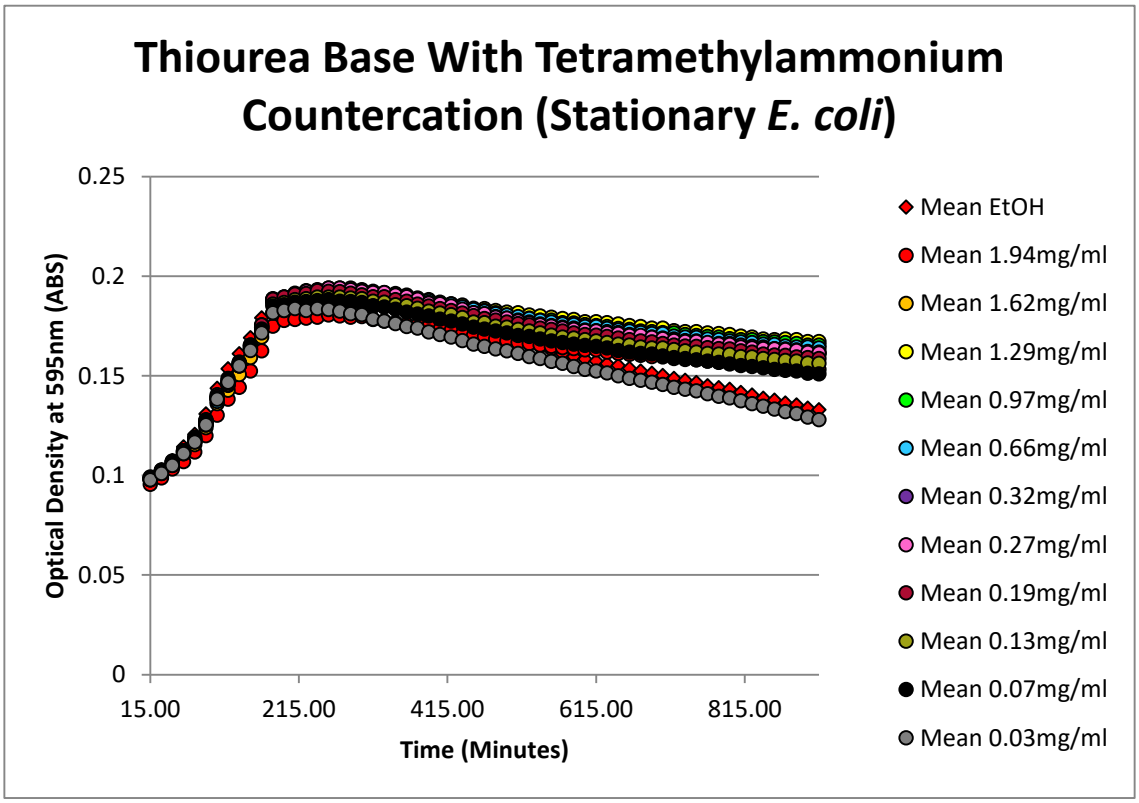

FIGURE 55 - GROWTH CURVE FOR THIOUREA BASED TETRAMETHYLAMMONIUM COMPOUND AGAINST STATIONARY *E. COLI*

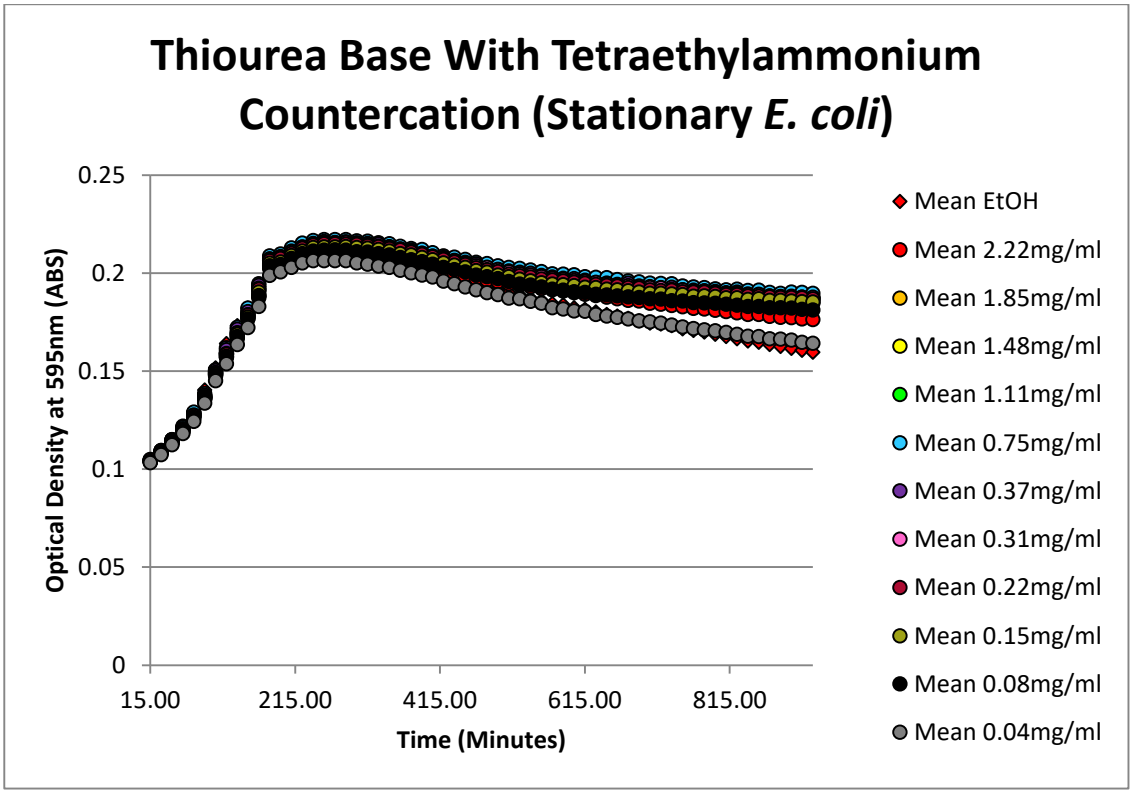

FIGURE 56 - GROWTH CURVE FOR THIOUREA BASED TETRAETHYLAMMONIUM COMPOUND AGAINST STATIONARY *E. COLI*

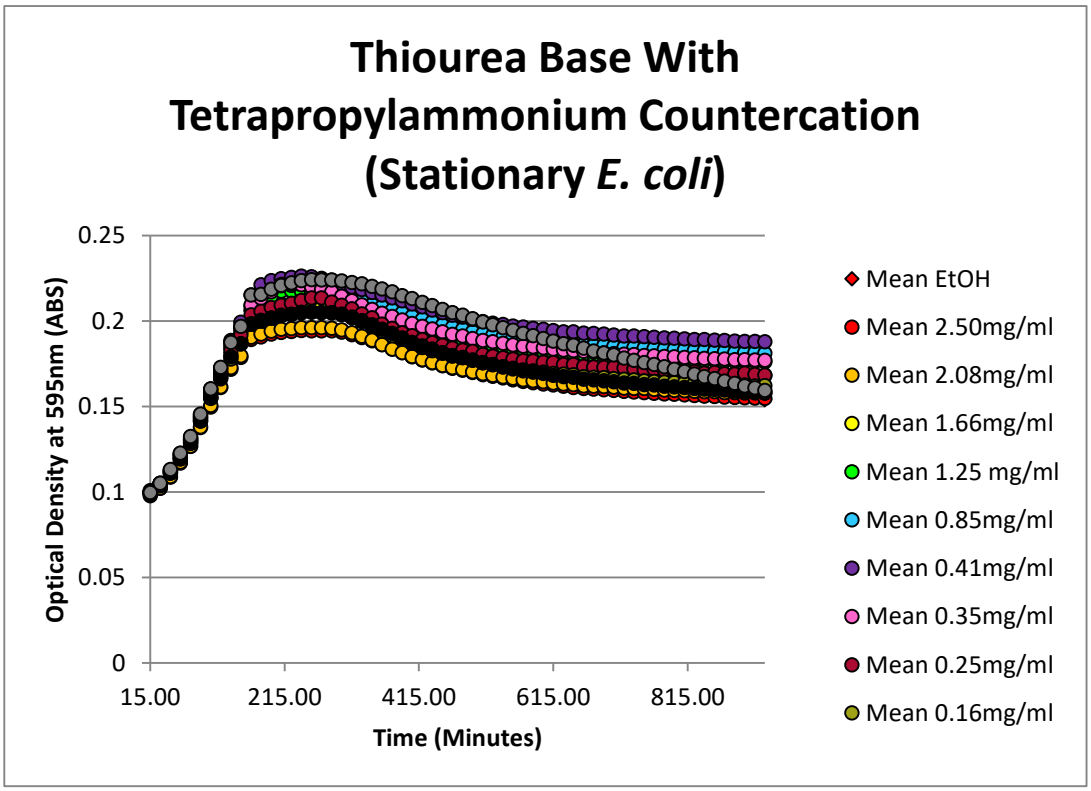

FIGURE 57 - GROWTH CURVE FOR THIOUREA BASED TETRAPROPYLAMMONIUM COMPOUND AGAINST STATIONARY *E. COLI*

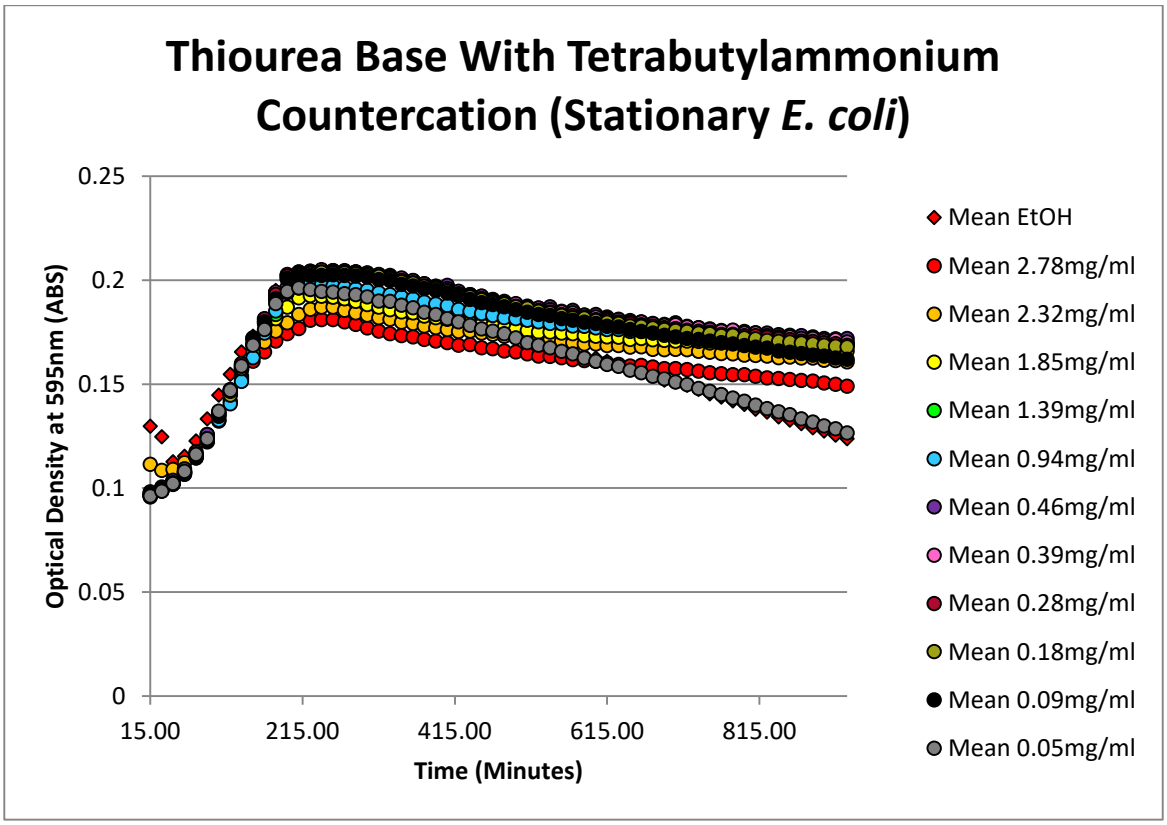

FIGURE 58 - GROWTH CURVE FOR THIOUREA BASED TETRABUTYLAMMONIUM COMPOUND AGAINST STATIONARY *E. COLI*

	Urea Base				**Thio Base**
MIC50	Log *S. aureus*	Stat *S. aureus*	Log *E. coli*	Stat *E. coli*	Log *S. aureus*
	µg/mL	µg/mL	µg/mL	µg/mL	µg/mL
Meth	0.45	5.58	N/a	N/a	N/a
Eth	19.14	39.39	N/a	N/a	N/a
Prop	21.60	10.64	N/a	N/a	N/a
But	7.35	209.13	N/a	412.08	54.13
Pent	N/a	N/a	N/a	N/a	N/a
Hex	29.08	464.14	237.00	450.99	N/a

	Urea Base				Thio Base
MIC100	Log *S. aureus*	Stat *S. aureus*	Log *E. coli*	Stat *E. coli*	Log *S. aureus*
	µg/mL	µg/mL	µg/mL	µg/mL	µg/mL
Meth	2.97	7.30	N/a	N/a	N/a
Eth	20.08	54.08	N/a	N/a	N/a
Prop	22.68	10.92	N/a	N/a	N/a
But	29.41	254.56	N/a	421.06	93.55
Pent	N/a	N/a	N/a	N/a	N/a
Hex	30.35	559.13	505.67	480.25	N/a

FIGURE 59 - MIC VALUES TABLE FOR THE FAMILY OF COMPOUNDS TESTED WITHIN THIS THESIS

3.3.9 The Tetraalkylammonium Chloride Salts with Log *S. aureus*

These experiments were to prove which part of the molecule being tested produced the therapeutic effect, and as the tetraalkylammonium counteraction was not present, and none of the results yielded antimicrobial effect, this shows the counteraction is responsible for the activity of the compound.

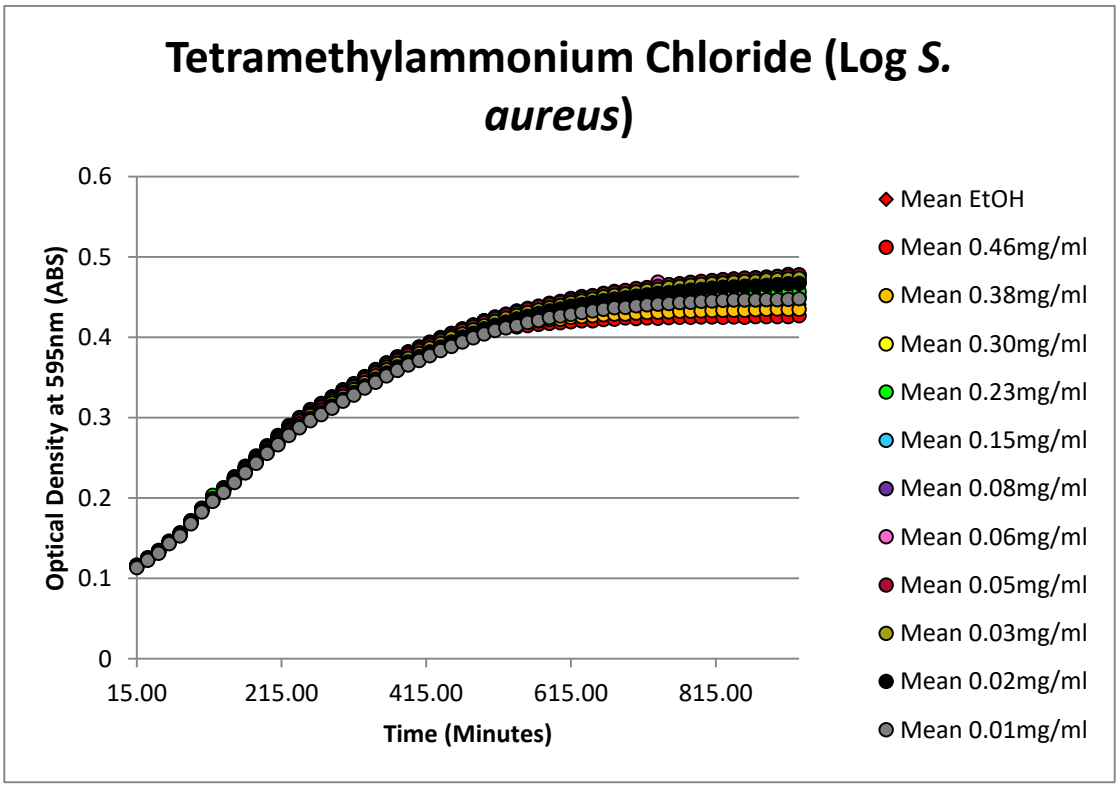

FIGURE 60 - GROWTH CURVE FOR TETRAMETHYLAMMONIUM CHLORIDE COMPOUND AGAINST LOG *S.AUREUS*

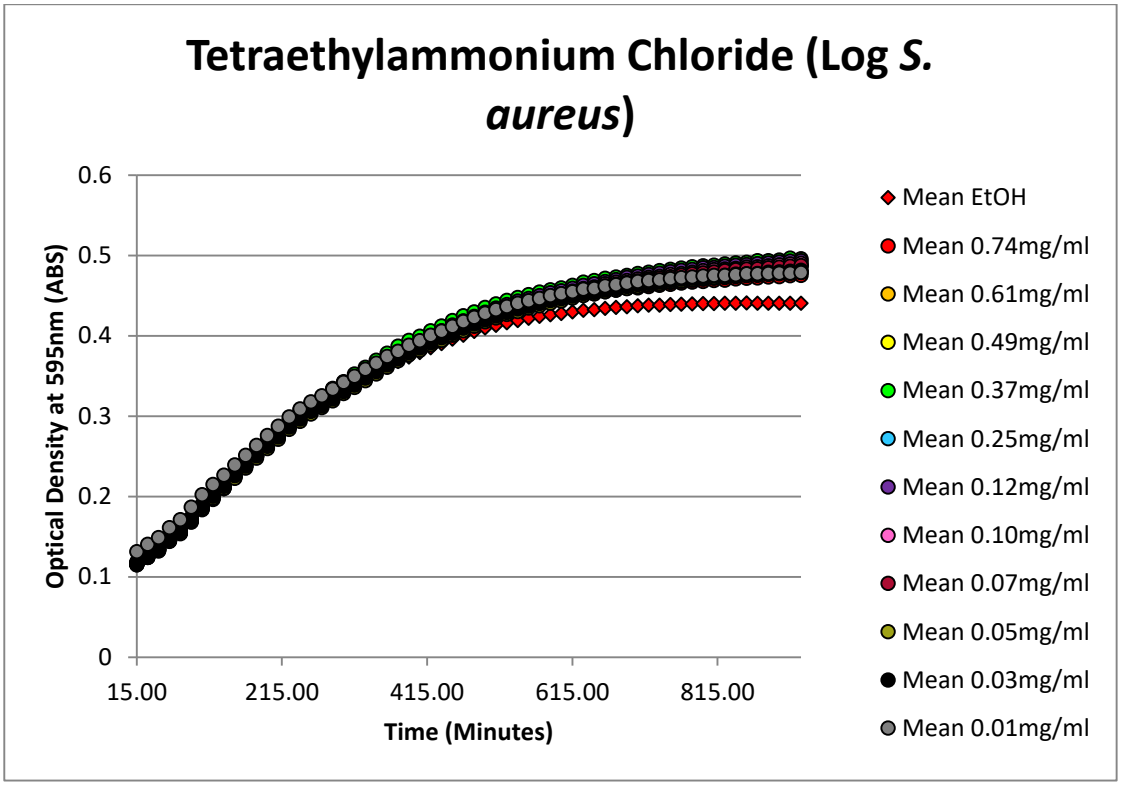

FIGURE 61 - GROWTH CURVE FOR TETRAETHYLAMMONIUM CHLORIDE COMPOUND AGAINST LOG *S.AUREUS*

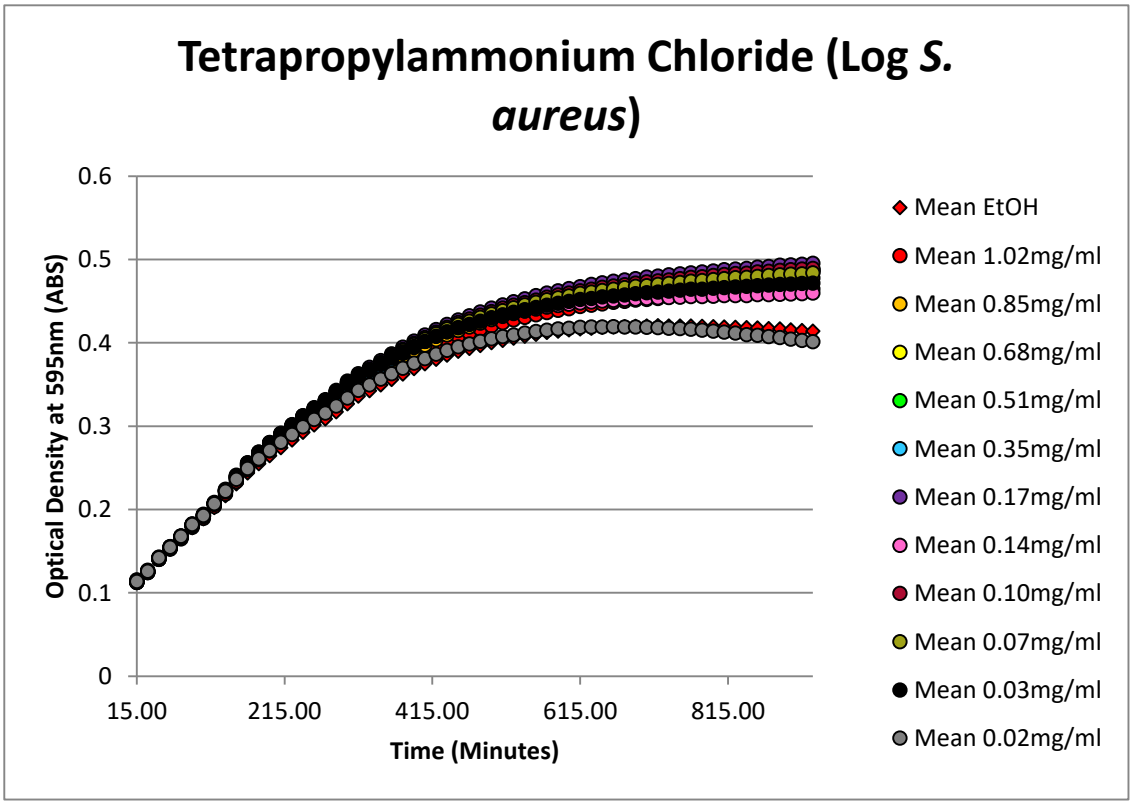

FIGURE 62 - GROWTH CURVE FOR TETRAPROPYLAMMONIUM CHLORIDE COMPOUND AGAINST LOG *S.AUREUS*

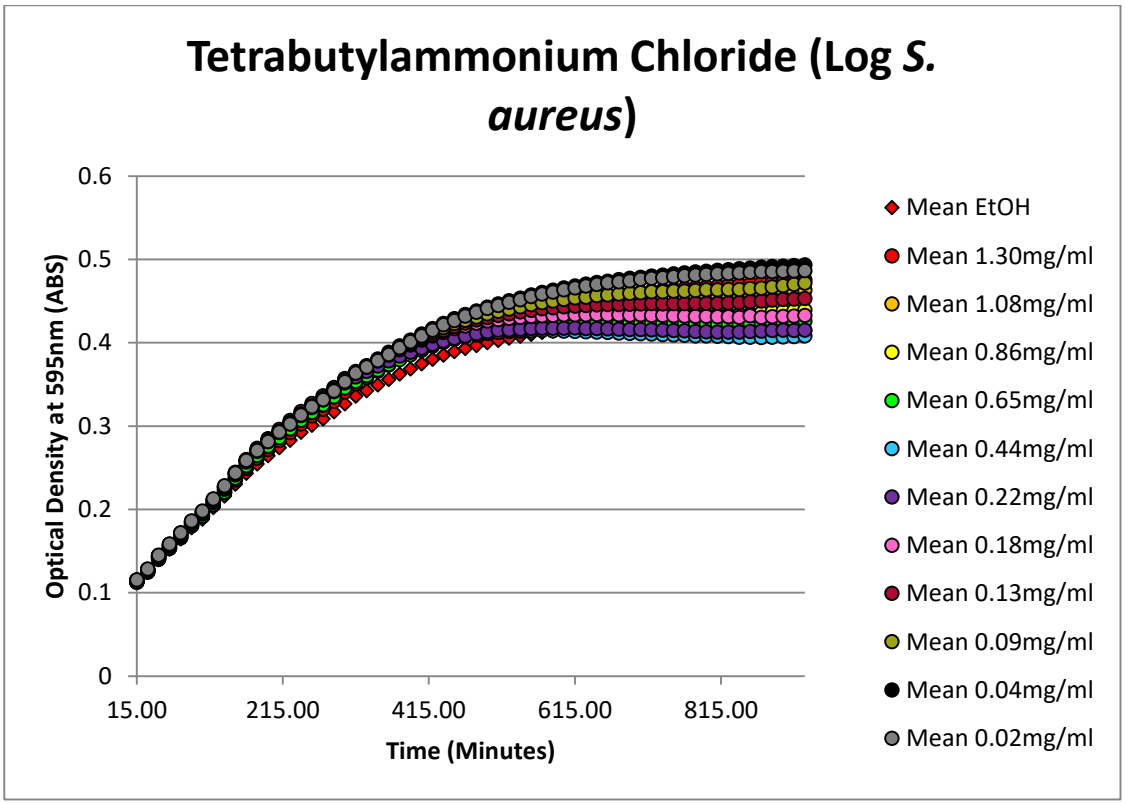

FIGURE 63 - GROWTH CURVE FOR TETRABUTYLAMMONIUM CHLORIDE COMPOUND AGAINST LOG *S.AUREUS*

3.3.10 The Tetraalkylammonium Chloride Salts with Log *E. coli*

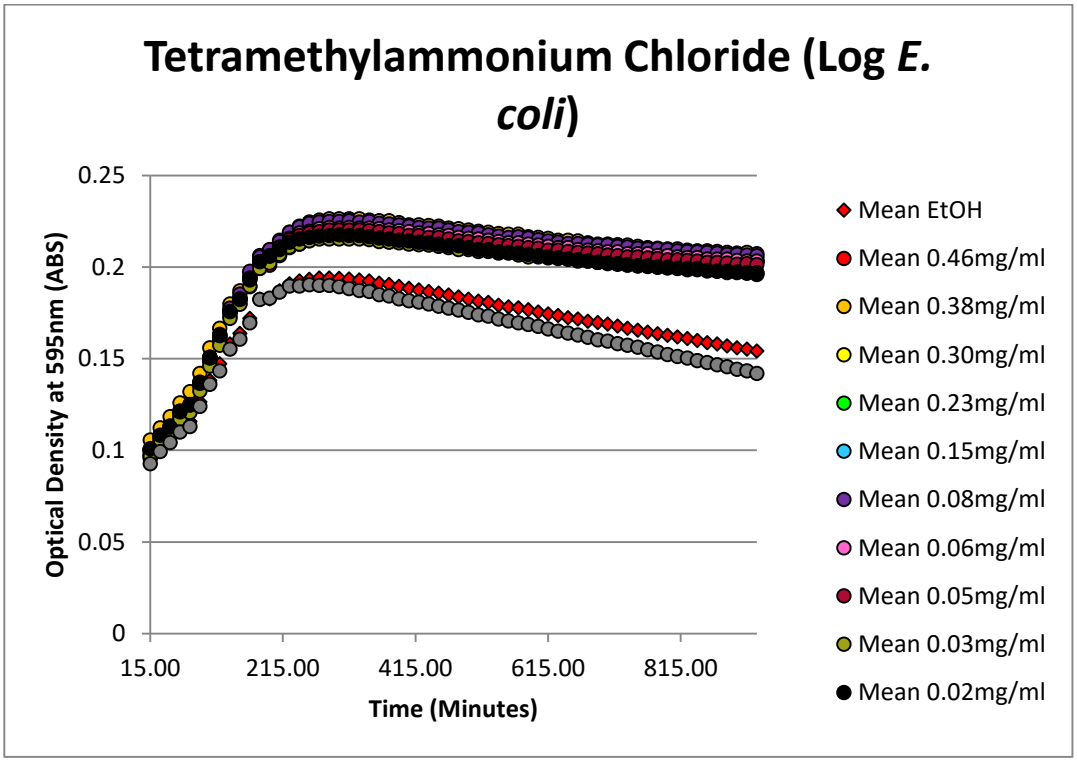

FIGURE 64 - GROWTH CURVE FOR TETRAMETHYLAMMONIUM CHLORIDE COMPOUND AGAINST LOG *E. COLI*

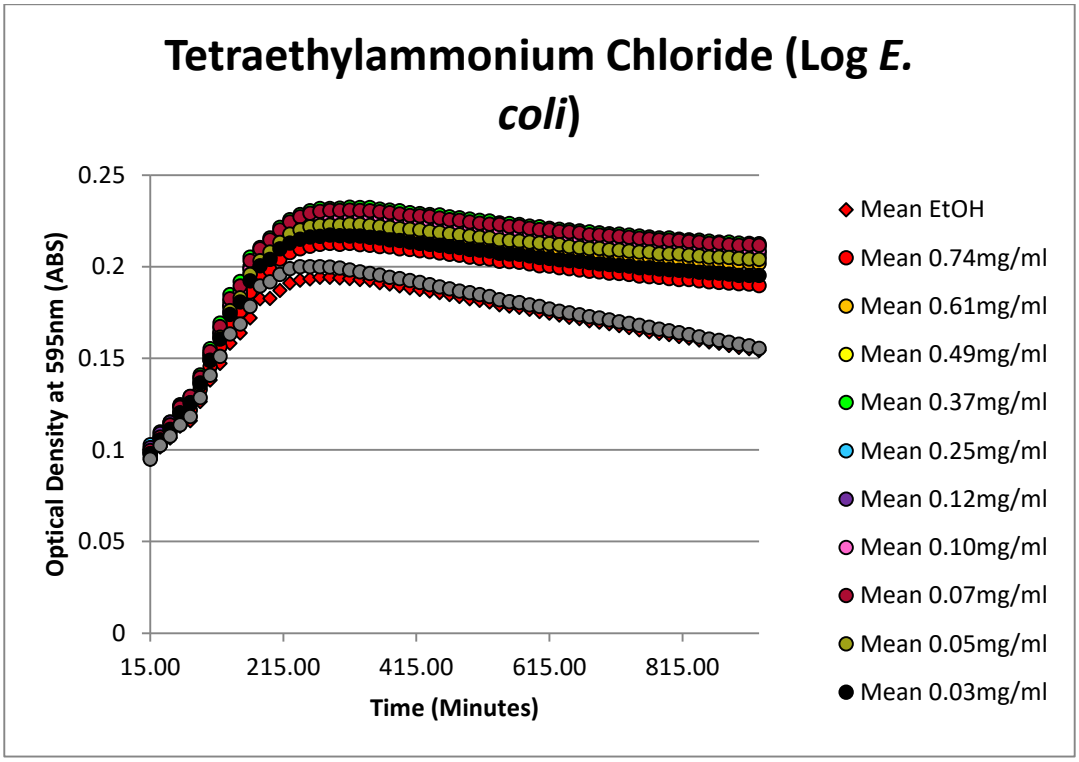

FIGURE 65 - GROWTH CURVE FOR TETRAETHYLAMMONIUM CHLORIDE COMPOUND AGAINST LOG *E. COLI*

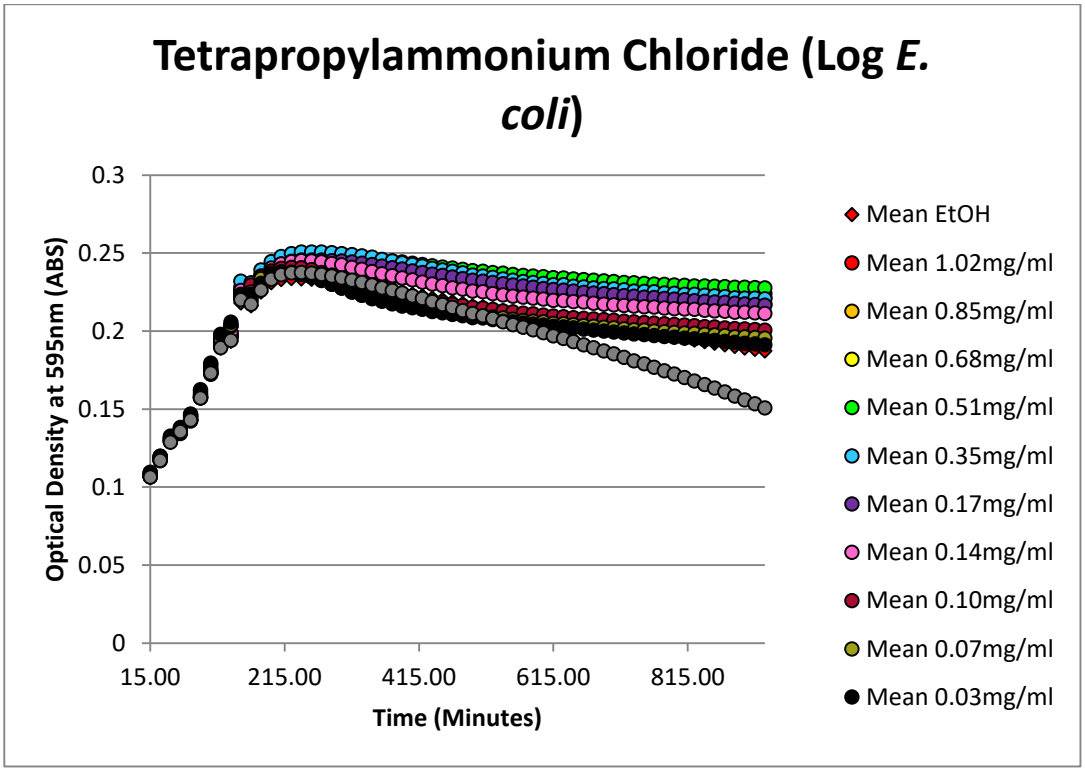

FIGURE 66 - GROWTH CURVE FOR TETRAPROPYLAMMONIUM CHLORIDE COMPOUND AGAINST LOG *E. COLI*

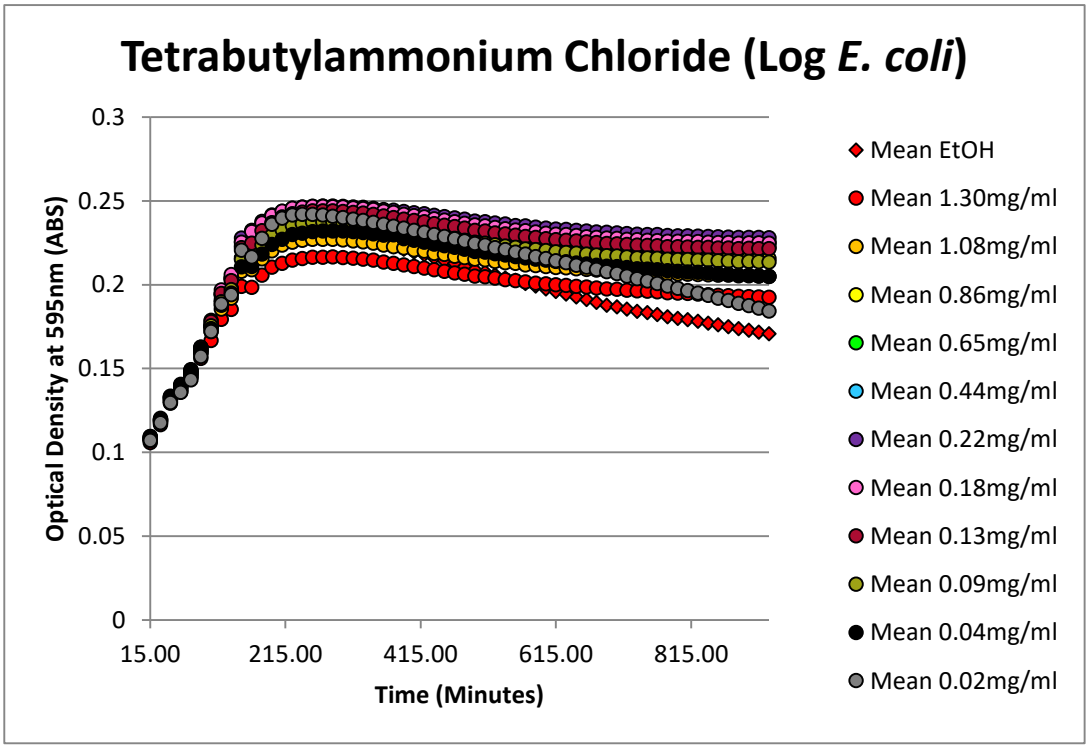

FIGURE 67 - GROWTH CURVE FOR TETRAHEXYLAMMONIUM CHLORIDE COMPOUND AGAINST LOG *E. COLI*

3.4 Results of the Robotic Drop Testing Method

Despite the drawback of the two LEGO brick modules not being able to communicate with each other, the time delayed dual program procedure was effective, allowing the dropping mechanism to move freely from the sample block to the petri dishes. As the microliter syringe was electronically and mechanically controlled, it was able to produce and reproduce similar sized droplets on the surface of the plate.

FIGURE 68 – RESULTS OF THE DROP SIZE TEST FOR THE ROBOTIC SCREENING SYSTEM

4 Discussion

4.1 Discussion of MIC Growth Rate Assay

All the urea based compounds that were tested exhibited antibacterial activity against both log and stationary phase cultures of *S. aureus*, with the most prolific compound being the tetramethylammonium with an MIC_{50} value of 0.45µg/ml. As the chain length of the tetraalkylammonium countercation increases, the efficacy of the compound decreases, but the tetrabutylammonium compounds do not follow the trend, exhibiting the second highest MIC_{50} value of 7.35µg/ml. The tetrabutylammonium and tetrahexylammonium also exhibited an antibacterial effect against *E. coli*, with the hexyl compound producing MIC values for both log and stationary phase cultures, and the butyl producing an MIC value for stationary phase culture. The butyl still exhibited antibacterial action against the *E. coli* cultures, but higher concentrations of drug need to be tested to give a clear calculation for the MIC values. (Figure 26-39)

All the thiourea based compounds except one were ineffective as antibacterials. Only the Tetrabutyl countercation exhibited an antibacterial effect, producing an MIC_{50} value of 54.13µg/ml against *S. aureus* in log phase. However, the compound did not exhibit the same effect against stationary phase, meaning higher concentrations will need to be investigated in further experimentation. None of the thiourea compounds were effective against the cultures of *E. coli*

All compounds tested within this thesis exhibited an effect when added to bacterial suspensions, when an antibiotic effect is not produced, the compounds exhibit an increase in the optical density of the suspension, this effect is hypothesised to be caused by the compounds self-associating to form aggregated nanostructures within the solution, or the association of the compounds with the cell membranes of the bacteria within the solution.

4.2 Discussion of Tetraalkylammonium Hydroxide Compounds

The tetraalkylammonium compounds were tested with the exact same protocols as the urea and thiourea based compounds tested within this thesis. This was to investigate which functional part of the molecule produced the antibacterial effect. In all the experiments performed, none of the tetraalkylammonium compounds exhibited antibacterial effects. All of the compound experiments exhibited an increase in the measured optical density of the bacterial suspensions, this was hypothesised to be caused by the self-association of the compounds, either causing aggregate structures within the solution, or aggregating around the membranes of the cells. This shows that the compounds either cause, or add to the increase in optical density, but do not contribute anything to the antibacterial effect of the compounds.

4.3 Discussion of the Robotic Drop Testing Method

Improvements for the system can be made, with the replacement of the NXT brick being replaced with the newer EV3 brick being the first step, allowing one program to be developed to control all of the motor functions of the robot. The final upgrade for the R.A.S.S. system is a complete replacement of all the motors and control system with component stepper motors and an electronic control unit powered by a microcomputer such as an Arduino board or a Raspberry Pi. This component overhaul would allow the actions of the robot to be even more customisable as stepper motors have much more accurate rotary encoders, allowing finer control of the needle positioning.

5 Conclusion and further work

The aim of this thesis was to investigate the testing methods for synthesised antibacterial compounds, and then apply these assays to a family of novel amphiphilic compounds. The investigation took the data from previously performed experiments concerning the reliability and accuracy of the Kirby Bauer disc diffusion assay, and used this information to develop the drop testing assay. This assay prevented false negative results within the compound screens performed, however suffered from limited repeatability due to the intricate process

of the manual addition of microliter droplets of solution onto an agar plate. This led to the development of the R.A.S.S. system, this modular robot allowed the precise dropping of solutions onto agar plates in an automatic and repeatable protocol. The robot can be programmed to dispense completely customisable grids of solution droplets on standard and large form petri dishes, with scope for a program that will automatically dose a 96 well plate.

After a screening protocol was developed, the MIC assay was investigated, the information gathered using this procedure was used to calculate the MIC values of the novel family of amphiphilic compounds. The methodology was validated by using the assay to calculate the value of known and clinically available antibacterial compounds.

The compounds investigated all exhibited effects against both Gram-positive and Gram-negative bacteria, either antibacterial effects, inhibiting the growth of the pathogenic cells (Gram-Positive), or increasing the optical density through forming aggregated structures (Gram Negative). The antimicrobial effects observed are also comparable to currently available clinical compounds, with the MIC_{50} value of 0.45 µg/ml for the Urea based Methyl compound competing with the values of 1 µg/ml and 2 µg/ml for Vancomycin and Amoxiclav respectively, and the MIC_{50} value of 7.35 µg/ml for the Urea based Butyl compound competing with the value of 8 µg/ml for Erythromycin.

Further investigation of this family of compounds is needed, particularly microscopy, this would confirm the mode of action of the self-association, showing whether the aggregate structures are free in solution of interacting with the bacterial cell membranes. After this, testing of the compounds on clinical bacterial strains such as the *ESKAPE* pathogens should also be investigated as well as further testing into the antibacterial mode of action. A component overhaul and upgrade of the R.A.S.S. system should also be investigated.

6 Appendix – ESI

6.1 Tetrapentylammonium Compound

Melting Point: 90 ºC; ^{1}H NMR (400 MHz, DMSO-d6): δ: 0.88 (t, 3H), 1.28 (m, 2H), 1.56 (s, 4H), 3.15 (t, 2H), 3.93 (d, 2H), 6.94 (s, 1H, NH), 7.55 (m, 4H) 9.24 (s, 1H, NH); ^{13}C{^{1}H} NMR (100 MHz, DMSO-d_6): δ: 56.38 (CH_2), 117.61 (CH), 121.16 (C), 121.48 (CH), 123.83 (C), 126.29 (C) 126.53 (C) 144.77 (C), 154.70 (C); IR (film): v = 3278 (NH stretch), 2964, 1544, 1321, 1161, 840; HRMS for ($C_{29}H_{52}F_3N_3O_4S$) (ESI$^-$): m/z: act: 297.0155 [M-H]$^-$ cal: 297.0162 [M-H]$^-$.

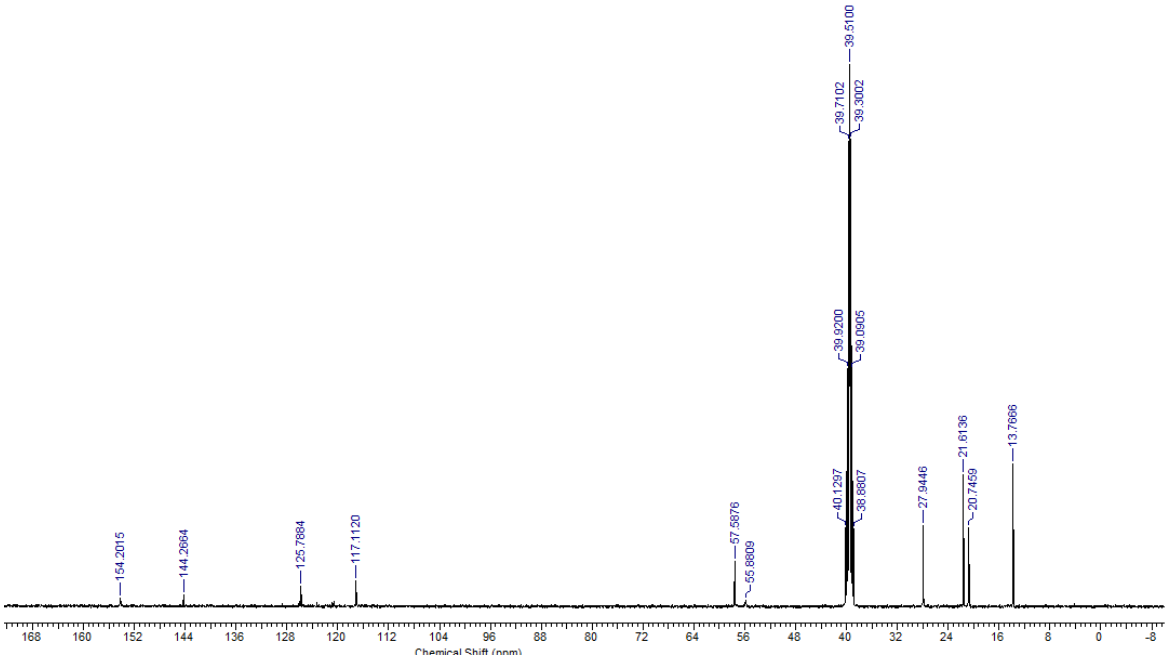

^{13}C{^{1}H} NMR of Tetrapentylammonium Compound

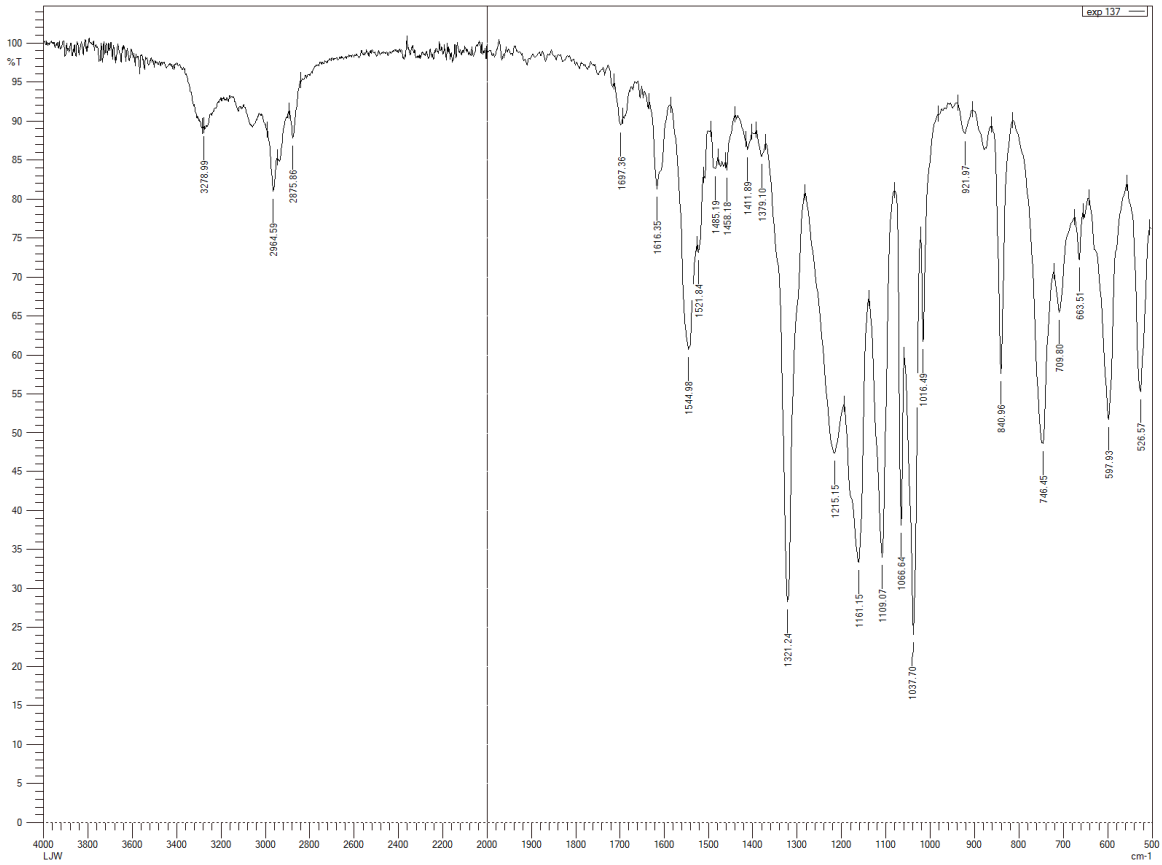

IR spectrum of Tetrapentylammonium Compound

6.2 Tetrahexylammonium compound

Melting Point: N/a – Compound is an oil; ^{1}H NMR (400 MHz, DMSO-d_6): δ: 0.83 (m, 3H), 1.24 (d, 2H), 1.52 (m, 2H), 3.11 (m, 2H), 3.87 (d, 2H), 6.85 (s, 1H, NH), 7.48 (m, 4H) 9.28 (s, 1H, NH); ^{13}C{^{1}H} NMR (100 MHz, DMSO-d_6): δ: 56.41 (CH_2), 117.62 (CH), 117.62 (CH), 121.30 (C), 126.24 (CH), 126.26 (C) 126.28 (CH) 144.82 (C), 154.76 (C); IR (film): v = 3288 (NH stretch), 1695, 1222, 1111, 840; HRMS for ($C_{33}H_{60}F_3N_3O_4S$) (ESI$^-$): m/z: act: 297.0141 [M-H]$^-$ cal: 297.0162 [M-H]$^-$.

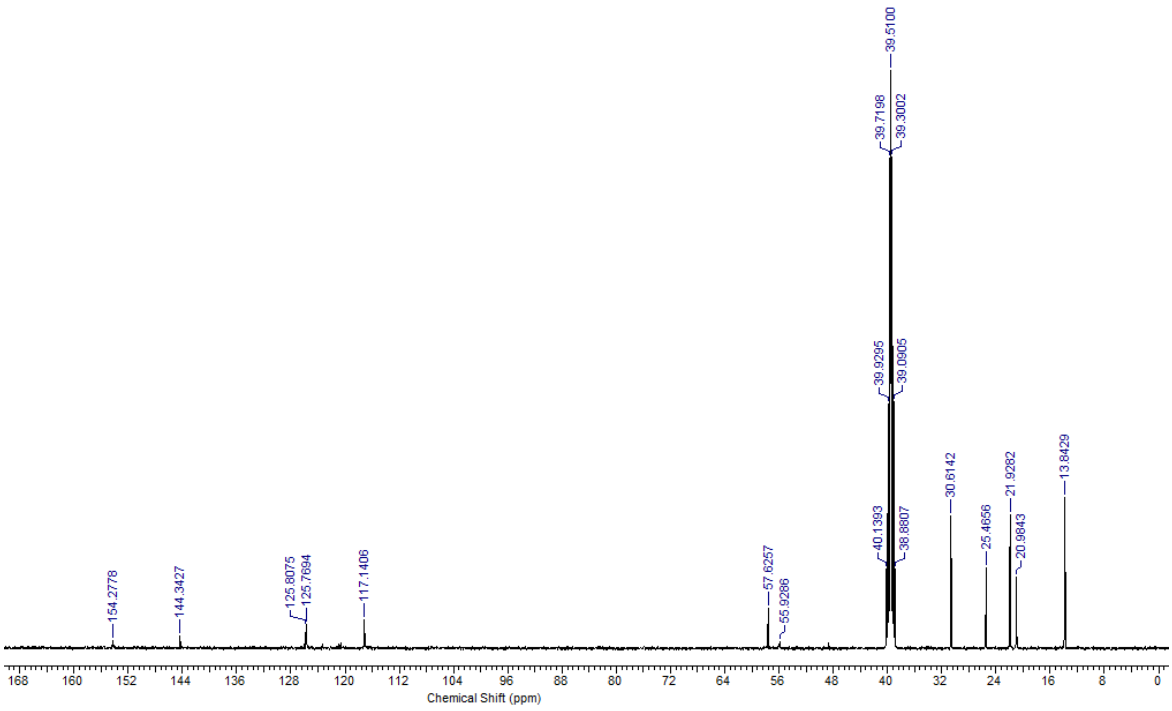

^{13}C{^{1}H} NMR of Tetrahexylammonium Compound

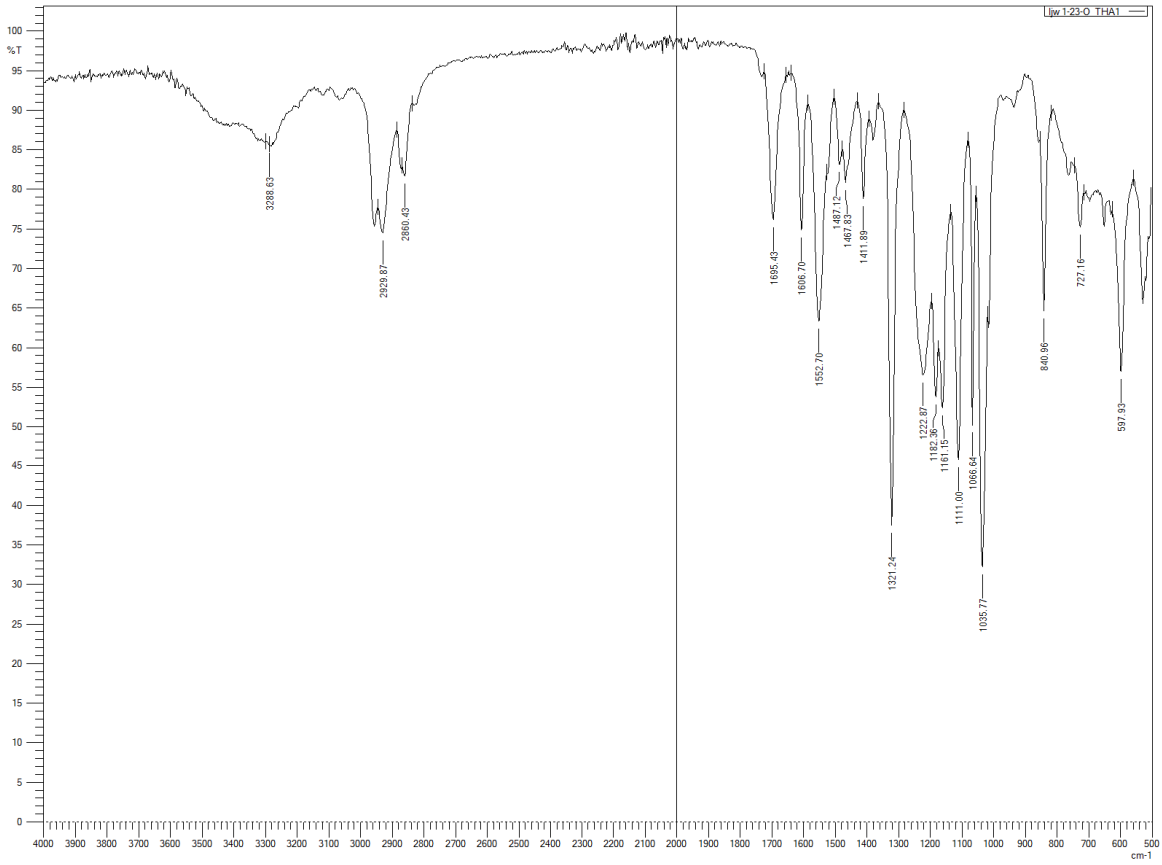

IR spectrum of Tetrahexylammonium Compound

7 References

1. Valiquette, L. & Laupland, K. B. Antimicrobial shortages: Another hurdle for clinicians. *Can. J. Infect. Dis. Med. Microbiol.* **26,** 67–8 (2015).

2. Ventola, C. L. The antibiotic resistance crisis: part 1: causes and threats. *P T A peer-reviewed J. Formul. Manag.* **40,** 277–83 (2015).

3. Speck, P. Antibiotics: Avert an impending crisis. *Nature* **496,** 169 (2013).

4. O'Neill, J. Review on Antimicrobial Resistance: Antimicrobial Resistance: Tackling a Crisis for the Health and Wealth of Nations. *Rev. Antimicrob. Resist.* (2014).

5. Shapiro, D. J., Hicks, L. A., Pavia, A. T. & Hersh, A. L. Antibiotic prescribing for adults in ambulatory care in the USA, 2007–09. *J. Antimicrob. Chemother.* **69,** 234–240 (2014).

6. Report, M. W. Office-related antibiotic prescribing for persons aged ≤14 years United States, 1993--1994 to 2007--2008. *MMWR. Morb. Mortal. Wkly. Rep.* **60,** 1153–1156 (2011).

7. Fleming-Dutra, K. E., Hersh, A. L., Shapiro, D. J. et al. Prevalence of Inappropriate Antibiotic Prescriptions Among US Ambulatory Care Visits, 2010-2011. *JAMA.* 2016 **315**(17):1864–1873

8. O'Neill, J. Antimicrobials in Agriculture and the Environment: Reducing Unnecessary Use and Waste. *Rev. Antimicrob. Resist.* **Dec.** (2015).

9. Ferber, D. WHO Advises Kicking the Livestock Antibiotic Habit. *Science* **301,** 1027 (2003).

10. Mathew, A. G., Cissell, R. & Liamthong, S. Antibiotic resistance in bacteria associated with food animals: a United States perspective of livestock production. *Foodborne Pathog. Dis.* **4,** 115–33 (2007).

11. Woolhouse, M., Ward, M., van Bunnik, B. & Farrar, J. Antimicrobial resistance in humans, livestock and the wider environment. *Philos. Trans. R. Soc. Lond. B. Biol. Sci.* **370,** 20140083 (2015).

12. European Medicines Agency. Reflection paper on the use of macrolides, lincosamides and streptogramins (MLS) in food-producing animals in the European Union: development of resistance and impact on human and animal health. *J. vet. Pharmacol. Ther.* **32,** 515–533 (2008).

13. Aiello, A. E., Larson, E. L. & Levy, S. B. Consumer Antibacterial Soaps: Effective or Just Risky? *Clin. Infect. Dis.* **45,** 137–147 (2007).

14. Rice, L. B. Federal Funding for the Study of Antimicrobial Resistance in Nosocomial Pathogens: No ESKAPE. *J. Infect. Dis.* **197,** 1079–1081 (2008).

15. Marrie, T. J., Nelligan, J. & Costerton, J. W. A scanning and transmission electron microscopic study of an infected endocardial pacemaker lead. *Circulation* **66,** 1339–1341 (1982).

16. Ghooi, R. B. & Thatte, S. M. Inhibition of cell wall synthesis; is this the mechanism of action of penicillins? *Med. Hypotheses* **44,** 127–131 (2017).

17. Ennis, H. L. Inhibition of protein synthesis by polypeptide antibiotics. *J. Bacteriol.* **90,** 1109–1119 (1965).

18. Usary, J. & Champney, W. S. Erythromycin inhibition of 50S ribosomal subunit formation in *E. coli* cells. *Mol. Microbiol.* **40,** 951–962 (2001).

19. Hartmann, G., Behr, W., Beissner, K.-A., Honikel, K. & Sippel, A. Antibiotics as Inhibitors of Nucleic Acid and Protein Synthesis. *Angew. Chemie Int. Ed. English* **7,** 693–701 (1968).

20. Kohanski, M. A., Dwyer, D. J., & Collins, J. J. (2010). How antibiotics kill bacteria: from targets to networks. *Nature Reviews. Microbiology*, *8*(6), 423–435.

21. Tan, S. Y. & Tatsumura, Y. Alexander Fleming: Discoverer of penicillin. *Singapore Med. J.* **56,** 366–367 (2015).

22. Yocum, R. R., Rasmussen, J. R. & Strominger, J. L. The mechanism of action of penicillin. Penicillin acylates the active site of Bacillus stearothermophilus D-alanine carboxypeptidase. *J. Biol. Chem.* **255,** 3977–3986 (1980).

23. M. Lawrence Podolsky. Cures Out of Chaos: How Unexpected Discoveries Led to Breakthroughs in Medicine and Health. *Harwood Acad. Publ.* (1997).

24. Singh, J. & Arrieta, A. C. New cephalosporins. *Semin. Pediatr. Infect. Dis.* **10,** 14–22 (1999).

25. Papp-Wallace, K. M., Endimiani, A., Taracila, M. A. & Bonomo, R. A. Carbapenems: Past, present, and future. *Antimicrob. Agents Chemother.* **55,** 4943–4960 (2011).

26. Bisacchi, G. S. Origins of the Quinolone Class of Antibacterials: An Expanded 'Discovery Story'. *J. Med. Chem.* **58,** 4874–4882 (2015).

27. Aldred, K. J., Kerns, R. J. & Osheroff, N. Mechanism of quinolone action and resistance. *Biochemistry* **53,** 1565–1574 (2014).

28. Administration, U. F. and D. FDA Drug Safety Communication on Quinolones. (2016).

29. Chopra, I. & Roberts, M. Tetracycline Antibiotics : Mode of Action , Applications , Molecular Biology , and Epidemiology of Bacterial Resistance. **65,** 232–260 (2001).

30. Biotechnology Information,Tetracycline. *PubChem* (2017). Available at: https://pubchem.ncbi.nlm.nih.gov/compound/54675776. (Accessed: 6th July 2017)

31. Toleman, M. A. *et al.* Aminoglycoside Modifying Enzymes. *Sci. York* **13,** 151–171 (2011).

32. Munita, J. M., Arias, C. A., Unit, A. R. & Santiago, A. De. Mechanisms of Antibiotic Resistance. **4,** 1–37 (2016).

33. Kaufman, G. Antibiotics: mode of action and mechanisms of resistance. *Nurs. Stand.* (2011).

34. Pages, J.-M., James, C. E. & Winterhalter, M. The porin and the permeating antibiotic: a selective diffusion barrier in Gram-negative bacteria. *Nat Rev Micro* **6,** 893–903 (2008).

35. Ughachukwu, P. O. & Unekwe, P. C. Efflux Pump-Mediated

Resistance in Chemotherapy. *Annals of Medical and Health Sciences Research* **2,** 191–198 (2012).

36. Blair, J. M. A., Webber, M. A., Baylay, A. J., Ogbolu, D. O. & Piddock, L. J. V. Molecular mechanisms of antibiotic resistance. *Nat Rev Microbiol* **13,** 42–51 (2014).

37. Burdett, V. Tet(M)-promoted release of tetracycline from ribosomes is GTP dependent. *J. Bacteriol.* **178,** 3246–3251 (1996).

38. Neda Gorgania, Scott Ahlbrandc, Andrew Pattersonc, and N. P. Detection of point mutations associated with antibiotic resistance in *Pseudomonas aeruginosa*. *Int. J.* **34,** 414–418 (2010).

39. Weisblum, B. Erythromycin resistance by ribosome modification. *Antimicrob. Agents Chemother.* **39,** 577–585 (1995).

40. van Meer, G. & de Kroon, A. I. P. M. Lipid map of the mammalian cell. *J. Cell Sci.* **124,** 5–8 (2011).

41. Virtanen, J. a, Cheng, K. H. & Somerharju, P. Phospholipid composition of the mammalian red cell membrane can be rationalized by a superlattice model. *Proc. Natl. Acad. Sci. U. S. A.* **95,** 4964–4969 (1998).

42. Zambrano, F., Fleischer, S. & Fleischer, B. Lipid composition of the golgi apparatus of rat kidney and liver in comparison with other subcellular organelles. *Biochim. Biophys. Acta - Lipids Lipid Metab.* **380,** 357–369 (1975).

43. Simons, K. & Van Meer, G. Lipid sorting in epithelial cells. *Biochemistry* **27,** 6197–6202 (1988).

44. Balouiri, M., Sadiki, M. & Ibnsouda, S. K. Methods for in vitro evaluating antimicrobial activity: A review. *J. Pharm. Anal.* **6,** 71–79 (2016).

45. Gautam, V., Singhal, L., Arora, S., Jha, C. & Ray, P. Reliability of Kirby-Bauer Disk Diffusion Method for Detecting Carbapenem Resistance in *Acinetobacter baumannii-calcoaceticus* Complex Isolates. *Antimicrob. Agents Chemother.* **57,** 2003–2004 (2013).

46. Joseph, N. *et al.* Reliability of Kirby-Bauer disk diffusion method for detecting meropenem resistance among non-fermenting gram-negative bacilli. *Indian J. Pathol. Microbiol.* **54,** 556–560 (2011).

47. Drew, W. L., Barry, A. L., O'Toole, R. & Sherris, J. C. Reliability of the Kirby-Bauer disc diffusion method for detecting methicillin-resistant strains of *Staphylococcus aureus*. *Appl. Microbiol.* **24,** 240–7 (1972).

48. Biemer, J. J. Antimicrobial Susceptibility Testing by the Kirby-Bauer Disc Diffusion Method. *Ann. Clin. Lab. Sci.* **3,** 135–140 (1973).

49. Hudzicki, J. Kirby-Bauer disk diffusion susceptibility test protocol. 1–14 (2009).

50. Magaldi, S. *et al.* Well diffusion for antifungal susceptibility testing. *Int. J. Infect. Dis.* **8,** 39–45 (2004).

51. Du Toit, E. A. & Rautenbach, M. A sensitive standardised micro-gel well diffusion assay for the determination of antimicrobial activity. *J. Microbiol. Methods* **42,** 159–165 (2000).

52. Hiscock, J. R., Bustone, G. P., Wilson, B., Belsey, K. E. & Blackholly, L. R. In situ modification of nanostructure configuration through the manipulation of hydrogen bonded amphiphile self-association. *Soft Matter* **12,** 4221–4228 (2016).

53. Koh, J. J. *et al.* Nonpeptidic Amphiphilic Xanthone Derivatives: Structure-Activity Relationship and Membrane-Targeting Properties. *J. Med. Chem.* **59,** 171–193 (2016).

54. Faig, A. *et al.* Biscationic Tartaric Acid-Based Amphiphiles: Charge Location Impacts Antimicrobial Activity. *Langmuir* **31,** 11875–11885 (2015).

55. Wang, H. *et al.* Antibacterial Activity of Geminized Amphiphilic Cationic Homopolymers. *Langmuir* **31,** 13469–13477 (2015).

56. He, M., Zhou, Y., Xiao, H. & Lu, P. Amphiphilic cationic copolymers with ciprofloxacin: preparation and antimicrobial activities. *New J. Chem.* **40,** 1354–1364 (2016).

57. Andrews, J. M. Determination of minimum inhibitory concentrations. *J. Antimicrob. Chemother.* **48,** 5–16 (2001).

58. Luber, P., Bartelt, E., Genschow, E., Wagner, J. & Hahn, H. Comparison of Broth Microdilution, E Test, and Agar Dilution Methods for Antibiotic Susceptibility Testing of *Campylobacter*

jejuni and *Campylobacter coli. J. Clin. Microbiol.* **41,** 1062–1068 (2003).

59. Trimble. Sketchup Software Download. (2017). Available at: https://www.sketchup.com/download. (Accessed: 25th July 2017)

60. B.V., U. Cura Software Download. (2017). Available at: https://ultimaker.com/en/products/cura-software.

61. Lego. Lego Mindstorms Software Download. (2016). Available at: https://www.lego.com/en-gb/mindstorms/downloads/download-software. (Accessed: 25th July 2017)

62. Cell Wall Diagram. Available at: https://cnx.org/contents/nnx1QFeU@11/Structure-of-Prokaryotes. (Accessed: 26th July 2017)

63. Penicillin Inhibition. Available at: https://commons.wikimedia.org/wiki/File:Penicillin_inhibition.svg. (Accessed: 25th July 2017)

64. Beta Lactamase Diagram. Available at: https://commons.wikimedia.org/wiki/File:PDB_1bsg_EBI.jpg. (Accessed: 24th July 2017)

65. Efflux Pump Diagram. Available at: http://www.frontiersin.org/files/Articles/40475/fmicb-04-00007-HTML/image_m/fmicb-04-00007-g001.jpg. (Accessed: 24th July 2017)